Characterization of Native Chromatin Structures Respectively Containing the Methyl-CpG Binding Domain Protein MeCP2 and the Histone Variant H2A.Z

by

Anita Annajothi Thambirajah
B.Sc., University of Victoria, 2003

A Dissertation Submitted in Partial Fulfillment
of the Requirements for the Degree of

DOCTOR OF PHILOSOPHY

in the Faculty of Graduate Studies, Department of Biochemistry and Microbiology

Supervisory Committee

Characterization of Native Chromatin Structures Respectively Containing the Methyl-CpG Binding Domain Protein MeCP2 and the Histone Variant H2A.Z

by

Anita Annajothi Thambirajah
B.Sc., University of Victoria, 2003

Supervisory Committee

Dr. Juan Ausió, (Department of Biochemistry and Microbiology)
Supervisor

Dr. Robert D. Burke (Departments of Biochemistry and Microbiology and Biology)
Departmental Member

Dr. Terry Pearson (Department of Biochemistry and Microbiology)
Departmental Member

Dr. Francis Choy (Department of Biology)
Outside Member

Abstract

Supervisory Committee
Dr. Juan Ausió (Department of Biochemistry and Microbiology)
Supervisor
Dr. Robert D. Burke (Departments of Biochemistry and Microbiology and Biology)
Departmental Member
Dr. Terry Pearson (Department of Biochemistry and Microbiology)
Departmental Member
Dr. Francis Choy (Department of Biology)
Outside Member

The maintenance of dynamic chromatin structures is critical for the proper regulation of cellular activities. The plasticity of chromatin structures can be mediated in several ways, two of which include the incorporation of histone variants and the activities of *trans*-acting factors. In this dissertation, biochemical methods were used to determine the effects of the histone variant H2A.Z or the methyl-CpG binding protein 2 (MeCP2) on the structural composition of native chromatin.

Early, independent biophysical studies of the stability of reconstituted H2A.Z chromatin structures yielded contradictory results. As these studies used H2A.Z expressed as a recombinant protein, it was possible that the absence of any essential folding or post-translational modifications (PTMs) may have been responsible for the diametric findings. To resolve this issue, the stability of various native chromatin structures containing H2A.Z was determined. Using gel filtration chromatography, sucrose gradient sedimentation, and hydroxyapatite chromatography, the partitioning of H2A.Z within dissociated octamers, mononucleosomes, and chromatin fibres were respectively assessed. Within all three structures, H2A.Z associated with stabilized forms. However, the salt-dependent thermal analysis of H2A.Z-H2B dimers by circular

dichroism showed that the variant dimer was largely unstructured. The deposition of H2A.Z also occurred independently of linker histones.

MeCP2 is a chromatin binding protein best known for its ability to repress transcription. While its roles in neuron development have been well-studied, little is known of its interactions within native chromatin. Shortly after MeCP2 was discovered, it was postulated that MeCP2 would behave as a global repressor. However, recent findings have contested this idea. If MeCP2 does act as a universal silencer, it was hypothesized that changes to global chromatin modifications would affect the distribution of MeCP2 within chromatin. HeLa S3 cultures were chemically treated with 3-aminobenzamide or butyrate to induce either DNA hypermethylation or histone hyperacetylation. Neither treated culture resulted in a redistribution of MeCP2 within chromatin. Moreover, the majority of MeCP2 was present within nuclease-accessible, active chromatin. Interestingly, the butyrate treatment resulted in proportional losses of MeCP2 within fractionated chromatin that were not due to changes in *MeCP2* transcription. MeCP2 was also observed to bind to mononucleosomes containing DNA that was >146 bp - ~160 bp. These results suggested that MeCP2 does not act as an indiscriminate silencer, but more likely as a specific transcriptional regulator.

Most studies of MeCP2 interactions with chromatin were performed using reconstituted chromatin templates *in vitro*. However, it is not known if MeCP2 interacts with chromatin in a tissue-specific manner. In addition, as MeCP2 has a broad distribution throughout all chromatin types, it is not known if histone variants or PTMs influence MeCP2 deposition. Therefore, the tissue specificity of MeCP2 binding and the influence of nucleosomal components were investigated. MeCP2 has a differential

distribution throughout chromatin extracted from rat brain, liver, and testis. The brain has significantly more MeCP2 than the liver or testis and this was reflected in the *MECP2* mRNA amounts. Using native co-immunoprecipitations, MeCP2 was shown to interact with mononucleosomes containing specific histone variants and PTMs: H2AX, $H3K27me_3$, and $H3K9me_2$. These novel interactions may further specialize the MeCP2-bound chromatin regions.

Finally, two novel hypotheses regarding the regulation of MeCP2 are proposed. In the first, the regulation of MeCP2 turnover is proposed to occur through the poly-ubiquitination of the two MeCP2 PEST domains, followed by proteolytic degradation. The second hypothesis proposes that the use of histone deacetylase inhibitors could be used to control the levels of MeCP2 expression, in conjunction with gene therapies, for the treatment of Rett syndrome.

Table of Contents

List of Figures

Abbreviations

3-ABA	3-aminobenzamide
26S UPS	26S ubiquitin proteasome system
Å	Angstrom
AUT	acetic acid – urea – Triton X-100
AU	acetic acid – urea
BDNF	brain-derived neurotrophic factor
bp	base pair
$CaCl_2$	calcium chloride
CaMK	calcium/calmodulin-dependent kinases
cDNA	complementary DNA
CDKL5	cyclin-dependent kinase like 5
CENP-A	centromere protein A
ChIP	chromatin immunoprecipitation
Chz1	chaperone for Htz1/H2A-H2B dimer
C-terminal	carboxy – terminal
DNA	deoxyribonucleic acid
DNMT	DNA methyltransferase
EDTA	ethylenedinitrilo-tetraacetic acid
GAPDH	glyceraldehyde-3-phosphate dehydrogenase
GPBP1	GC-rich promoter binding protein 1
H2A.Bbd	H2A barr body deficient

HAP	hydroxyapatite
HCl	hydrochloric acid
HDAC	histone deacetylase
HEPES	N-2-hydroxyethylpiperazine-N'-2-ethanesulfonic acid
HMR	hidden MAT (mating locus) right
HP1-α	heterochromatin protein 1 – alpha
HPLC	high performance liquid chromatography
KAT	lysine (K) acetyl-transferase
Kat5	lysine (K) acetyltransferase 5
KCl	potassium chloride
kDa	kilo dalton
KMT	lysine methyltransferase
LSD1	lysine specific demethylase 1
MART	mono-ADP-ribosyltransferase
MBD	methyl-CpG binding domain
MBD2	methyl-CpG binding domain protein 2
MBD3	methyl-CpG binding domain protein 3
MBD4	methyl-CpG binding domain protein 4
MCF-7	Michigan Cancer Foundation – 7
me_2	dimethylated
me_3	trimethylated
MeCP2	methyl-CpG binding protein 2
$MgCl_2$	magnesium chloride

MNase	micrococcal nuclease
mRNA	messenger RNA
NaCl	sodium chloride
NAD	nicotinamide adenine dinucleotide
Nap1	nucleosome assembly protein 1
NCP	nucleosome core particle
NHR	non-histone region
NLS	nuclear localization signal
NP-40	nonyl phenoxylpolyethoxylethanol
N-terminal	amino – terminal
P	pellet
PAGE	polyacrylamide gel electrophoresis
PARP-1	poly(ADP-ribose) polymerase 1
PCR	polymerase chain reaction
PDB	protein data base
PEST	proline, glutamate, serine, threonine
PTM	post-translational modification
RNA	ribonucleic acid
RT-PCR	reverse-transcriptase polymerase chain reaction
RTT	Rett syndrome
S1	first supernatant
S.D.	standard deviation
S.E.	standard error

SDS	sodium dodecyl sulphate
SE	EDTA supernatant
SRA	SET and ring finger-associated
SUMO	small ubiquitin-related modifier
SWI/SNF	switch mating type/sucrose non-fermenting
SWR1	sick with rat8 ts 1
TAE	Tris – acetic acid - EDTA
TRD	transcriptional repression domain
WW domain	tryptophan – tryptophan containing domain
Xist	X-inactivated specific transcript

Acknowledgements

I would like to first thank my supervisor, Dr. Juan Ausió, for his mentorship, guidance, and the opportunity to study in his lab. I have learned a great deal from him, both scientific and otherwise, from his experience and by his giving me the independence to pursue my ideas and experimental adventures.

I am grateful for the support of my supervisory committee: Dr. Ausió, Dr. Robert Burke, Dr. Terry Pearson, and Dr. Francis Choy. I am deeply appreciative of the time that they have taken to guide my progress over the past number of years, for their insightful advice and their continued support of my scientific development. Thank you to Dr. Jim Davie for taking the time to be my external examiner.

Thank you also to Deb Penner, Melinda Powell, and Sandra Boudewyn for all of their friendly help. I would like to particularly acknowledge Deb and Melinda for their very kind and experienced advice over the years, especially with all things administrative.

Thank you to the gentlemen in the technical shop, Scott Scholz, Albert Labossier, and Steven Horak, for keeping the lab (and my experiments!) running. I greatly appreciate the invaluable help that Scott has provided (*i.e.*, rescuing my laptop) and for his patient and knowledgeable explanations of the inner workings of lab equipment.

To my colleagues and friends in the lab, the mutual support and comradery have been particularly meaningful. Thank you to the past and present lab members: Lindsay Frehlick, Begonia Silva Moreno, Ron Finn, Toyotaka Ishibashi, Deanna Dryhurst, Wade Abbott, Chema Eirín-López, Alison Calestagne-Morelli, Andra Li, Kim Curry, Allison Maffey, Brad Williamson, Lyndsay Sprigg, and the many visiting scientists.

I am profoundly grateful for the unabating support, encouragement, and understanding of my sisters, my friends, and most particularly, of my parents. Thank you also to my friends who generously shared their library e-journal access at other universities with me.

I would like to thank Dr. Steve V. Evans for his assistance in preparing the SETOR H2A.Z structure model. Thanks also to Dr. Cornelia Bohne for generously permitting the use of her spectropolarimeter for the circular dichroism studies.

Thank you to Dr. Nik Veldhoen and Deanna Dryhurst for many helpful qPCR discussions. I would like to thank Dr. Brian Christie for providing the male rats used in the RT-qPCR work and Michael Peterson for the lamb brains.

My experimental work was supported indirectly by a Canadian Institute of Health Research (CIHR) grant MOP-97878 (J.A.). I gratefully acknowledge the various funding I have received over the years: a CIHR CGS Master's scholarship, a Michael Smith Foundation for Health Research (MSFHR)-UVic fellowship, and a Natural Sciences and Engineering Research Council (NSERC) CGS doctoral fellowship.

Dedication

I dedicate this dissertation to my parents with thanks for their love, support, encouragement and faith.

Chapter 1 – Introduction to Chromatin

This chapter was adapted in part from the publication:

Thambirajah, A.A. and Ausió, J. (2009) A moment's pause: Putative nucleosome-based influences on MeCP2 regulation. Biochemistry and Cell Biology. **87**:791-798.

Chromatin Fundamentals

Chromatin organization provides for the functionally dynamic, structural compaction of genetic information within the nucleus of a cell. Chromatin is the large, macromolecular complex derived from the packaging of DNA with histone and non-histone proteins. The tremendous informational capacity stored within chromatin must be precisely regulated during developmental and homeostatic processes. Any aberrations in this regulation of information can jeopardize the health of an organism and lead to disease.

The fundamental repeat unit of chromatin is the nucleosome core particle. The nucleosome is formed by 146 base pairs (bp) of DNA wrapping 1.65 times around a core of histone proteins (Kornberg and Thomas, 1974; Luger et al., 1997; Olins and Olins, 1974; Oudet et al., 1975; Richmond and Davey, 2003). The histone core is an octamer formed of two copies each of histones H2A, H2B, H3 and H4 (Figure 1). Copies of H3 and H4 together form a tetramer which is flanked by two H2A-H2B dimers, resulting in the histone core octamer:

$$(H3\text{-}H4)_2 + 2\cdot(H2A\text{-}H2B) \rightarrow (H2A\text{-}H2B):(H3\text{-}H4)_2:(H2A\text{-}H2B).$$

Hydrophobic interactions exist between the individual histone contacts within the dimer and tetramer forms, while the tetramer and dimers associate through hydrogen bonding (Eickbush and Moudrianakis, 1978). Adjacent nucleosomes are joined by an intervening piece of linker DNA that can range from 10-60 bp in length. Linker histones, either H1 or H5, can bind to this region and facilitate compaction of the chromatin fibre, and thereby have pivotal transcription- and replication-dependent implications. The

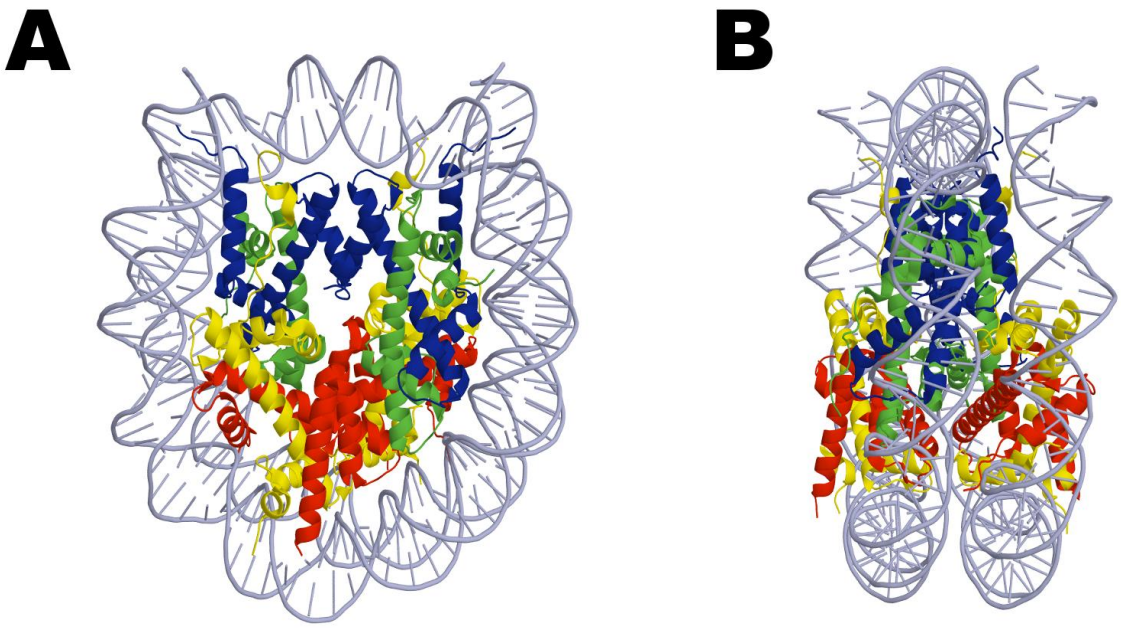

Figure 1. ***Front (A) and side (B) view representations of the nucleosome core particle composition.*** **These depictions are based on the X-ray structure of the nucleosome (structure 1KX3) determined to a resolution of 1.9Å (Davey et al., 2002). The figures were prepared using PyMOL (DeLano, 2002) and rendered using POVray. 146 bp of DNA are shown in light grey wrapping around the histone octamer in approximately 1.65 turns. The histone octamer is composed of two copies each of H2A (yellow), H2B (red), H3 (blue), and H4 (green). The H3-H4 tetramer is flanked by two H2A-H2B dimers. The nucleosome core particle forms the fundamental repeat unit of chromatin.**

chromatosome particle is composed of ~160 – 170 bp of DNA wrapped around the histone octamer with the linker DNA bound by the linker histone (Simpson, 1978).

Within most nucleated cells, histones are the major protein complement that organize the DNA. However, in sperm, alternative sperm nuclear basic proteins may be utilized that can enhance the tight compaction of DNA. Depending on the type of

organism, these proteins may be histones, protamines or intermediate protamine-like proteins. For a good review, refer to (Eirin-Lopez and Ausió, 2009).

The successive compaction of the chromatin fibre initially goes through a 30 nm fibre intermediate (Thoma et al., 1979), which then condenses into higher order chromatin structures. The extent of packing of the chromatin fibres can vary immensely. More open and accessible chromatin regions are referred to as euchromatin and typically correlate to being transcriptionally active. Conversely, tightly arrayed chromatin domains are often refractory to nuclease digestion and are transcriptionally quiescent. These regions are known as heterochromatin. However, neither are absolute definitions and a well-known exception is the expression of the non-coding *Xist* RNA from the heterochromatinized inactivated X chromosome (Brown et al., 1991; Kalantry et al., 2009).

The highly organized folding of the DNA-protein complex permits the nearly 2 m long DNA to fit within the cell's nucleus, which has a diameter of approximately 2-5 μm. Aside from this being an incredibly impressive structural feat, this compaction of the DNA has tremendous relevance for the functional expression of genetic information. But how is access to this information regulated in a temporal and spatial manner? To accomplish the functional genetic requirements of the cell, the chromatin structure must be dynamically regulated.

Histone types

In early chromatin research, it was thought that the histone complement were static proteins whose primary importance was to serve as a physical scaffold for the DNA

(Wilkins, 1959). However, this largely outdated viewpoint has now been replaced with the understanding that the histones themselves have a tremendous informational capacity and play key roles in transcription and replication (Jenuwein and Allis, 2001; Shogren-Knaak et al., 2006).

Histone proteins are among the most evolutionarily conserved proteins. Analogous architectural proteins have been described in archaea and bacteria, underscoring the importance of histone proteins in regulating gene metabolism (Luijsterburg et al., 2008). As described earlier, there are two main types of histone proteins: core histones and linker histones. Each individual histone protein exists as a family comprised of several different isoforms or variants. These have been described as two main classes: heteromorphous and homomorphous isoforms. The homomorphous isoforms display a minimal sequence divergence of only a few amino acids compared to the canonical forms, while the heteromorphous possess a significant sequence variation (West and Bonner, 1980). Heteromorphous histones are typically non-allelic variants that are expressed throughout the cell cycle and independently of the S phase, unlike the majority of canonical, homomorphous histones. The genes of heteromorphous histones may include introns and the mRNAs are often polyadenylated. These genes are not clustered on chromosomes as characteristic of homomorphous isoforms.

Core Histone Variability

The core histones have a distinctive globular central domain known as the histone fold (Arents and Moudrianakis, 1995; Baxevanis et al., 1995). The histone fold consists of three α-helices in a helix-fold-helix motif (Arents and Moudrianakis, 1993;

Moudrianakis and Arents, 1993). When paired in the heterodimer, the histone folds of the two interacting histones form a handshake motif (Luger et al., 1997). Emanating from either side are the N- and C-terminal histone tails, which are the sites of considerable sequence variability. The tails are also the major sites of post-translational modification.

The H2A family of isoforms is one of the largest and perhaps best studied group of histones (Ausió, 2006). A number of heteromorphous H2A variants have been characterized extensively and play key roles in a diverse range of processes including poising genes for transcriptional activation, DNA damage repair, and X chromosome inactivation [for recent reviews, see (Altaf et al., 2009; Thambirajah et al., 2009b)]. Examples of variants involved in these roles include H2A.Z, H2AX, macroH2A, and H2A.Bbd. The carboxyl-terminal (C-terminal) tails of these replacement variants are the major sites of sequence divergence.

H2A.Z has broad, and sometimes conflicting, functional roles; it is postulated to be involved in activating and silencing gene expression (Bruce et al., 2005; Dhillon and Kamakaka, 2000; Larochelle and Gaudreau, 2003; Rangasamy et al., 2003). This will be described in more detail in Chapter 2. H2AX is present in approximately every 10 nucleosomes and becomes phosphorylated at serine 139 (γ-H2AX) within its SQE motif following DNA double strand breaks (Rogakou et al., 1998). γ-H2AX then recruits factors involved in the repair of DNA damage. MacroH2A is an atypical histone variant in that its long C-terminus contains a large, globular macro domain known as the non-histone region (NHR) (Pehrson and Fried, 1992). The NHR is connected to the histone fold through a basic hinge region. Altogether, macroH2A is about 3 times larger than

canonical H2A forms (Thambirajah et al., 2009b). In addition to its role in X chromosome inactivation, phosphorylation of the macroH2A hinge region is proposed to have a role in chromatin condensation during mitosis (Bernstein et al., 2008).

Like the H2A family, the H3 family of variants has also been well-studied, though the H3 variants are fewer in number. Aside from the homomorphous isoforms, such as H3.1, H3.2 and H3.3, the centromeric H3 heteromorphous variant is the best known of its kind. CENP-A is required to epigenetically maintain the identity of the centromeres (Torras-Llort et al., 2009). A testis-specific variant, H3t, has also been described in mammals (Tachiwana et al., 2008).

There are 14 separate H4 genes in humans, all of which encode the same H4 amino acid sequence (Albig and Doenecke, 1997; Happel and Doenecke, 2009). Similarly, H2B was thought to have very few isoforms. In 2006, the detection of 11 H2B variants in Jurkat cells (a human T lymphocyte cell line) was described. Although the functional relevance of these variants is yet to be determined, the major sequence variation is present in the first 39 amino acids. In addition, some variation is present in the globular domain, as in some H2A variants (Bonenfant et al., 2006). Testis-specific human isoforms of H2B (hTSH2B) may undertake important roles in decondensation during fertilization (Zalensky et al., 2002).

Linker Histones

The linker histones are distinguished from their core histone counterparts by several key features. Similar to core histones, the lysine-rich linker histones have a tripartite structure consisting of N- and C-terminal tails that flank a globular domain.

However, the globular core has a winged helix motif comprised of three α-helices and three antiparallel β-sheets (Clark et al., 1993). Of all the histone families, the H1 linker histone group has the greatest heterogeneity (Happel and Doenecke, 2009). A unique avian and amphibian linker histone variant, H5, is expressed in nucleated erythrocytes (Doenecke and Tonjes, 1986; Neelin et al., 1964). H5 was used to determine the crystallographic structure of linker histones (Clark et al., 1993; Ramakrishnan et al., 1993).

Linker histones bind asymmetrically near the pseudo-dyad axis of the nucleosome, although exactly where H1 binds has been contentious (Bradbury and van Holde, 2004; Happel and Doenecke, 2009). The long C-terminal tail of H1 is able to constrain the ends of the DNA entering and exiting the nucleosome, and consequently, alters the conformation of the chromatin fibre (Lu and Hansen, 2004). H1 has tremendous influence over the organization and compaction of higher order chromatin structures. As such, H1 isoforms play critical roles in regulating transcription as they can limit the access of non-histone regulatory proteins to chromatin (Catez et al., 2006; Zlatanova et al., 2000).

There are eleven different mammalian H1 variants whose expression in somatic cells occurs either during S phase or independently of the cell cycle. As well, there are germline variants, three of which are testicular forms (H1t, H1T2, and HILS1) and one oocytic variant (H1oo) [see (Happel and Doenecke, 2009) for review]. There is some limited redundancy between the different H1 histones. The expression of some H1 subtypes is linked to particular developmental stages and could indicate a specialization among the different H1 variants.

Maintaining a Dynamic Chromatin State

It is imperative that the plasticity of chromatin be maintained in order to accommodate any replication or transcription requirements in response to developmental, homeostatic, or stress stimuli. A dynamic chromatin state can be maintained in several different ways. The introduction of histone variants into nucleosome structures and the chemical modification of DNA or histones can impart structural and functional variability to chromatin. The methylation of DNA at specific dinucleotides and the post-translational modification (PTM) of histones will be discussed briefly in more detail later in this chapter. Recently, RNA has been shown to play a role in regulating chromatin structure; for example, the *Xist* mRNA. In combination with histone variants, DNA methylation and histone PTMs, changes can be imparted to local or global chromatin structures in *cis* or in *trans* by the recruitment of non-histone chromatin binding proteins. The combination of all these factors and the enzymes that confer chemical modifications together constitute a multitude of epigenetic signals that can modulate transcriptional states (Probst et al., 2009; Tost, 2009; Wu et al., 2009).

Other mechanisms altering chromatin dynamics include, but are not limited to, the activities of non-histone proteins such as chromatin remodelling complexes or the methyl binding domain (MBD) family proteins. Examples of ATP-dependent remodelling complexes include the SWI/SNF complex or SWR1. Their activities are specific to particular histones or variants, and regulate access to DNA sequences (Korber and Horz, 2004; Yoo and Crabtree, 2009). The MBD family of proteins recognizes specific nucleosome-constrained DNA sites and recruits other modifying proteins to affect

changes in transcriptional activites. These are a few examples of non-histone chromatin binding proteins that can affect chromatin structure.

Post-Translational Modification of Histones

Histone tails are subject to a number of different chemical modifications and these include: acetylation, phosphorylation, methylation, ubiquitination, sumoylation, poly-ADP ribosylation, N-formylation and deimination (Jiang et al., 2007; Kouzarides, 2007). PTMs permit the diversification of roles that a particular histone may undertake, potentially in combination with other modified histones. The establishment of epigenetic marks permits cells to respond to internal and external stimuli and to create transcriptional memory. Transcriptional memory refers to the establishment of an epigenetic signature that primes a cell to respond to stimuli it has previously encountered (Francis and Kingston, 2001). The modification of histones is a dynamic event; for instance, the gain and loss of particular PTMs can be detected throughout the cell cycle (Bonenfant et al., 2007).

Phosphorylation

The addition of a phosphate moiety by one of many kinases to specific serine or threonine residues of histones has been extensively described (Davie, 2004). Phosphorylation of H2AX and macroH2A can lead to different, specialized functional outcomes. For instance, phosphorylation of serine 10 of H3 has been linked to chromatin condensation during mitosis (Bradbury, 1992) and increases during mitosis and meiosis

(Wei et al., 1999). Phosphorylated H3S10 is correlated to learning and memory as well (Stipanovich et al., 2008). Phosphorylated H1 increases during the cell cycle and colocalizes with replicating DNA. It has been proposed that the phosphorylation of H1 promotes decondensation to facilitate replication (Alexandrow and Hamlin, 2005). Conversely, during M phase, H1 phosphorylation is associated with chromatin condensation (Baatout and Derradji, 2006).

Acetylation

Acetylation involves the covalent linkage of an acetyl group from acetyl-coenzyme A to the ε-amino group of lysine residues within the N-terminal tails of histones. This transfer is mediated by lysine acetyltransferases (KATs) and the complementary reversal of this process is accomplished by histone deacetylases (HDACs). The effects of acetylation can be localized to a few nucleosomes including gene promoters, but can also result in the global modification of several kilobases of DNA (Calestagne-Morelli and Ausió, 2006). Acetylation has typically been associated with active transcription, whereas deacetylation of histones confers a repressed state. It is thought that acetylation facilitates transcription by opening up the chromatin structure through weakened histone – DNA interactions (Garcia-Ramirez et al., 1995).

Methylation

Unlike acetylation, the modification of histone tails by methylation is associated with activated and repressed chromatin states. Protein arginine methyltransferases can either monomethylate arginine residues or produce symmetrical or asymmetrical dimethylation marks (Agger et al., 2008). The ε-amino group of lysine residues are similarly modified by lysine methyltransferases (KMTs) with mono-, di-, and trimethyl

groups (Zhang and Reinberg, 2001). Methylation of histone H3 lysine residues 4 ($H3K4me_3$) and 36 ($H3K36me_3$) are associated with active transcription conditions. Examples of heterochromatin methylation marks include those of H3K27 and H3K9 (Peters et al., 2003). The chromodomain of the heterochromatin protein 1 (HP1) is able to recognize and bind methylated H3K9 and promote heterochromatinization (Lachner et al., 2001). Interestingly, the subtle differences between mono-, di-, and trimethylation marks of the same histone residue can affect its localization within different chromosome locations (*i.e.* facultative heterochromatin, pericentric heterochromatin, euchromatin) (Peters et al., 2003).

It was initially thought that methylation was an irreversible PTM. However, in 2004, a lysine specific demethylase (LSD1) was discovered that demethylates H3K4 through an oxidative reaction. As such, LSD1 also functions as a transcriptional corepressor (Shi et al., 2004; Wysocka et al., 2005). Subsequently, the Jumonji family of histone demethylases, which demethylate trimethylated residues, has been described. The Jumonji protein family is not only able to demethylate specific H3 lysines, but methylated arginine, too (Agger et al., 2008).

Ubiquitination

Ubiquitination involves the covalent bonding of ubiquitin monomers to histones as either a single addition or as a polyubiquitin chain through a series of enzymatic reactions. An isopeptide bond is formed between the 76 amino acid ubiquitin molecule and a lysine residue of either the histone or the preceding ubiquitin moiety (Pickart and Fushman, 2004). Depending on the type of linkage between successive ubiquitin moieties, polyubiquitin chains can direct the modified protein for signalling, trafficking,

degradation, or other purposes (Shukla et al., 2009). This will be discussed in more detail in Chapter 5.

The C-terminal tail of histone H2A is subject to the addition of single and polyubiquitin chains. As the C-terminal tail of H2A protrudes near the entry and exit site of the DNA within the nucleosome, it is thought that this bulky modification may alter the local chromatin structure (Jason et al., 2002). Monomeric ubiquitination of the C-terminal tail of H2B has been associated with transcriptional stimulation, elongation, and nucleosome remodelling (Shukla et al., 2009). Ubiquitination of H2B is a reversible process. The tails of H1 and H3 can also be ubiquitinated (Chen et al., 1998; Pham and Sauer, 2000).

Sumoylation

The small ubiquitin-like modifier (SUMO) is another bulky modification, approximately 10 kDa in mass, which is covalently linked to histones. In vertebrates, there are three different paralogues. Like ubiquitination, SUMOylation targets lysine residues (Kouzarides, 2007), but within a unique consensus sequence: ΨKxE (Ψ = large hydrophobic residue and x = any amino acid) (Hay, 2007). Sumoylation of histones has been identified for all four core histones and specific sites of modification have been identified for all but H3 (Nathan et al., 2006). In yeast, sumoylation of histones is associated with transcriptional repression (Nathan et al., 2006).

ADP-ribosylation

ADP-ribosylation can occur in either mono- or poly- modified forms and distinct enzymes are responsible for these PTMs. These include mono-ADP-ribosyltransferases (MARTs) and poly(ADP-ribose) polymerases (PARPs) (Kouzarides, 2007). ADP ribosyl

monomers are covalently attached to glutamic residues in a transfer from β-NAD+ substrates (Ausió et al., 2001). While the functional significance of this histone PTM is not well understood, one modified site in H2B (gluatamic acid 2) has been determined (Ogata et al., 1980). It has also been suggested that the histone variant macroH2A may be poly-ADP ribosylated (Abbott et al., 2005).

DNA Methylation

The methylation of cytosines to create the 5-methyl-deoxycytidine (5-meC) is often referred to as the fifth nucleotide. This post-replicative DNA modification occurs through the enzymatic activities of DNA methyltransferases (DNMTs) that transfer a methyl group from S-adenosyl methionine to cytosines (Roberts and Cheng, 1998; Zhu, 2009). In mammals, DNA methylation occurs exclusively within 5'-CpG regions, whereas in plants, methylation can occur within CpNpG and CpHpH sequences (N = any base, H = C, A, T) (Fischle, 2008). In mammals, 2% - 8% of cytosines are methylated and in plants, approximately 50% are methylated. CpG islands (CGIs), which contain a high concentration of this dinucleotide, are typically unmethylated. However, a small portion of CGIs are differentially methylated (Illingworth and Bird, 2009). CGIs are often associated with gene promoter regions, although not exclusively (Bird et al., 1985; Bogdanovic and Veenstra, 2009; Illingworth and Bird, 2009).

Methylated DNA regions are typically associated with transcriptional repression, whether it is present in heterochromatin or euchromatin regions. DNA methylation occurs in exons and intergenic regions, and has pivotal roles in X chromosome inactivation, imprinting of parental genes, tissue-specific gene regulation and other

functions (Zhu, 2009). Existing methylation marks are replicated by semiconservative DNMTs such as DNMT1; thereby mediating their epigenetic continuance. It is becoming increasingly clear that cross-talk or an interdependence between DNA methylation and histone PTMs is required to maintain the fidelity of transmission of these marks (Fischle, 2008).

DNA methylation is not an irreversible modification as once thought. DNA demethylase activities have been demonstrated in eukaryotes including plants and vertebrates (Metivier et al., 2008; Rai et al., 2008; Zhu, 2009). Demethylation can occur through deamination followed by base-excision mechanisms that involve the removal of the methylated cytosine by DNA glycosylases and other *trans*-acting factors. The mechanism of the subsequent replacement with an unmodified cytosine is yet unknown (Zhu, 2009).

Methyl-CpG Binding Domain Proteins

Methylated DNA can be recognized and bound by different families of proteins: the methyl-CpG binding domain (MBD) family of proteins, Kaiso proteins, and the SET and ring finger-associated (SRA) domain family (Clouaire and Stancheva, 2008). The MBD protein family consists of five members: MBD1, MBD2, MBD3, MBD4 and methyl-CpG binding protein 2 (MeCP2). Each protein possesses a distinct functional and structural variability (Clouaire and Stancheva, 2008; Hendrich and Bird, 1998; Hendrich and Tweedie, 2003). During the 1990's, Adrian Bird's group in Edinburgh discovered this then-unique family of proteins based on their ability to bind methylated DNA (Hendrich and Bird, 1998; Lewis et al., 1992). Each MBD member has been implicated

in transcriptional repression, due in part to the recruitment of interacting partners involved in silencing (*i.e.*, HDACs, Sin3a) (Bogdanovic and Veenstra, 2009). However, unlike the other MBD proteins, MBD3 is unable to bind methylated CpG regions due to the presence of two different amino acids in its MBD (Hendrich and Bird, 1998). As such, it requires MBD2 to facilitate its association with methylated CpG sequences (Sansom et al., 2007). MBD4 has a unique enzymatic ability not found in the other MBD proteins; it possesses a thymine DNA glycosylase activity and is involved in DNA repair (Hendrich et al., 1999; Sansom et al., 2007). MeCP2 is perhaps one of the better studied members (Meehan et al., 1992), due in large part to mutations in this protein being the primary cause of Rett syndrome (RTT) (Amir et al., 1999; Lewis et al., 1992). A comparison of the major structural features of the MBD family of proteins is shown in Figure 2.

MeCP2: The Early Years

Early *in vitro* work demonstrated that MeCP2 is able to bind to reconstituted chromatin templates through its MBD and compete with H1 binding (Nan et al., 1997; Nan et al., 1993). MeCP2 binds to the DNA linker region and does so preferentially within 10 base pairs of the DNA entry and exit site of the nucleosome (Ishibashi et al., 2008; Nikitina et al., 2007a). The preference for binding to a longer linker DNA was shown *in vivo* through the sedimentation of native mononucleosomes to which MeCP2 was bound (Ishibashi et al., 2008). While MeCP2 can bind to unmethylated DNA, it preferentially binds to (reconstituted) methylated DNA templates in the presence of competitor DNA (Ishibashi et al., 2008; Meehan et al., 1992). MeCP2 binds to its

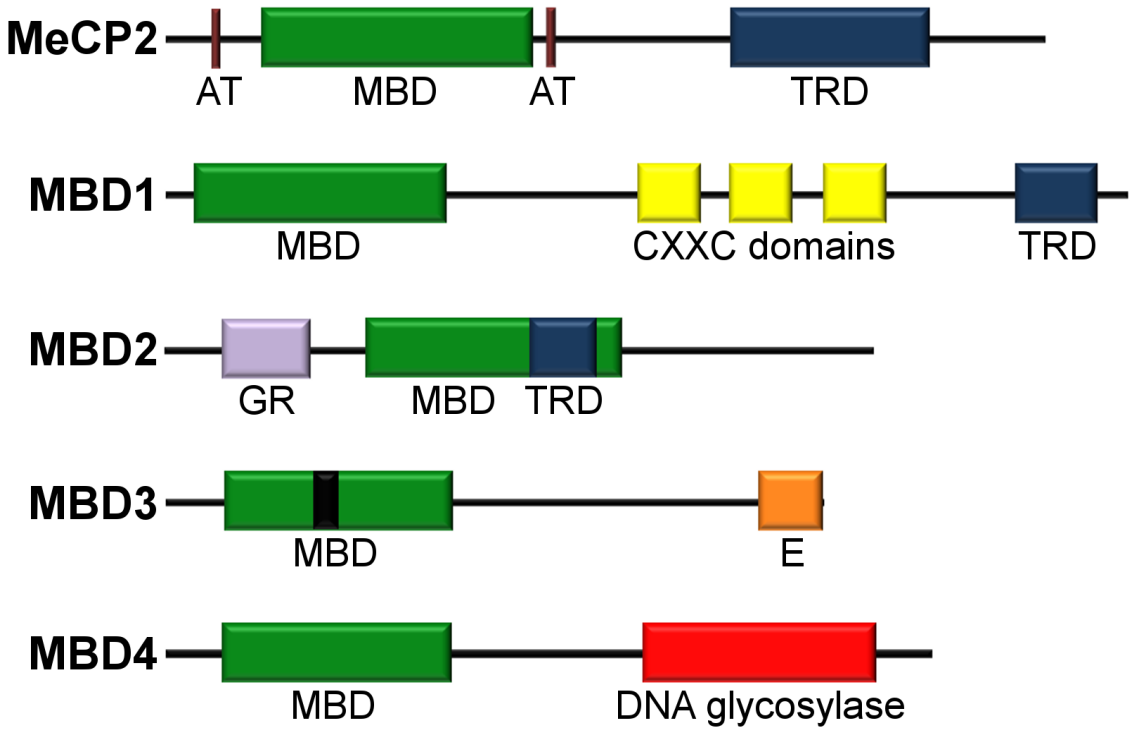

Figure 2. ***Schematic representation of the major functional domains within the different MBD proteins (MeCP2, MBD1, MBD2, MBD3, and MBD4).*** **All members contain a methyl binding domain (MBD), although the MBD of MBD3 is unable to bind methylated DNA due to amino acid sequence differences. MeCP2, MBD1, and MBD2 each contain a transcription repressor domain (TRD). MeCP2 contains two AT – hook motifs which flank the MBD. MBD1 contains three cysteine-rich zinc finger domains (CXXC). Towards the N-terminal portion of MBD2, a glycine – arginine (GR) repeat region is located. MBD3 contains a glutamate-rich region near its C-terminal end (E). MBD4 has a DNA glycosylase domain that is involved in the removal of CG:TG mismatches. This figure was adapted from (Clouaire and Stancheva, 2008; Sansom et al., 2007).**

methylated target with a variable affinity and can exchange with chromatin in a similar manner to linker histone H1 (Klose et al., 2005; Meehan et al., 1992; Nan et al., 1993).

Because the two proteins compete for the same region of the nucleosome, it is not surprising that MeCP2 can displace H1 (Nan et al., 1997).

Co-immunoprecipitation studies showed that MeCP2 interacts with HDACs and Sin3a through its transcriptional repressor domain, and this helped establish its role as a transcriptional repressor through its ability to recruit *trans*-acting factors (Jones et al., 1998; Nan et al., 1998; Suzuki et al., 2003). Additionally, MeCP2 has been shown to interact with HP1 (Agarwal et al., 2007). In the absence of salt, MeCP2 can condense chromatin fibres *in vitro* and does so independently of other factors (Georgel et al., 2003). Interactions of MeCP2 with other chromatin proteins such as HMTs and DNMTs also support the notion that MeCP2 activities are associated with the repression of gene activity (Fuks et al., 2003b). Further to this, confocal microscopy of MeCP2 showed that it associates with (pericentromeric) heterochromatin regions in a variety of mouse tissues including, the cortex and cerebellum, cells undergoing myogenic differentiation, and fibroblasts (Agarwal et al., 2007; Brero et al., 2005; Collins et al., 2004; Kumar et al., 2008; Marchi et al., 2007). Similar investigations using MCF-7 cells, a human breast cancer cell line, showed that MeCP2 has a granular distribution throughout the nucleus (Koch and Stratling, 2004). These cytological variations may reflect differences in the cell type and not the species type as the murine and human MeCP2 share a high sequence similarity (Thambirajah et al., 2009a). MeCP2 also interacts with the Brahma subunit of the SWI/SNF complex, although this interaction can vary depending on the cell type investigated (Harikrishnan et al., 2005; Hu et al., 2006).

A new perspective on MeCP2 behaviour began to emerge at the end of 2007 and the beginning of 2008 when two groups independently demonstrated that the majority of

MeCP2-bound promoters were actively expressed (Chahrour et al., 2008; Yasui et al., 2007). In addition to this, a small percentage of promoters associated with MeCP2 were transcriptionally silent (Yasui et al., 2007). Indeed, fractionation of HeLa S3 chromatin showed that the majority of MeCP2 is present in the more nuclease-accessible, active regions of chromatin (Ishibashi et al., 2008). Furthermore, a smaller portion of MeCP2 was associated with heterochromatin (Ishibashi et al., 2008). Although these recent findings may seem contradictory compared to earlier findings, the association of MeCP2 with active promoters and its purported role in gene repression are not necessarily mutually exclusive. It may be that MeCP2 represses gene expression in a temporally-dependent, cyclical manner. Under repressive conditions, MeCP2 is bound to its target gene promoter, but upon induction of gene activation, MeCP2 is released. This scenario appears to be the case at the promoters of inducible genes (Metivier et al., 2008). What is clear, however, is that MeCP2 does play a role in the dynamic regulation of specific gene activity. Possible support of this proposed idea is illustrated in the following paragraph.

Perhaps one of the best examples of MeCP2 target genes is that of the *brain-derived neurotrophic factor* (*BDNF*). MeCP2 binds to the third promoter of *BDNF*, which has eight promoters, and upon (calcium influx or) KCl-triggered membrane depolarization, MeCP2 becomes phosphorylated via a CaMK II-dependent pathway (Chen et al., 2003; Martinowich et al., 2003). MeCP2 is subsequently released from the promoter and transcription ensues. Certainly, given the abundance of information on BDNF and its importance in neuronal development and maintenance, this is not a target that one would expect MeCP2 to permanently silence. Gene repression would need to be

relieved in response to specific stimuli and at particular times. But does MeCP2 always regulate in this manner?

MeCP2 binding requirements and dynamics

Any discourse on how MeCP2 may differentially regulate genes, particularly those located in distinct chromatin regions (euchromatin or heterochromatin) should be prefaced by a discussion of what is known of the MeCP2 – chromatin binding constraints. As mentioned, MeCP2 binds symmetrically methylated 5'-CpG regions that are proximal to at least four adenine or thymine nucleotides in the adjacent 11 nucleotides (Klose et al., 2005). However, the necessity for methylated DNA is not an absolute requirement. MeCP2 can bind to unmethylated DNA four-way junctions or cruciform-type structures, which approximates well the observations that MeCP2 binds to the linker DNA close to the nucleosome dyad axis of symmetry (Galvao and Thomas, 2005).

A solution structure of the MeCP2 MBD determined using NMR spectroscopy showed that it forms an asymmetric wedge-shaped structure composed of an anti-parallel β-sheet with four strands on one side while the other half was more helical in nature (Wakefield et al., 1999). Based on the structure, it was suggested that the symmetry of the binding target was not key in recognition. Furthermore, a conserved hydrophobic pocket within the β-sheet was postulated to be in close proximity to the methyl groups of the cytosines (Wakefield et al., 1999). Similarly, the structure of the methyl binding domain for chicken MeCP2 has been determined (Heitmann et al., 2003). However, a recent publication suggested that recognition of the MeCP2 MBD for methylated DNA involves the hydrated DNA major groove and not the methylated cytosines themselves

(Ho et al., 2008). Using methylated DNA-MBD co-crystals and X-ray analysis, the hydrophilic MBD region, in the presence of water molecules, associates with the methyl groups (Ho et al., 2008). As of yet, the crystal structure of the full-length MeCP2 has not been determined. This is perhaps due in part to MeCP2 exhibiting a high degree of intrinsic disorder (Adams et al., 2007). Despite this lack of more detailed information, it is of interest to understand what other factors influence and modulate MeCP2 binding to its target sequences.

Places to go, genes to regulate: the ubiquitous MeCP2

Early studies showed that phosphorylation of MeCP2 releases it from its target sequence, resulting in gene transcription. Phosphorylation of MeCP2 at S421 in response to neuron depolarization is needed for activation (Zhou et al., 2006) (Figure 3). The ability to phosphorylate this residue is important for dendrite branching and neuron maturation and appears to occur exclusively in the brain. Other phosphorylated residues have also been observed, S80 and S229 and more recently, the list has expanded to include T148/S149, S164, and S424 (Tao et al., 2009; Zhou et al., 2006). Like S421, the functional relevance of phosphorylation at S80 has been characterized. In contrast to S421, S80 becomes dephosphorylated following depolarization and this is correlated with a response in neuronal activity. S80 dephosphorylation also attenuates the association of MeCP2 with chromatin (Tao et al., 2009) (Figure 3).

These two polar phosphorylation events do not appear to directly affect each other and are likely the result of two separate signalling cascades or regulatory events. The inhibition of CaMK II and CaMK IV activities ablated S421 phosphorylation, but S80

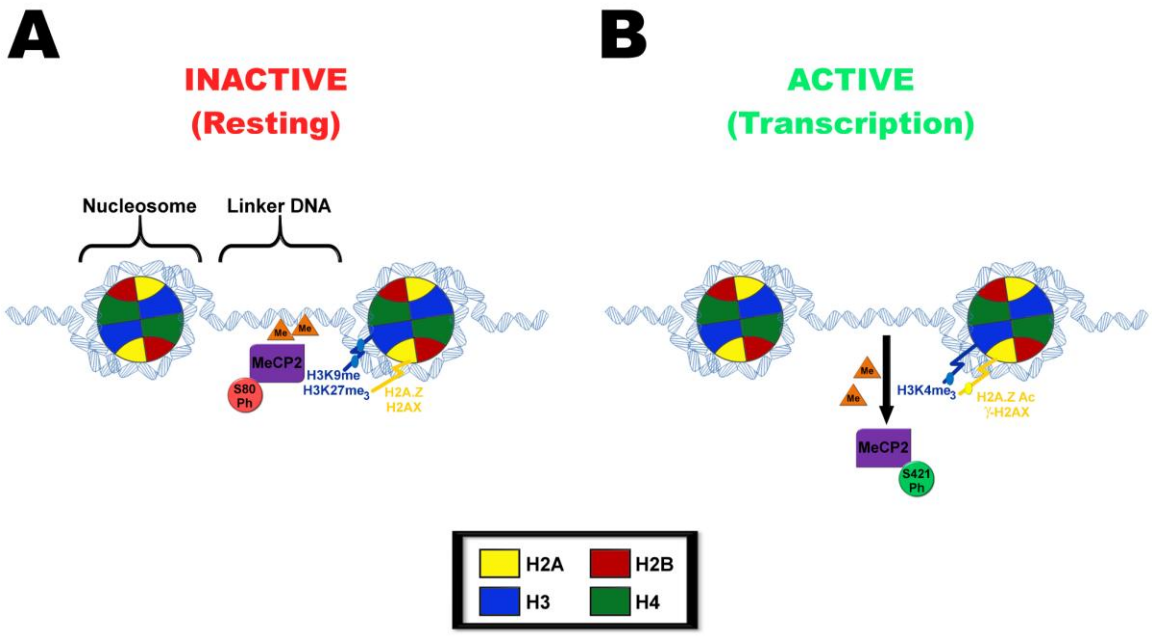

Figure 3. ***Potential nucleosome components that could influence MeCP2 association and regulatory behaviour.*** **A. A transcriptionally inert state involving MeCP2 requires binding of the protein to its methylated target sequence and also the phosphorylation of MeCP2 at S80 (Tao et al., 2009). As MeCP2 has been shown to interact with the KMT responsible for H3K9 methylation (Fuks et al., 2003b) and as the H3 N-terminal tail binds to the linker DNA (Leuba et al., 1998), it is possible that this mark may be in close association with MeCP2. Similarly, other PTMs marking inactive states, such as H3K27me$_3$ for facultative heterochromatin, may also modify nucleosomes proximal to the MeCP2 binding site. The H3 tail regions are denoted in dark blue with the potential PTM sites marked by light blue ovals. It is additionally possible that nucleosomes close to the binding site of MeCP2 may contain histone variants such as H2AX or H2A.Z. The latter variant has been shown to be present in the 5' ends of promoters (Raisner et al., 2005). The potential H2A variant C-terminal tail is shown in orange in the figure and a PTM site is indicated by a yellow oval. B. Following the initiation of transcriptional activation, MeCP2 is phosphorylated at S421 and is released from its binding site (Zhou et al., 2006). The loss of MeCP2 may also occur concurrently with the demethylation of the previously modified 5'-CpG (Metivier et al., 2008). The H3K4me$_3$ PTM, which marks active chromatin regions (Benevolenskaya, 2007), may now be incorporated**

into these nucleosomes. Furthermore, as demethylation has been shown to occur through base-excision, it is possible that H2AX, if nearby, may become phosphorylated. Also, although not necessarily in the same nucleosome, H2A.Z may become acetylated and this would then be associated with the active state of the promoter region.

dephosphorylation was not affected (Tao et al., 2009). The kinase responsible for S80 phosphorylation has not been ascertained, nor has the phosphatase responsible for its dephosphorylation. The analysis of S80A mutants of MeCP2 revealed the presence of locomotor deficits in affected mice and the reduced association of MeCP2 with several euchromatin gene promoters in resting neurons. The S80A MeCP2 mutants did not alter the association of MeCP2 with heterochromatin (Tao et al., 2009).

It is evident that how MeCP2 is post-translationally modified can not only strongly influence MeCP2 regulatory behaviour in specific chromatin locales, but also in response to various stimuli impinging on different signalling pathway cascades. It is possible that S80 phosphorylation may allow MeCP2 to bind chromatin in resting-state neurons or cells, while S421 phosphorylation facilitates MeCP2 discharge following depolarization and transcriptional induction (Figure 3). When considering the array of other phosphorylation sites identified, it is possible that a plethora of other PTM combinations may exist, which would further diversify the portfolio of MeCP2 epigenetic effects. These effects may not be limited to MeCP2 – based interactions with chromatin, but may extend into other functions, including the involvement of MeCP2 in mRNA splicing (Buschdorf and Stratling, 2004; Young et al., 2005).

Post-translational modification of MeCP2 is not the only means through which specific MeCP2 behaviour may be modulated in relation to chromatin. The development of the histone code hypothesis (Jenuwein and Allis, 2001; Jiang et al., 2008; Tsanev and Sendov, 1971) and the emergence of inter-related epigenetic effects (Fischle, 2008) underscore yet another level of complexity in understanding how MeCP2 elicits its own outcomes. A lot of focus has been paid to the methylation status of DNA that MeCP2 recognizes, but little attention has been paid to the local nucleosome composition. Using a mouse model with a genetically disrupted MeCP2 locus, no global changes in H3 or H4 acetylation and methylation were observed (Urdinguio et al., 2007). Specific modifications investigated included $H3K9me_3$, $H4K20me_3$, and $H3K79me_2$ for which no differences were observed for any PTM between wild-type and MeCP2-null mice. Despite this, the local distribution of these PTMs at pertinent gene promoters remains uncharacterized.

It is well appreciated that the presence of PTMs on histone tails or the incorporation of histone variants can modulate local chromatin structure through either direct structural changes (Ausió, 2006) or the recruitment of remodelling machinery and other chromatin-interacting partners (Wu et al., 2009). Is there a nucleosomal signature, based on variable histone composition, that MeCP2 recognizes and how do PTMs of MeCP2 influence this identification? Through the synergistic combination of variable DNA methylation, histone PTM or variant incorporation, and MeCP2 PTMs, a broad range of possibilities exist to fine-tune MeCP2 response to specific stimuli or transcriptional needs in either particular chromatin locations or cell types. This regulation may become even more complex in consideration of the two splice variant

isoforms of MeCP2, MeCP2e1 and MeCPe2, which are differentially expressed in the brain compared to other tissues (Kriaucionis and Bird, 2004; Mnatzakanian et al., 2004).

There has been a strong neural focus to MeCP2 research, particularly in the functional studies of MeCP2 that have been carried out. However, MeCP2 is a ubiquitously expressed protein and is expressed in many, if not most, tissues of the body (Shahbazian et al., 2002; Zhou et al., 2006), Thambirajah, unpublished results). If MeCP2 were to regulate the same set of genes, regardless of tissue origin, the question of how MeCP2 differentially regulates or silences these genes in different tissues arises. In non-brain tissues, does MeCP2 terminally silence brain-specific genes that it would otherwise transiently repress in the brain? Are there different nucleosomal cues – histone or MeCP2 PTMs – to signal or facilitate such transcriptional outcomes? However, it is likely that seemingly brain-specific genes are not exclusively expressed in the brain; rather, they may be expressed in other tissues for alternative functions. This has been shown for certain transcripts and protein forms of *BDNF* and other neurotrophins (Lomen-Hoerth and Shooter, 1995; Prakash et al., 2009), but such expression patterns may not apply to all potential tissue-specific genes regulated by MeCP2. It is also conceivable that MeCP2 may not regulate or even associate with the same gene(s) in different tissues as it does in the brain. Regardless of how and what target genes MeCP2 binds to in a given tissue, the PTMs of MeCP2 and the local nucleosome environment may be fundamental in defining the regulatory role of MeCP2.

MeCP2 and its nucleosomal signature

No studies yet have addressed what parameters of nucleosome composition are critical for MeCP2 binding other than DNA methylation. Some studies have investigated the effects of disease [Rett syndrome (RTT)]–relevant mutations of MeCP2 on histone PTMs, but no clear trends were outstanding. Comparison of different brain regions (midbrain, cortex, and cerebellum) of MeCP2– knockout and wild-type mice did not reveal in any significant differences in either histone H3 or H4 acetylation or methylation (Urdinguio et al., 2007). However, contrasting results were observed from samples or cell lines derived from RTT patients. One study found an increase in H4K16 acetylation with no changes in H3 acetylation, while another study found no changes in global acetylation of histone H3 or H4 (Balmer et al., 2002; Wan et al., 2001). Adding to the complexity of these findings is another study that detected no changes in H4 PTMs, but differences in H3 methylation and acetylation (Kaufmann et al., 2005). Whether these changes are directly dependent on a MeCP2 deficiency, or even the type of MeCP2 mutation, is of particular interest, but MeCP2 dysfunction may not necessarily be the cause. Perhaps the more relevant question is: What are the histone PTMs that influence MeCP2 interaction?

What is (are) the nucleosomal signature(s) that MeCP2 recognizes? Is MeCP2 able to mediate post-translational changes to its environment? MeCP2 has been shown to interact with the KMT responsible for mediating methylation of H3K9. By doing so, H3K9 becomes methylated within the immediate chromatin region (Fuks et al., 2003b). But, are there other modified or variant histones that MeCP2 recognizes? Although no others have been thoroughly explored at present, there are some strong candidates. In

consideration of recent findings that MeCP2 is predominantly associated with active genes, it may be prudent to consider what chromatin conditions prime particular gene regions for activation. Bivalent modification of histone tails have been observed to predispose the proximal gene for either activation or silencing, depending on the transcriptional cue(s) received. H3K27 trimethylation ($H3K27me_3$, silencing) and H3K4 trimethylation ($H3K4me_3$, activation) is one such example (Delcuve et al., 2009; Gan et al., 2007; Soshnikova and Duboule, 2008). If the gene becomes poised for activation, the $H3K4me_3$ mark is perpetuated while the $H3K27me_3$ PTM is lost; the opposite occurs for the converse scenario (Figure 3). As research progresses into the study of histone PTMs, it is apparent that there is an interplay and cross-talk between histone PTMs and DNA methylation (Fischle, 2008). It is quite likely that the nature of the chromatin environment MeCP2 interacts with will be more complex than what this discussion anticipates.

The other consideration is the histone variant partners that MeCP2 may have. A recent study demonstrated the cycling of MeCP2 and MBD2 deposition at activated promoters that was also accompanied by the demethylation of these promoter regions. Of interest was that this demethylation occurred through base excision of the modified nucleotides (Metivier et al., 2008). With well-documented roles in double-strand break repair and oxidative stress damage responses (Crowe et al., 2006; Vasko et al., 2005), is it possible that H2AX, and particularly, phosphorylated H2AX may be localized within these regions (Thambirajah et al., 2009b)? Moreover, is there a close association between MeCP2 and H2AX? Another histone variant candidate could be H2A.Z. Although there is a multitude of putative roles ascribed to this histone variant, H2A.Z is

incorporated into nucleosomes at the boundaries between euchromatin and heterochromatin and also at the promoters of active genes (Meneghini et al., 2003; Raisner et al., 2005). H2A.Z is often found to be acetylated near actively transcribed genes (Bruce et al., 2005). Is it possible that such nucleosomes may be the sites of MeCP2 interactions or may be localized proximal to these binding sequences (Figure 3)?

It is likely that the differential association of MeCP2 with nucleosomes containing a combination of different PTMs and histone variants may specialize the transcriptional role that MeCP2 takes on. This may pertain to its partitioning within different chromatin fractions (*i.e.*, euchromatin or heterochromatin), which would strongly correlate to whether or not its bound genes are transiently active or terminally repressed (Henikoff et al., 2009). Furthermore, this differentiation would have critical implications for the temporal- and tissue-dependent regulation of gene activity. Thus, it is conceivable that by simply changing the PTM status of MeCP2 and the nucleosome composition, genes that are active in one tissue could be silenced in another. SUMOylation of MeCP2 has been demonstrated (Miyake and Nagai, 2007) and a recent publication has proposed a hypothesis regarding the regulation of MeCP2 turnover through PTM (Chapter 5, (Thambirajah et al., 2009a). There are other yet-to-be-determined PTMs of MeCP2 that could further diversify the nuanced regulatory roles MeCP2 undertakes.

Implications for Rett Syndrome

As alluded to earlier, a broad range of mutations in MeCP2 result in approximately 90% of all diagnosed incidences of RTT. These mutations, 300 of which have been documented, include missense, nonsense and truncations that affect the entire

X-linked *MECP2* gene (Chahrour and Zoghbi, 2007; Christodoulou et al., 2003) (Amir et al., 1999; Ausió et al., 2003; Shahbazian and Zoghbi, 2001). A smaller cohort of RTT cases is caused by mutations in the cyclin dependent kinase-like 5 (CDKL5) gene, which is a putative kinase for MeCP2 (Bertani et al., 2006; Mari et al., 2005; Tao et al., 2004; Weaving et al., 2004).

Perhaps one of the best studied diseases of the broad spectrum of autism disorders, RTT predominantly afflicts young girls (Hagberg et al., 1983; Rett, 1966). RTT is considered a neurodevelopmental disorder, based in part on the clinical pathology. RTT manifests after 6-18 months of age following an ostensibly normal post-natal development. Most RTT patients begin to lose learned speech or locomotive functions and then regress, eventually developing any of a wide, diversified range of cognitive and physical disabilities. First described in 1966 by the Austrian physician Andreas Rett, RTT is now considered one of the most prevalent neurodevelopmental disorders (Hagberg et al., 1983; Rett, 1966).

When considering the delayed onset of the disease, it is apparent that the developmentally-regulated timing of MeCP2 expression and/or activity in neurons (notwithstanding other cell types) is of critical importance to healthy infant post-natal development. The absence of functional MeCP2 during development results in abnormal and decreased neuronal branching. In contrast, the opposite phenotype of superfluous axonal and dendritic branching is a consequence of MeCP2 overexpression (Armstrong et al., 1998; Jugloff et al., 2005). Both scenarios culminate in the inability to form proper, mature synaptic connections, which is a hallmark of RTT. Therefore, understanding

what cues govern MeCP2 activity and regulation are of critical importance, particularly during neuronal development.

As well-studied as the effects of MeCP2 mutations, overexpression and knock-outs in neurons have been, there has been little attention paid to other cell types. However, a recent paper showed that glial cells harboured mutated MeCP2 forms as well (Ballas et al., 2009). Moreover, mutant MeCP2 astrocytes affected the dendritic morphology of both wild-type and mutated *MeCP2* neurons grown under *in vitro* conditions. It was suggested that this conferred damage to otherwise healthy neurons was the result of aberrantly secreted factors (Ballas et al., 2009). This recent finding underscores an important point that it is not only neurons that are affected by abnormalities arising from MeCP2, but other cell types and potentially different tissues as well. Should the latter prove to be true, it may prompt a reconsideration of how RTT etiology is perceived. For instance, the constellation of symptoms experienced by girls with RTT, including respiratory and gastrointestinal difficulties, may not be just a corollary of brain dysfunction (Isaacs et al., 2003). Rather, such symptoms may arise from a localized dysregulation within the affected tissues due to MeCP2 mutations. Of course, it is also possible that these irregularities may ensue from improper autonomous function. Regardless of what the primary cause is of these other symptoms, it is possible that, if combined, both factors could exacerbate the symptom severity.

Concluding thoughts on MeCP2

Because of active research efforts into MeCP2 and RTT, much has been elucidated about how this protein operates at the molecular level, and of its downstream

effects on a larger, physiological scale. However, as more information emerges about MeCP2 involvement in chromatin-based phenomena and cellular development, it is apparent that this protein does not behave as was anticipated. At the molecular level, the interplay between the PTMs of MeCP2, the status of DNA methylation, and the nucleosome composition may all strongly influence the transcriptional states of particular genes, depending on the cues received and the tissue in question. To better understand the context of MeCP2 function, it will be imperative to fathom the interplay between these superimposed layers, and not only to consider them in isolation.

Dissertation Outline

The intent of this dissertation is to discuss work done to characterize the conformation of native chromatin structures containing the histone variant H2A.Z or MeCP2. In the following chapter, the structural effects imparted by H2A.Z to the hierarchical organization of chromatin structures will be described. Early structural studies of recombinantly expressed H2A.Z reconstituted into chromatin fibres produced contradictory results. It is hypothesized that the absence of essential PTMs or folding may be responsible for the opposing findings. To test this hypothesis, the stability of various chromatin structures (dimers, octamers, nucleosomes, fibres) containing native H2A.Z were characterized. A more detailed background relevant to the experimental work will be provided in this chapter as well.

The third to fifth chapters are devoted to studies characterizing the nature of MeCP2 interactions with native chromatin. Chapter 3 describes work done to determine whether MeCP2 behaves as a global or specific chromatin repressor *in situ*. Shortly after

MeCP2 was discovered, it was proposed to act as a global repressor of transcription. However, since then, evidence has been produced that suggested MeCP2 does not globally regulate gene expression. It is hypothesized that if MeCP2 behaves as a universal regulator, then changes to chromatin modifications could affect its distribution within chromatin. DNA hypermethylation and histone hyperacetylation were chemically induced and the effects on MeCP2 distribution within fractionated chromatin were investigated.

Having studied the nature of MeCP2 interactions with chromatin in cultured cells, it was of interest to determine how MeCP2 distributed within chromatin derived from different tissues. It is hypothesized that if MeCP2 undertook different regulatory roles in different tissues, this may be reflected in a distinct distribution of MeCP2 within fractionated chromatin. MeCP2 has a broad, tissue-specific distribution within fractionated chromatin. It is also hypothesized that the presence of histone variants or PTMs in the bound nucleosomes may facilitate the association of MeCP2 with different chromatin regions. Studies undertaken to determine the distribution of MeCP2 and the nucleosomal interacting partners of MeCP2 are discussed in Chapter 4.

A hypothetical model of MeCP2 regulation through proteasome-mediated turnover is explored in Chapter 5. Two PEST domains were identified within MeCP2 and it is proposed that the poly-ubiquitination of these motifs target MeCP2 for proteolytic degradation. A second hypothesis proposes the use of histone deacetylase inhibitors to control the levels of MeCP2 in conjunction with potential gene therapies for the treatment of Rett syndrome. The final chapter summarizes the major findings of this dissertation.

Chapter 2 – Native Chromatin Structures, Except Dimers, are Stabilized by the Histone Variant H2A.Z

This chapter was adapted in part from the publication:

Thambirajah, A.A., Dryhurst, D., Ishibashi, T., Li, A., Maffey, A.H., Ausió, J. (2006) H2A.Z stabilizes chromatin in a way that is dependent on core histone acetylation. Journal of Biological Chemistry. **281**:20036-44.

D. Wade Abbott performed the Olins chromatin fractionation described in this chapter. A.A.T. then took the fractions prepared, acid extracted them, and normalized the loading for the AUT-PAGE. Other than this exception, A.A.T. performed all of the experimental work described. Thanks to José Maria Eirín-López and Ron Finn for their skillful assistance in the preparation of the figures.

Abstract

One way of introducing variability into chromatin dynamics is through the incorporation of histone variants into chromatin structure. The histone variant H2A.Z has been implicated in transcriptional activation and silencing, but until recently, it was not understood how it accomplishes these contradictory roles. Structural studies in the last decade mirrored the functional dichotomy presented by H2A.Z. The crystal structure of the H2A.Z nucleosome was determined in 2000 and it was suggested that H2A.Z destabilized the nucleosome (Suto et al., 2000). However, subsequent, independent biophysical studies of reconstituted H2A.Z chromatin produced results in support of, and in disagreement with this model. The intent of this chapter was to resolve this discrepancy by characterizing the hierarchical organization of chromatin structures using native chromatin sources. Therefore, any post-translational modification(s) or folding effects lost in a prokaryotic expression system would be accounted for in native H2A.Z. Gel filtration chromatography of H2A.Z-containing octamers showed that it associated with stable forms at physiological pH. Similarly, H2A.Z was stably associated with mononucleosomes that were dissociated in the presence of increasing concentrations of NaCl. The association of H2A.Z within chromatin fibres was assessed by hydroxyapatite chromatography and had a late elution with H3-H4 following H2A-H2B. This indicates either a stronger association with the DNA or with the H3-H4 tetramer. The deposition of H2A.Z in nucleosomes occurred independently of linker histones. In contrast, circular dichroism analysis of the H2A.Z-H2B dimer showed that it was unstable and lacked secondary structure when compared to the canonical H2A-H2B dimer.

Introduction

The heteromorphous histone H2A variant, H2A.Z, was first discovered in 1980 and was estimated to account for approximately 5% of the total H2A content (West and Bonner, 1980). In the past thirty years, H2A.Z has become one of the best studied histone variants and is implicated in a broad range of functions. These functions have often been in diametric opposition and early structural characterizations seemed to follow these functional contradictions.

Initial characterizations of H2A.Z revealed some interesting distinctions between it and its major H2A counterparts. H2A.Z showed a high interspecific sequence conservation (90%) compared to a lower intraspecific homology with the major H2A forms (~65%) (Hatch and Bonner, 1995). This divergence from the canonical forms is also emphasized by the replication-independent expression of H2A.Z that occurs outside of the S phase and from transcripts that contain introns and poly-adenylated 3' tails (Hatch and Bonner, 1990). H2A.Z is essential for viability in several organisms including *Drosophila* (van Daal and Elgin, 1992), *Tetrahymena* (Liu et al., 1996), and mice (Faast et al., 2001) and for proper development in *Saccharomyces cerevisiae* (Jackson and Gorovsky, 2000). The C-terminal tail of H2A.Z in *Drosophila* is crucial for its viability (Clarkson et al., 1999). It should be noted that these studies were done by deleting or disrupting the first described single copy gene of H2A.Z. However, it was recently shown that H2A.Z is actually comprised of two different isoforms, H2A.Z-1 and H2A.Z-2, which are expressed from two different genes (alleles) (Coon et al., 2005). There are only four amino acid substitutions between these two isoforms: A12T, A14T,

T38S, and A128V (Coon et al., 2005). H2A.Z-1, the first characterized form, may play a more dominant or distinct role from that of H2A.Z-2.

H2A.Z is implicated in a myriad of functions. H2A.Z is involved in transcriptional activation (Santisteban et al., 2000) and in silencing at the *S. cerevisiae* HMR locus (Dhillon and Kamakaka, 2000). This duality was mirrored by the presence of H2A.Z in transcribed regions in euchromatin and similarly within non-transcribed heterochromatin regions in *Drosophila* polytene chromosomes (Leach et al., 2000). H2A.Z is known to play important roles during mammalian development and is localized to pericentromeric heterochromatin upon differentiation of the inner cell mass in mice (Rangasamy et al., 2003). H2A.Z is also found to localize with HP1-α in pericentromeric heterochromatin.

In budding yeast (*S. cerevisiae*), Htz1 (the yeast H2A.Z form) is found at the borders of heterochromatin and euchromatin and prevents the spread of ectopic heterochromatin into adjacent euchromatin regions (Meneghini et al., 2003). This maintenance of anti-silenced states in gene regions near telomeres is accomplished synergistically with the associated boundary element (Meneghini et al., 2003). To further contrast the association of H2A.Z with heterochromatin, the presence of H2A.Z at active promoters has been described (Meneghini et al., 2003). Regions within the H2A.Z C-terminal tail have been reported to facilitate the positioning of H2A.Z within promoters that are poised for activation (Larochelle and Gaudreau, 2003). H2A.Z is present at the 5' end of inactive and active promoters in euchromatin (Raisner et al., 2005). However, a hyperacetylated form of H2A.Z predominates at active loci (Bruce et al., 2005). In further support of an active role in gene expression, H2A.Z interacts with components of

the RNA polymerase II machinery (Adam et al., 2001). How H2A.Z accomplishes such diverse functions could be accounted for by the different H2A.Z PTMs (Figure 4), the activity of remodelling complexes responsible for its deposition, and other proteins associated with these regions, such as Sir proteins (Dryhurst et al., 2004; Krogan et al., 2003; Luk et al., 2007; Mizuguchi et al., 2004; Ren and Gorovsky, 2001; Ren and Gorovsky, 2003).

In many respects, early structural studies of H2A.Z-containing chromatin were similarly divisive and consequently inconclusive as to the influence of H2A.Z on chromatin folding stability. The crystal structure of the H2A.Z nucleosome suggested that there would be a destabilization of the nucleosome core particle (NCP) compared to the canonical H2A nucleosome (Suto et al., 2000). A glycine at position 106 in the H2A.Z C-terminal tail was postulated to interfere with the interactions of H3 and the H2A.Z docking domain in the nucleosome (Figure 4) (Suto et al., 2000). As such, there would possibly be a less stable interaction between the H2A.Z-H2B dimer and the $(H3\text{-}H4)_2$ tetramer. Initial studies done of reconstituted NCPs and chromatin fibres containing H2A.Z supported this model; a loss of chromatin stability was imparted by the incorporation of H2A.Z compared to canonical H2A (Abbott et al., 2001). NCPs were partially destabilized, and it was proposed that the H2A.Z-H2B dimer bound less tightly to the nucleosome and that chromatin fibres were also decondensed (Abbott et al., 2001).

Shortly after the publication of these recombinant H2A.Z studies, another group published contradictory findings using similar methods (Fan et al., 2002). Using reconstituted nucleosome arrays and recombinantly expressed H2A.Z, they found that H2A.Z facilitated intranucleosome interactions and that the NCP was more stable. In

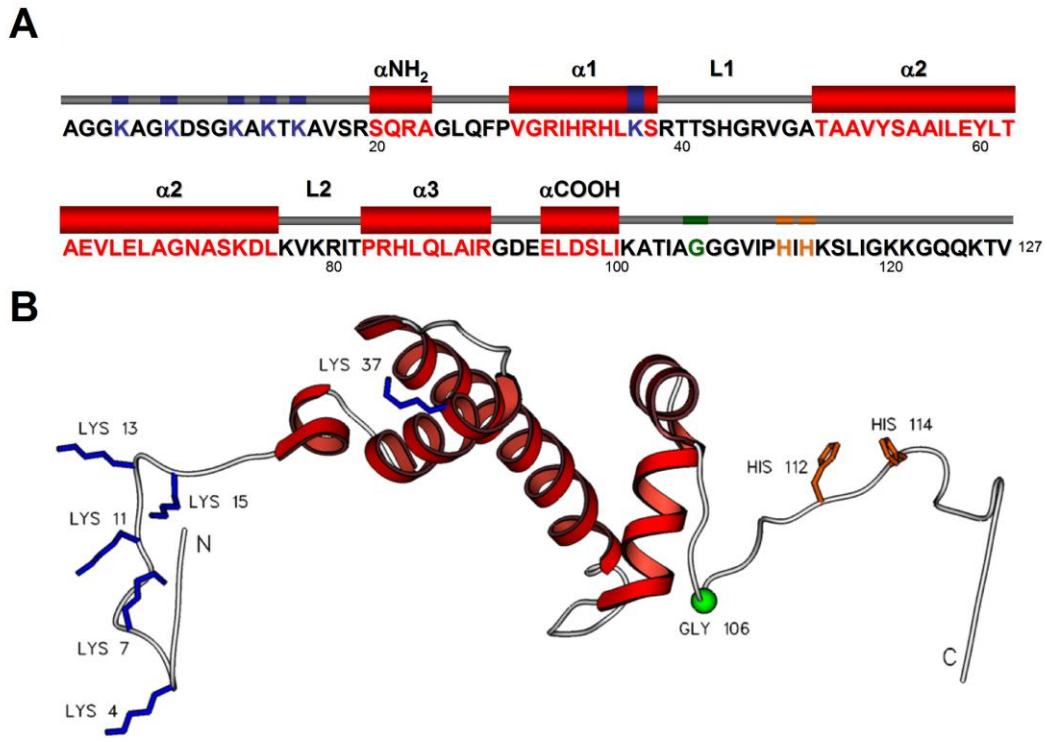

Figure 4. ***Human H2A.Z: highlights of some of its characteristic structural features.*** **A. H2A.Z primary sequence. Based on the similarity to the acetylatable lysine residues of the N-terminal tail of *Tetrahymena thermophila* (4, 7, 10, 13, 16, and 21) (Ren and Gorovsky, 2001), five correlating lysine residues were identified in the human sequence (4, 7, 11, 13, and 15) and are shown in blue. In contrast to *Tetrahymena* H2A.Z, no other lysines are present in human H2A.Z until position 37. In the C-terminal tail, Gly106 (shown in green, it corresponds to Gln104 in H2A) causes a minor destabilization of H3 interactions with the H2A.Z docking domain in the nucleosome (Suto et al., 2000). His112 and His114 (shown in orange) of H2A.Z create a distinct metal ion-binding region. This results in a unique nucleosomal interface for interacting *trans*-acting factors not found on H2A (Suto et al., 2000). The amino acids participating in the formation of α-helices are shown in red. B. The tertiary structure of H2A.Z based on the coordinates generated from the crystallographic data of H2A.Z-containing nucleosomes (Suto et al., 2000). The full structure, including the N- and C- termini, was generated using SETOR (Evans, 1993) from a predicted structure obtained using the Swiss-Model First Approach**

and based on the human H2A.Z sequence. The H2A.Z sequence was obtained from the NCBI Entrez Protein data bank (1F66C). This figure was prepared for the publication (Dryhurst et al., 2004).

contrast, the presence of H2A.Z in these arrays prevented the formation of positive intermolecular interactions, leading to a more decondensed, higher order chromatin structure (Fan et al., 2002). Both studies proposed that their findings supported a model in which H2A.Z-induced structural changes assisted transcriptional activation.

With such polar findings, and as both studies used recombinantly expressed H2A.Z, it was possible that the *in vitro* recapitulations of chromatin structure did not accurately reflect the *in vivo* situation. In order to resolve these contradictory findings, the objective of this study was to determine the structural composition of chromatin containing native H2A.Z. Therefore, any essential folding or PTMs of H2A.Z, that would otherwise be lost in a recombinant system, would be accounted for in native-derived H2A.Z. Through such an approach, it would be possible to determine how chromatin structure is influenced by the inclusion of H2A.Z. To this end, the effects of H2A.Z on the structural organization of the H2A-H2B dimer, histone octamer, NCP, and chromatin fibres were characterized.

Materials and Methods

Chromatin preparation. Chicken blood and liver were used to prepare nuclei for chromatin extraction as described previously (Abbott et al., 2005; Ausió et al., 1989). Chromatin was fractionated from chicken blood and liver nuclei following a five minute

micrococcal nuclease (MNase) digestion according to protocols established by (Abbott et al., 2005; Ausió et al., 1989). Following centrifugation, the S1 supernatant was obtained (10-20% chromatin) and the resulting pellet was resuspended in 0.25 mM EDTA (pH 8.0) and lysed by shearing. Shearing was accomplished by stirring a thin layer of the suspension in an erlynmeyer with a stir bar at 4^{o}C. The suspension was then centrifuged to yield the SE supernatant (containing the majority of the soluble chromatin) and an insoluble pellet (P) (Ausió et al., 1989).

Olins chromatin fractionation. This modified chromatin fractionation procedure was initially described by Olins and Olins (Abbott et al., 2005; Olins et al., 1976) and allowed the separation of different chromatosome and nucleosome forms. Nuclei were prepared as described above, subjected to an extensive MNase digestion (for 12, 24, or 32 minutes), and subsequently centrifuged. A P1 pellet was produced and the resulting S1 supernatant contained more than 30% of the total chromatin. The S1 was dialyzed against 0.1 M KCl in Tris buffer (pH 7.5) to precipitate the H1/H5-containing nucleosome forms. The turbid suspension was centrifuged to produce the S2 supernatant, which primarily contained mononucleosomes composed of ~146 bp of DNA that were depleted of linker histones. The P2 pellet contained chromatosomes having ~168 bp DNA and linker histones. The P2 also had some larger oligonucleosome forms whose contribution became increasingly negligible as the time of MNase digestion increased (Abbott et al., 2005). The P1, P2, and S2 samples were dounced in a final concentration of 0.4 N HCl to acid-extract the histones for further gel electrophoretic analysis.

Preparation of mononucleosomes and histone octamers. Mononucleosomes were prepared from chicken erythrocytes following a timed MNase digestion of SE chromatin (Ausió et al., 1989). The digested chromatin was then separated by sucrose gradient fractionation to purify the NCPs (~146 bp DNA). Histone octamers were generated from either NCPs or SE chromatin stripped of the linker histones that were adsorbed onto a 5.5 cm X 4.4 cm Bio-Gel HTP hydroxyapatite (HAP) DNA-grade resin (Bio-Rad) column in 20 mM potassium phosphate buffer, pH 6.8. Histone octamers were eluted free of contaminating DNA in 2.5 M NaCl, 20 mM potassium phosphate, pH 6.8.

SDS- and AUT-PAGE and agarose gel electrophoresis analyses. SDS-PAGE and AUT (acetic acid – urea – Triton X-100) – PAGE were performed for the analysis of histone protein composition and agarose gel electrophoresis was done for the analysis of DNA (Abbott et al., 2001; Rabbani et al., 1999).

Analysis of the pH-dependent stability of histone octamers containing H2A.Z. Histone octamers prepared from nucleosomes were concentrated to ~2mg/mL and 1 mg was dialyzed against 2 M NaCl (buffered with either Tris-HCl or sodium phosphate) at different pH values (5.5, 6.0, 7.5) at 4^{o}C for 4 – 6 hours (Eickbush and Moudrianakis, 1978). The dissociating octamers were fractionated by gel filtration chromatography at 4^{o}C using a Sephacryl S-300 HR column having the dimensions of 120 cm X 1.5 cm (flow rate 5 mL/min) and using the same freshly prepared buffer as was used for dialysis.

Ionic-strength dependent analysis of mononucleosome stability. The folding stability of NCPs was determined by sucrose gradient sedimentation analysis of mononucleosomes under increasing NaCl concentration (Abbott et al., 2005). Mononucleosomes were loaded onto 5% - 20% sucrose gradients in the presence of 10 mM Tris pH 7.5, 0.1 mM EDTA and 0.1 M, 0.6 M, 0.9 M, 1.2 M, or 1.5 M NaCl. Prior to loading, mononucleosomes were dialyzed against their respective buffered NaCl solution without sucrose. Following centrifugation, 1 mL fractions were collected and the absorbance at 260 nm was measured.

Scanning densitometry analysis of the ionic strength–dependent association of H2A.Z with mononucleosomes. Scanning densitometry was used to quantify the relative distribution and amounts of H2A.Z within dissociated mononucleosomes following NaCl-dependent sucrose gradient fractionation. The ChemiImager 4000 scanner was used with the AlphaEase™ Version 3.3d software (Alpha Innotech Corp.). Density measurements were made in triplicate of H2A.Z, H2A and of the background levels in each lane. The density scale was adjusted so that black was assigned a value of 255 and white, 0. The background readings were subtracted from the values for both H2A.Z and H2A. Corrected H2A.Z values were divided by H2A to create the normalized amount in each lane. GraphPad Prism (GraphPad Software, Inc.) was used to plot the normalized H2A.Z/H2A values with error bars indicating the standard mean ± S.E.

Hydroxyapatite chromatography of chromatin fibres. Chromatin was adsorbed onto HAP resin (15 cm x 1.5 cm) as described above and the histones were eluted under an

increasing NaCl gradient in 20 mM potassium phosphate pH 6.8 buffer (Abbott et al., 2004). Chromatin fractions characterized included chicken liver SE and chicken erythrocyte S1, SE and linker-histone stripped SE.

High performance liquid chromatography (HPLC) purification of native H2A.Z. H2A.Z was purified from chicken erythrocyte histones by several repeated rounds of HPLC which involved the use of both preparative 1 X 25 cm (300 Å and 5 µm) C_4 and analytical 0.46 X 25 cm (300 Å and 5 µm) C_{18} Vydac® columns. Histones were eluted by an increasing acetonitrile gradient (to 100%) in 0.1% trifluoroacetic acid (TFA) in distilled water (Ausió and Moore, 1998).

Reconstitution of H2A.Z-H2B and H2A-H2B dimers. Histones for each respective dimer pair were combined in equivalent amounts and reconstituted using methods previously described (Ausió and Moore, 1998). The reconstituted dimers were then purified using gel filtration chromatography (120 X 1.5 cm Sephacryl S-300 HR column) and eluted with 2 M NaCl, 20 mM Tris-HCl (pH 7.5) at 4^{o}C.

Circular dichroism analysis of histone dimer folding. To determine the melting profiles of the H2A-H2B and H2A.Z-H2B dimers, respectively, spectra were recorded at 222 nm with a spectral bandwidth of 1 nm and a response time of 1 s. The temperature was increased at a rate of 1^{o}C per minute, from 5^{o}C to 80^{o}C. The Jasco J-810 spectropolarimeter used was connected to a circulating water bath and a temperature controller. Spectra of the dimers were recorded in 0.1 mM EDTA, 10 mM HEPES (pH

7.5) and increasing NaCl concentrations (50 mM, 100 mM, 200 mM, 400 mM, and 1000 mM) (Karantza et al., 2001).

Results

The H2A.Z-containing histone octamers are stable at physiological pH and less stable at low pH

The heterotypic histone core octamer is composed of an H3-H4 tetramer, which is flanked on either side by two H2A-H2B dimers. The addition of 146 bp of DNA wrapped about this octamer forms the NCP. Within the histone octamer, the tetramer and dimers weakly interact through hydrogen bonds primarily between histidine-lysine and histidine-tyrosine residues (Eickbush and Moudrianakis, 1978). At physiological ionic conditions in solution, the octamer exists in a multiform equilibrium as a consequence of its tripartite organization. This equilibrium consists of the H2A-H2B dimers, the $(H3\text{-}H4)_2$ tetramers, the $(H3\text{-}H4)_2$–(H2A-H2B) hexamer, and the octamer form. The octamer is stably associated *in vitro* in solution in 2 M NaCl (or higher) and does not require the presence of DNA. Under these conditions, and by adjusting the pH of the solution, it is possible to understand the nature of the interactions which govern octamer association from tetramer and dimer subunits (Eickbush and Moudrianakis, 1978).

A modified approach to that of the Eickbush and Moudrianakis study was taken to determine the association of H2A.Z within the histone octamer equilibrium. Using gel filtration chromatography, the stability of the octamer was determined under decreasing pH conditions (Figure 5). The distribution of the dissociated canonical histone core octamer was very similar to that described previously [Figure 7a of

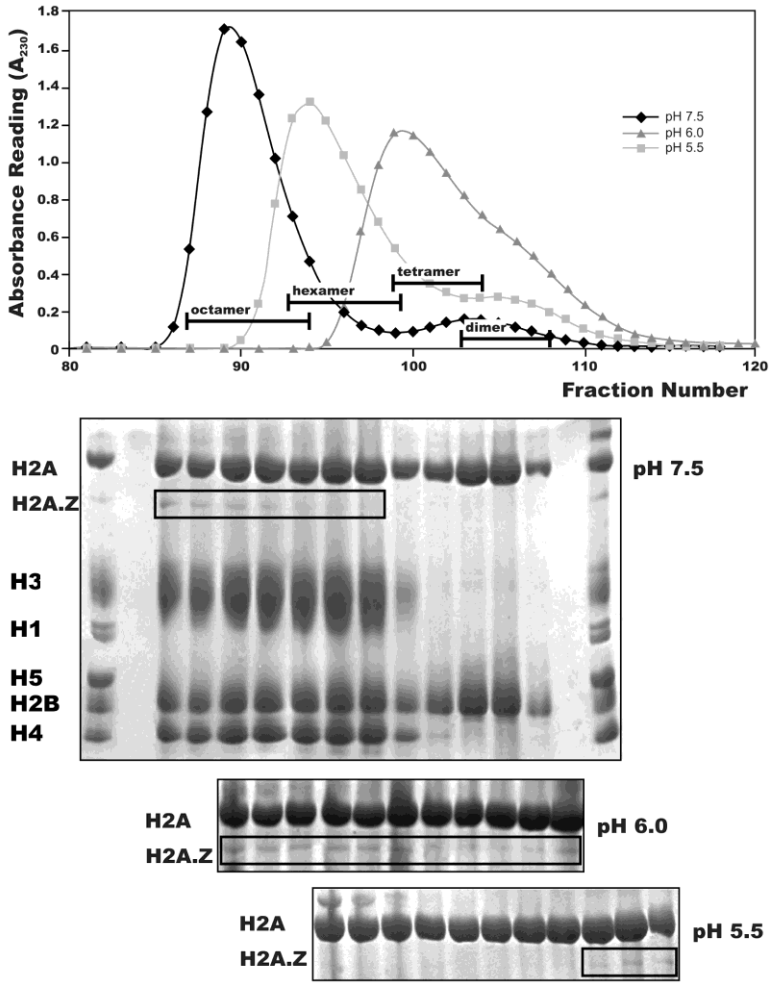

Figure 5. ***The dissociation of histone octamers under decreasing pH as characterized by gel filtration chromatography.*** **Chicken erythrocyte octamers in 2 M NaCl at pH 7.5, 6.0, and 5.5 were fractionated using an equilibrated Sephacryl S-300 HR gel filtration column and eluted with each respective buffer. The elution of histones was assessed by measuring the absorbance at 230 nm (A_{230}) of each fraction as is depicted in the plot. The AUT-PAGE analyses of selected fractions from each pH profile are shown below the plot. The gels are aligned to each respective pH profile such that the first and last lane of the gel corresponds to the first and last fraction of the pH elution profile. For the pH 7.5 gel, the full AUT-PAGE is shown. A chicken histone marker has been run on either end of the gel as shown in the pH 7.5 AUT-PAGE (but not in the others). For the pH 6.0 and 5.5 AUT-PAGE analyses, only the portion of the gel including H2A and H2A.Z is shown. The distribution of H2A.Z in all three gels is highlighted by the open rectangular boxes. Loadings of each**

fraction were normalized according to approximately equivalent H2A amounts. Gels were stained with Coomassie blue dye.

(Eickbush and Moudrianakis, 1978)]. At physiological pH (7.5) conditions, H2A.Z was associated with stable octamer forms. However, at pH 6.0, H2A.Z was additionally present in dissociated hexamer, tetramer, and dimer forms. At pH 5.5, H2A.Z was no longer present in octamer forms, and was primarily in dimer form (Figure 5).

Upon a decrease in pH from 6.0 to 5.5, the histidine imidazole ring (pK 6.0) becomes ionized, resulting in the loss of hydrogen bonding and the consequent instability between the tetramer and dimer components (Eickbush and Moudrianakis, 1978). The crystallographic structure of the H2A.Z NCP showed that the loop L1 between helix $\alpha 1$ and $\alpha 2$ of the H2A.Z histone fold displays some significant changes between residues 38 and 44 (^{38}SRTTSGH^{44}) when compared to the equivalent region in H2A (^{36}KGNYAE^{41}) (Suto et al., 2000). These regions are located within the interface of the two H2A molecules in the octamer. There is a highly conserved histidine residue (His^{43}) present within the H2A.Z interface and another proximal histidine (His^{35}), both of which are not present in canonical H2A isoforms. There are no differences in histidine amino acids located at the interface between either H3/H2A or H4/H2A (Marino-Ramirez et al., 2005). These departures from the canonical H2A forms may influence the stability of H2A.Z within the octamer.

The H2A.Z-H2B dimer is destabilized compared to the H2A-H2B canonical form

Having determined that under physiological conditions H2A.Z is predominantly partitioned within stable octamers, it was of interest to characterize the stability of the native H2A.Z-H2B dimer and understand its individual contribution to the octamer form. The salt-dependent thermal stability of native H2A.Z-H2B dimers was determined as described previously (Karantza et al., 1995; Karantza et al., 2001). As a control for the NaCl-dependent melting temperature profile of the H2A.Z-H2B dimer, the melting curve of the native H2A-H2B dimer was determined initially. The results produced were compared to those of an earlier study (Karantza et al., 1995; Karantza et al., 1996) and were in good agreement (Figure 6.A). However, efforts made to produce a similar melting curve for the H2A.Z-H2B dimer were unsuccessful. Under any of the buffered NaCl concentrations used, the native H2A.Z-H2B dimers displayed an unfolded conformation (Figure 6.B). During the time that these experiments were being conducted, another group published similar findings in which recombinantly expressed H2A.Z-H2B dimers were shown to be unstable (Placek et al., 2005). Our results corroborate those of Placek et al; under physiological ionic and temperature conditions, the native H2A.Z-H2B heterodimer adopts an unfolded state *in vitro*. There are several possible reasons for this instability, though the contributing factors are not known. Differences in the amino acid composition at the extensive interface between H2A.Z and H2B are one possible reason for a pH dependent stability. Another could be a requirement for a specific H2B interacting partner that may stabilize the variant dimer. A specialized metazoan H2B variant that specifically interacts with H2A.Z in *Trypanosomes* has been described (Lowell et al., 2005).

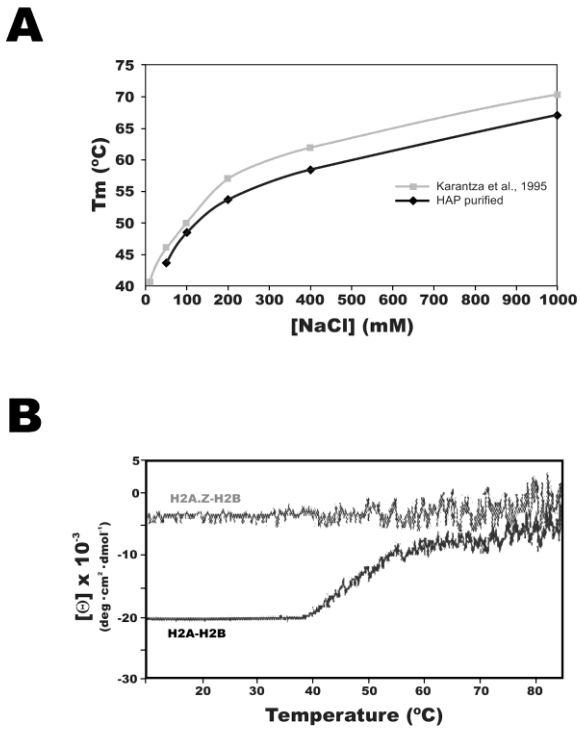

Figure 6. ***Circular dichroism analysis of the salt-dependent thermal stability of H2A.Z-H2B dimers compared to canonical H2A-H2B dimers.*** **A. The NaCl-dependent melting temperature (T_m) profile of native H2A-H2B dimers in solution. The light grey lines and square boxes represent the H2A-H2B melting profile determined in a previous publication (Karantza et al., 1995; Karantza et al., 2001). The melting temperature profile determined experimentally in this chapter of native H2A-H2B dimers purified by HAP chromatography is depicted by the dark black line and black diamonds. The thermal unfolding of the H2A-H2B dimers was performed in 10 mM HEPES pH 7.5, 0.1 mM EDTA and increasing NaCl concentrations. The change in molar ellipticity was measured at 222 nm as the temperature was increased from 5°C to 80°C. B. The change in the residual molar ellipticity of the H2A.Z-H2B dimer compared to the H2A-H2B dimer as a function of increasing temperature. These experiments were conducted using the same buffers as in (A), but with 100 mM NaCl. The H2A-H2B dimer displays a typical melting profile at 222 nm and it is possible to determine the T_m from these data. The H2A.Z-H2B dimer, in contrast, does not display a thermal-dependent unfolding profile as it is largely destabilized.**

H2A.Z-containing NCPs display a slight stabilization in an ionic strength – dependent manner

The salt-dependent stability of native H2A.Z – containing NCPs was characterized by sucrose gradient fractionation under increasing NaCl concentrations. The NCP dissociation was visualized by AUT electrophoretic analysis (Figure 7) (Abbott et al., 2005). AUT-PAGE loadings for each fraction were normalized according to approximately equivalent H2A amounts. With an increase in NaCl concentration from 0.6 M to 0.9 M, a small, but apparent loss of H2A.Z from fractions 19-21 in the upper portion of the gradient (associated with lower sucrose concentrations) occurred. This loss was quantified by scanning densitometry Figure 7. The increasing salt concentration interferes with the ionic interactions within the nucleosome between the DNA and histones. At 0.6 M to 0.9M NaCl, the association of the H2A-H2B dimer within the NCP begins to be disrupted. Higher NaCl concentrations from 0.9 M to 1.2 M showed a marked decrease in H2A.Z within the lower sucrose concentrations with a concomitant relative increase in H2A.Z in more stable mononucleosomes. These latter populations partitioned within higher sucrose concentrations (Figure 7). This slight shift in H2A.Z partitioning from dissociated to more stably associated NCPs under 0.6 M to 1.2 M NaCl indicated that H2A.Z conferred a stabilization to these NCP structures. Reconstituted native H2A.Z-NCPs are also slightly stabilized compared to canonical NCPs by sedimentation analytical ultracentrifuge analysis (Thambirajah et al., 2006). These results agree with previously published results of reconstituted recombinant H2A.Z-containing NCPs (Park et al., 2004), but disagree with similarly produced data from our lab (Abbott et al., 2001).

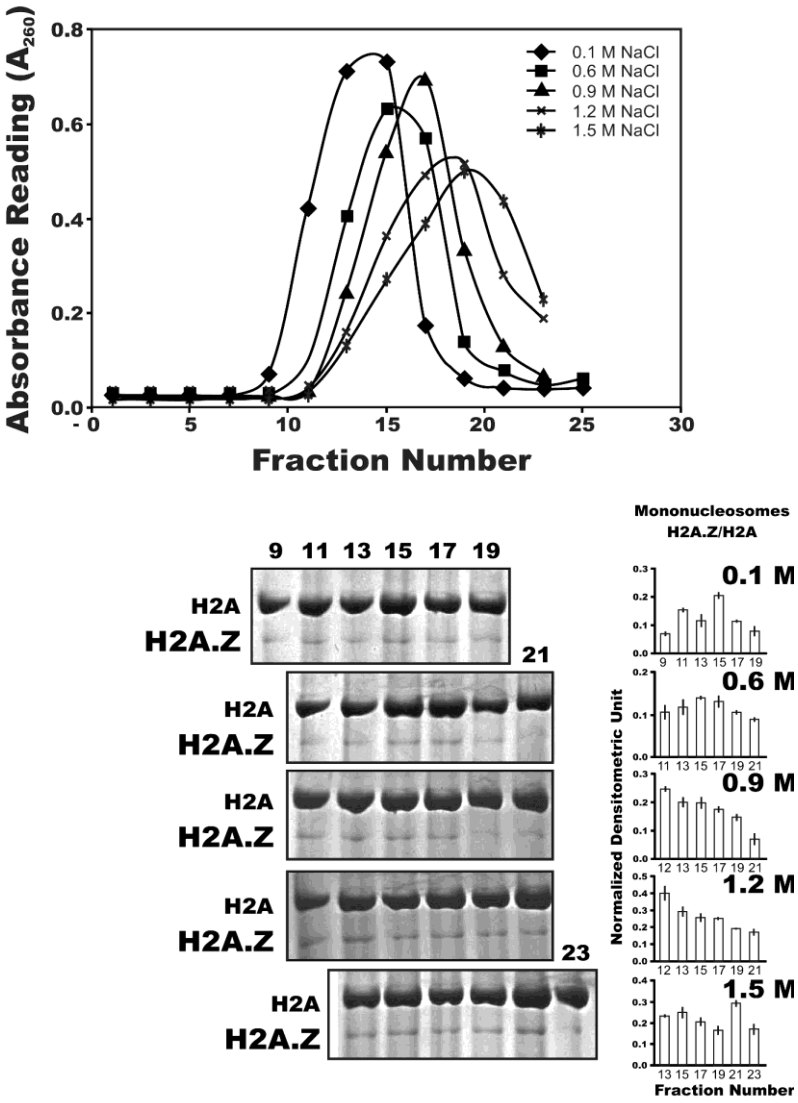

Figure 7. ***The salt-dependent sedimentation of H2A.Z-containing mononucleosomes by sucrose gradient fractionation.*** **Native chicken erythrocyte NCPs were equilibrated in 10 mM Tris-HCl pH 7.5, 0.1 mM EDTA and increasing NaCl concentrations. NCPs were loaded and separated on 5% - 20% sucrose gradients prepared with each respective salt buffer. The absorbance at 260 nm (A_{260}) was measured for each fraction in the different NaCl gradients and the plotted profiles are shown at the top. The lower fraction numbers correlate to a higher sucrose concentration and a corresponding decrease in sucrose concentration occurs with the increase in fraction number. Selected fractions (as numbered) from each gradient were analyzed by AUT-PAGE and these gels are shown below. In each**

panel, only the portion depicting H2A and H2A.Z is shown. The first panel is the 0.1 M NaCl gradient, the second, 0.6 M NaCl, the third, 0.9 M NaCl, the fourth, 1.2 M NaCl, and the final, 1.5 M NaCl. Sample loadings were normalized according to the total H2A amount in each fraction. Scanning densitometry was done of each gradient to determine the relative normalized amounts of H2A.Z/H2A in each fraction analyzed by AUT-PAGE. These averaged results are represented by the bar graphs to the right of the gels for the 0.6 M, 0.9 M, and 1.2 M NaCl gradients. The error bars indicate the mean ± S.E. When the H2A-H2B dimer interactions within the mononucleosome are disrupted at 0.9 M and 1.2 M NaCl, H2A.Z distributes within the more stabilized NCP populations.

The deposition of H2A.Z within chromatin is not affected by the presence or absence of linker histones (H1/H5)

H2A.Z is present in transcriptionally active (Bruce et al., 2005; Santisteban et al., 2000) and repressed domains (Fan et al., 2004; Guillemette et al., 2005) in yeast and higher eukaryotes. How H2A.Z accomplishes such a broad genomic distribution has been a source of considerable debate. The previous set of experiments investigated the effects of the histone variant H2A.Z on NCP structure in the absence of linker histones. What is not known is whether the presence of linker histones affects the distribution of H2A.Z throughout chromatin regions.

Micrococcal nuclease digestion of chromatin within intact nuclei initially proceeds through the linker histone-deficient euchromatin regions. A time-course analysis of an extensive digestion can be used to fractionate linker histone-containing chromatosomes from NCPs (Olins et al., 1976). Such a process can be used to infer the cohabitation of histone variants with the linker histone H1 or H5 (Abbott et al., 2005).

A similar approach was adopted and H2A.Z was found to be equally distributed within all fractionated chromatin populations, irrespective of the duration of digestion (Figure 8). H2A.Z was present in linker histone-containing (Figure 8, fraction P2) and linker histone-depleted (Figure 8, fraction S2) nucleosomes and also in the highly nuclease-resistant P1 fraction. The P1 fraction consists of tightly folded heterochromatin and insoluble active regions tethered to transcription complexes (Henikoff et al., 2009). These results show that H2A.Z deposition or partitioning between different chromatin regions is not based on the local linker histone content. This finding agrees with those of another study in which H2A.Z was found to be widely, though non-randomly, distributed across euchromatin and heterochromatin regions of the *Drosophila* polytene chromosomes (Leach et al., 2000).

H2A.Z binds more tightly to chromatin than H2A, regardless of the chromatin type

An early characterization of the association of H2A.Z within chromatin fibres showed that H2A.Z eluted from HAP-adsorbed chromatin at a much higher NaCl concentration than the canonical H2A form (Li et al., 1993). This suggested that the H2A.Z variant either bound to the nucleosomal DNA more strongly or that it had an enhanced interaction with the H3-H4 tetramer within the NCP. We pursued this observation and investigated the influence of several different parameters on the elution of H2A.Z from HAP-adsorbed chromatin. First, the effect of different tissue sources (chicken liver *versus* erythrocytes) on H2A.Z – chromatin association was tested in addition to the type of chromatin (S1, SE) and the absence of linker histones (SE-H1) (Figure 9).

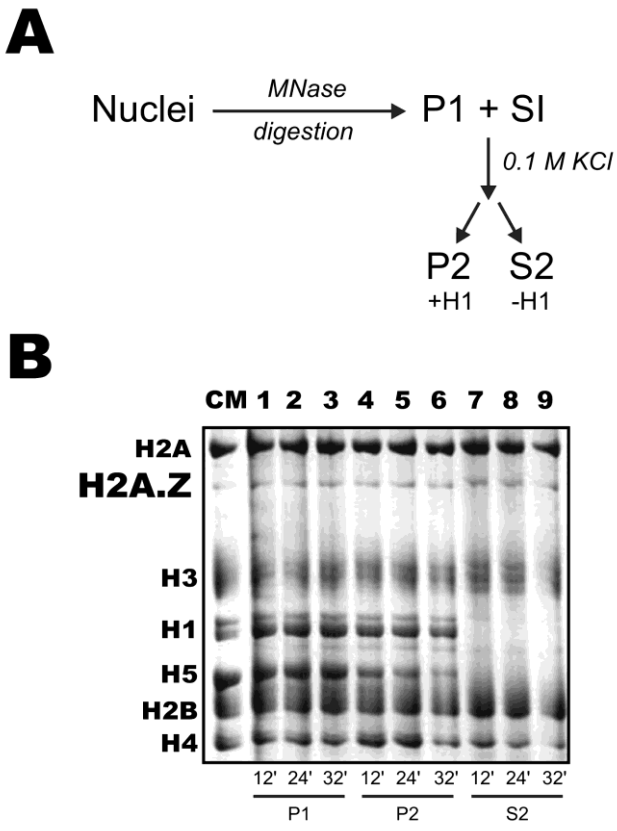

Figure 8. ***0.1 M KCl fractionation of chromatin particles following an extensive micrococcal nuclease digestion of chicken erythrocyte nuclei.*** **A. An abbreviated outline of the fractionation procedure based on the protocol developed by Olins (Olins et al., 1976). Chicken erythrocyte nuclei were digested with MNase for 12, 24, and 32 minutes and the reaction was stopped with the addition of EDTA. The digested nuclei were centrifuged to produce a nuclease-resistant insoluble pellet, P1, and an S1 supernatant. The S1 supernatant was dialyzed against 0.1 M KCl, which, following centrifugation, yielded an NCP-containing supernatant (S2) devoid of linker histones and a pellet (P2) that contained chromatosomes and nucleosome oligomers associated with linker histones. B. AUT-PAGE analysis of the P1, P2, and S2 fractions obtained following the fractionation procedure in A. H2A.Z is broadly distributed throughout all chromatin fractions and its localization is not dependent upon the presence or absence of H1 or H5 linker histones.**

Figure 9A shows a typical elution profile of histones under an increasing NaCl gradient from an SE chromatin fraction extracted from chicken liver. The AUT-PAGE analysis of selected fractions from this profile is shown in the first panel of Figure 9B. In agreement with previously published results (Li et al., 1993), H2A.Z had a late elution after H2A/H2B that was attendant with H3/H4 (Figure 9.A). Similar HAP chromatography was conducted to determine the effects of tissue specificity (chicken erythrocyte SE, Figure 9.B, panel 2), the presence or absence of linker histones (panels 2 and 3), and the chromatin type (chicken erythrocyte S1, a euchromatin fraction containing smaller chromatin fragments, panel 4). In all instances, H2A.Z showed a similar late co-elution with the H3/H4 histones. This late elution of H2A.Z was abrogated when H2A.Z became acetylated. Upon hyperacetylation of chromatin by the treatment of chicken erythroleukemic cells with sodium butyrate, acetylated H2A.Z demonstrated an early elution with H2A (Thambirajah et al., 2006). The lower NaCl concentration elution of acetylated histones from HAP has been described before (Hirose, 1988) and this early H2A.Z elution indicates that the acetylation of the core histones and/or acetylated H2A.Z can mitigate the stability conferred by the unmodified H2A.Z (Thambirajah et al., 2006).

It was necessary to ensure that the late elution of H2A.Z was not due to a differential interaction of this variant with the HAP resin as compared to the other histones. Depending upon the phosphate buffer and ionic conditions, histones can differentially interact with the HAP resin (Faulhaber and Bernardi, 1967). Different combinations of H2A/H2A.Z and H2A-H2B and H2A.Z-H2B dimers were loaded onto HAP columns under similar conditions and eluted with a 1 M – 2 M NaCl gradient, as the

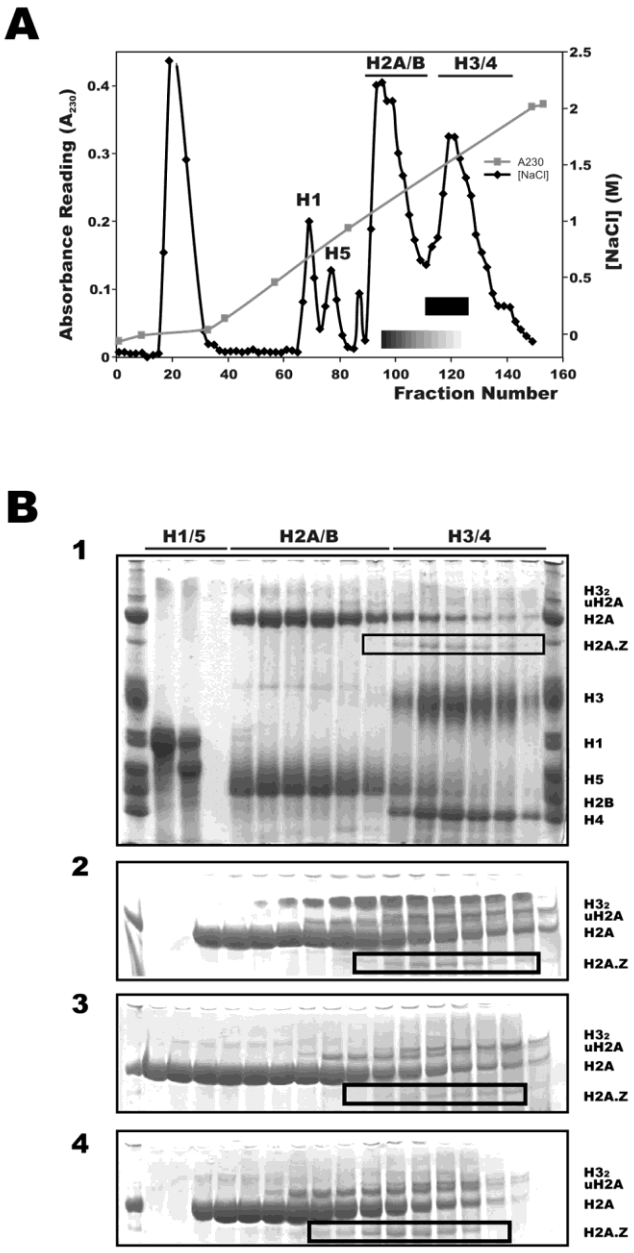

Figure 9. ***The NaCl-dependent elution of histones from hydroxyapatite-adsorbed chromatin complexes.*** **A. A representative plot of the elution of histones from EDTA-solubilized chicken liver SE chromatin that had been adsorbed onto a 15 cm X 1.5 cm HAP column. The column had been equilibrated in 20 mM phosphate buffer pH 6.8 and the histones were eluted in this buffer with a 0 – 2.5 M NaCl gradient. The absorbance at 230 nm (A_{230}) was measured of each fraction and the elution profile is shown with the dark black line and diamonds. The NaCl**

concentration gradient is plotted in the light grey line and square boxes. The black bar refers to the region of H2A.Z elution. B. AUT-PAGE analyses of the eluted histones from the different chromatin types that were loaded onto separate HAP columns. The AUT-PAGE lanes containing the H1/H5 linker histones and the H2A/H2B and H3/H4 core histones are marked to correspond to the respective elution peaks in A. The chromatin types in B are: 1. chicken liver SE; 2. chicken erythrocyte SE; 3. linker histone – stripped chicken erythrocyte SE; and 4. chicken erythrocyte S1. For gels 2 – 4, only the upper portion of the AUT-PAGE containing H2A and H2A.Z is shown.

core histone elution did not begin until ~1.2 M NaCl. In all instances, the histones eluted within a single peak (Thambirajah et al., 2006). This indicated that under 20 mM phosphate buffer and salt concentrations greater than 1 M NaCl, any differential affinities for the HAP resin by H2A or H2A.Z were abolished and did not artifactually influence the elution characteristics of the histones (Thambirajah et al., 2006).

Discussion

I sought to determine the effects mediated by the heteromorphic histone variant H2A.Z on the hierarchical organization of native chromatin structure. Interestingly, some contrasting structural features were observed. Under physiological pH conditions, H2A.Z was present predominantly within stabilized octamer forms. However, with the pH-dependent destabilization of the octamer, the exclusive association was lost and H2A.Z was present within all dissociated forms of the octamer (Figure 5). The H2A.Z-H2B dimer, in opposition to what was observed in other structures, displayed a negligible

secondary structure and was destabilized (Figure 6). Within the NCP, however, H2A.Z showed a salt-dependent stabilization of the particle (Figure 7). This stabilizing tendency was reinforced by studies of chromatin fibres that showed, compared to H2A, H2A.Z had either a stronger association with the DNA or the H3-H4 tetramer or both (Figure 9). Moreover, the association of H2A.Z within chromatin occurred independently of the deposition of linker histones (Figure 8 and Figure 9).

At pH conditions below 7, the loss of stability in H2A.Z–octamers and that of the variant dimers could reflect changes in the interactions at the different interfaces between H2A.Z and the complementary core histones. Although these phenomena are considered in isolation, they may affect the highly dynamic nature of the nucleosome. The instability of the H2A.Z-H2B dimer has been proposed to be responsible for the equilibrium shift from one involving the physiologically relevant sequential dissociation of H2A-H2B dimers from the NCP (van Holde et al., 1992) to a more stable nucleoprotein complex (Placek et al., 2005). Such stability of the NCP would not favour the dissociation of the unstable H2A.Z-H2B dimer (Placek et al., 2005). The same report proposed that the highly charged nature of the H2A-H2B tails also contributes to the stability of the dimer (Gloss and Placek, 2002; Placek and Gloss, 2002) such that neutralization of the charged regions (through acetylation) would increase the dimer stability. Consequently, dissociation of the dimer from the NCP would be enhanced (Placek et al., 2005). However, this has not been demonstrated, and molecular details of the mechanism involved in the H2A.Z-H2B dimer instability remain to be established. In yeast, Nap1, a chaperone for H2A-H2B dimers, can behave similarly for unincorporated Htz1-H2B dimers (Mizuguchi et al., 2004). Nap1 forms a heterotrimer with the variant

dimer and delivers Htz1-H2B for SWR1–mediated replacement. More recently, a specific chaperone for H2A.Z has been described: Chz1 (Luk et al., 2007). The formation of the Chz1-Htz1-H2B heterotrimer is considerably more stabilized when compared to their component parts (Luk et al., 2007). It is possible that the H2A.Z-H2B dimer requires the presence of a chaperone in order to maintain an ordered secondary or tertiary structure.

Two important structural considerations need to be made in regards to the chromatin stabilization imparted by H2A.Z. First, the histone H2A N-terminal tail binds two defined positions centered at 25 – 35 nucleotides from the ends of the 146 bp DNA in the NCP (Lee and Hayes, 1997; Zheng and Hayes, 2003). Second, these nucleotide stretches are within the region of DNA where the interaction with the octamer in the NCP is loosened following histone acetylation (Garcia-Ramirez et al., 1995; Norton et al., 1989).

That the flanking ends of the DNA at the entry and exit site of the NCP are potentially involved in chromatin stabilization is supported by the lower salt-dependent stability of the NCP (Figure 7) compared to the stability of full chromatin (Figure 9). That acetylation results in a destabilized H2A.Z association may be due to a weakened interaction of H2A.Z with the DNA in the chromatin complex. If so, then the interaction of H2A.Z with DNA could be mediated by the unique N-terminal region of H2A.Z, which can be acetylated. Studies of *Drosophila* H2A.Z and H2A.1 swapping mutants showed that the exchange of the first 12 N-terminal amino acids resulted in a lethality rate only second to the swapping of the indispensable C-terminal docking domain (amino acids 81-119) (Suto et al., 2000) of the two H2A isoforms (Clarkson et al., 1999).

Acetylation of H2A.Z occurs primarily at Lys^4, Lys^7, and Lys^{11} (Bruce et al., 2005). Acetylation of at least one lysine within the N-terminal tail of H2A.Z is essential for survival in *Tetrahymena* (Ren and Gorovsky, 2001; Ren and Gorovsky, 2003). It is thought that the post-translational modification of a charge patch encompassing these residues reduces the charge of the H2A.Z tail domain (Ren and Gorovsky, 2001; Ren and Gorovsky, 2003).

The results of this work may have important implications for understanding the dual functions of H2A.Z (Dryhurst et al., 2004). In its native form, H2A.Z is stably associated within octamer and NCP chromatin forms. The stability of H2A.Z interactions in native chromatin fibres is exchanged for an H2A-like association when it, and/or the surrounding chromatin, is acetylated. The deposition of H2A.Z has been described in transcriptionally active (Adam et al., 2001; Bruce et al., 2005; Farris et al., 2005; Larochelle and Gaudreau, 2003; Raisner et al., 2005; Santisteban et al., 2000; Zhang et al., 2005), inactive (Dhillon and Kamakaka, 2000; Fan et al., 2004; Raisner et al., 2005; Rangasamy et al., 2003; Swaminathan et al., 2005), and boundary (Meneghini et al., 2003) chromatin domains. The chromatin remodelling complex of the Swi2/Snf2-related ATPase Swr1p has been shown to deposit H2A.Z into yeast chromatin (Kobor et al., 2004). The Kat5 acetyltransferase has recently been shown to acetylate the N-terminal tail of H2A.Z in yeast once it is deposited (Kim et al., 2009). It is possible that unmodified H2A.Z is stably remodelled into euchromatin promoter regions which are transcriptionally inert. Additionally, its presence in heterochromatin regions may see the stabilizing effects of H2A.Z enhanced by the synergistic association with other *cis* elements or non-histone proteins such as HP1-α (Fan et al., 2004). In the complementary

situation, when H2A.Z and the surrounding chromatin environment are acetylated (such as during elongation) (Myers et al., 2003; Myers et al., 2001), the subsequent destabilization could favour transcriptional activation as has been reported at the 5’ end of promoters (Bruce et al., 2005).

Chapter 3 – Effects of Global Chemical Modifications to Chromatin on the Qualitative Distribution of MeCP2

This chapter is adapted from the following published paper and manuscript submitted for review:

Ishibashi, T., **Thambirajah, A.A.**, and Ausió, J. (2008) MeCP2 preferentially binds to methylated linker DNA in the absence of the terminal tail of histone H3 and independently of histone acetylation. FEBS Letters. **582**:1157-62.

Thambirajah, A.A. and Ausió, J. (2010) The tissue-specific chromatin distribution of MeCP2 is influenced by histone variants and post-translational modifications. Submitted.

A.A.T. was primarily responsible for the experimental design and carried out all of the experimental work described in this chapter. A.A.T. wrote this chapter, the second manuscript and contributed to the writing of the first publication listed above.

Abstract

Because of the relative abundance of methylated 5'-CpG sites and its ability to interact with histone deacetylases and Sin3a, the methyl-CpG binding protein 2 (MeCP2) was initially considered to be a global repressor of transcription. Support for this model began to wane as evidence emerged that MeCP2 may act as a specific regulator of gene activity. However, the debate persisted as experimental findings were produced in support of both arguments. In the work described in this chapter, the underlying assumption made was that if MeCP2 acted as a universal transcriptional repressor, then changes to global chromatin modifications should affect the distribution of MeCP2 within chromatin. To this end, HeLa S3 cultures were treated with either 3-aminobenzamide, to induce DNA hypermethylation, or butyrate, to promote histone hyperacetylation. Compared to an untreated culture, neither treated culture resulted in a rearrangement of MeCP2 within fractionated chromatin. Moreover, the majority of the MeCP2 was present in the nuclease-accessible, active chromatin fraction, regardless of treatment. However, the butyrate treatment resulted in a proportional loss of MeCP2 within all chromatin fractions. This loss was not due to butyrate-dependent effects on *MeCP2* transcription. As well, in order to further understand the nature of MeCP2 binding to native chromatin, it was shown that MeCP2 bound to nucleosomes that contained DNA that ranged in length from 146 bp to approximately 160 bp. This work supports an evolving paradigm of MeCP2 acting as a specific regulator of transcription and not as an indiscriminate silencer.

Introduction

MeCP2 was first identified based on its ability to bind methylated CpG dinucleotides. Given the relative abundance of this dinucleotide and the demonstrated ability of MeCP2 to impede transcription, it was postulated early on that MeCP2 could act as a global repressor of gene expression (Lewis et al., 1992; Meehan et al., 1992; Nan et al., 1997). MeCP2 was shown to associate with (class I) HDACs, Sin3a, and with components of silencing complexes including KMTs and DNMTs. Additional interactions of MeCP2 with the co-repressors c-Ski and N-CoR helped to cement the behaviour of MeCP2 as a transcriptional repressor (Kokura et al., 2001).

About 7 years after MeCP2 was first described, it was discovered that mutations in MeCP2 caused the neurodevelopmental disorder Rett syndrome (RTT) (Amir et al., 1999). Some doubt as to the ability of MeCP2 to act as a global repressor began to emerge a few years later when genetic profiling of a RTT *MECP2*-null mouse model showed only subtle changes in large scale gene expression patterns (Tudor et al., 2002). It seemed counterintuitive that a purported universal regulator should elicit such a small range of changes. Could it be that MeCP2 did not behave as a global repressor of gene activity?

Further support for the global paradigm of regulation came with studies investigating the changes in reconstituted chromatin fibre folding upon MeCP2 binding. In the absence of physiological ionic conditions, MeCP2 was observed to condense the chromatin fibres into ellipsoidal particles and oligomeric suprastructures. It was inferred that such a compaction would be refractory to gene activation (Georgel et al., 2003). However, that same year, two groups independently described the activity-dependent

activation of the *BDNF* gene which was repressed by MeCP2 at one of its several promoters (Chen et al., 2003; Martinowich et al., 2003). For the first time, it was shown that MeCP2-mediated repression could be relieved by the calcium-dependent release of MeCP2.

Despite the emergence of increasing information that MeCP2 played critical roles in neurogenesis, neuron maturation and the development of dendritic spines (Jugloff et al., 2005), the debate as to whether MeCP2 acted in a global versus specific manner still persisted. Support for a global model of regulation was beginning to wane, as other studies investigated the impact of *MeCP2* mutations on histone methylation and acetylation profiles. Multiple studies generated inconclusive findings on wide-scale changes in H3 or H4 acetylation or methylation profiles (Urdinguio et al., 2007). Could a protein that plays such important roles during early post-natal development still be considered a global regulator when mutations in the protein do not always result in a lethal phenotype? Certainly, the range of symptoms experienced by those with RTT is wide-ranging not only in type, but severity as well. That girls do survive this major genetic deficit could be due to a number of factors. X chromosome dosage compensation could certainly be one key element, while other possibilities include that there is a limited redundancy between other similar methyl-binding domain proteins or that MeCP2 regulates only a specific set of genes (Christodoulou and Weaving, 2003).

My objective was to attempt to settle some of this debate regarding the nature and scope of MeCP2 regulation. Many of the previous studies had emphasized the influence of MeCP2 on histone PTMs on a broad scale. The approach adopted in this study took another perspective. As discussed, MeCP2 binding is dependent (though not absolutely)

on the methylation of a CpG dinucleotide located proximal to $[A/T]_{\geq 4}$ nucleotides. If MeCP2 were an indiscriminate repressor, would global changes to the underlying chromatin modifications perturb the binding and distribution of MeCP2 within chromatin? Chemical treatment could be used to induce widespread modifications that would reflect either a repressive or active transcriptional state. If the DNA was hypermethylated, resulting in a repressive environment, would there be an excess of MeCP2 binding within heterochromatin regions? In the opposite scenario, would the hyperacetylation of histones result in the loss of MeCP2 from actively-regulated gene regions or a chromatin-based rearrangement of MeCP2?

This hypothesis was tested and no large scale rearrangements of MeCP2 were observed following either treatment when compared to native chromatin. This strongly indicated that the regulatory behaviour of MeCP2 does not extend to a universal genome level, but is more likely focussed within a specific set of genes. As well, the binding of MeCP2 within mononucleosome fractions was determined to occur within the linker DNA region *in vivo*.

Materials and Methods

***Preparation of nuclei*. HeLa S3 cell cultures**. Cells were grown in suspension as described before (Wang et al., 2001). Cultures were treated with 2 mM 3-aminobenzamide (3-ABA) from a 0.5 M stock for 22 hours to induce DNA hypermethylation (de Capoa et al., 1999). In a separate culture, cells were treated with 10 mM butyrate, resulting in histone hyperacetylation. Cells were harvested and nuclei

were prepared as in (Perry and Chalkley, 1981; Perry and Chalkley, 1982; Wang et al., 2001).

Digestion and fractionation of chromatin. Isolated nuclei were resuspended in buffer B (50 mM NaCl, 10 mM PIPES pH 6.8, 5 mM $MgCl_2$, 1 mM $CaCl_2$, and Roche Complete Protease Cocktail Inhibitor) to a final concentration of 4 mg/mL based on the A_{260} readings of a nuclear suspension in 0.5% SDS. Chromatin was digested using MNase (Worthington) at a concentration of 30 units/mg of DNA at 37^{o}C for 15 minutes as described previously (Ishibashi et al., 2008). 5 mM EDTA was added to stop the reaction on ice and the digested nuclei were centrifuged at 9000 rpm for 5 minutes at 4^{o}C to produce the S1 supernatant. A Beckman centrifuge and JA-20 rotor were used. The digested nuclei pellet underwent a hypotonic lysis with stirring in 0.25 mM EDTA at 4^{o}C for 1 hour. Following centrifugation at 10 000 rpm for 20 minutes at 4^{o}C, the SE supernatant was produced and an insoluble, lysis-resistant pellet (P) (Wang et al., 2001).

Sucrose gradient separation of HeLa S3 S1 mononucleosomes. 1.0 mg of S1 mononucleosomes were separated on a 5 – 20% sucrose gradient (in 10 mM Tris pH 7.5, 0.1 mM EDTA) by centrifugation at 25 000 rpm for 23 hours at 4^{o}C using a Beckman L8-70M ultracentrifuge and SW28 rotor. Deceleration was done without using a brake. Fractions were pooled into four groups: A, B, C, and D, and normalization for loading was done according to the total histone content by SDS-PAGE. The length of DNA associated with the mononucleosomes was assessed by native PAGE. Western blotting

was used to determine the relative abundance of bound MeCP2 within the fractionated mononucleosomes (Wang et al., 2001).

Gel electrophoreses. SDS-PAGE was performed as described previously (Laemmli, 1970). AUT-PAGE was done as in (Abbott et al., 2001). AU-PAGE were performed according to (Ausió and van Holde, 1986). 4% native PAGE gels were run as in (Yager and van Holde, 1984). 0.7% agarose gels were run at 100 V for 1 hour in 1x TAE buffer and then subsequently stained in ethidium bromide prior to visualization of the DNA under UV light.

Western blotting. Western blotting was done according to the protocol previously described in (Ishibashi et al., 2008). Blots were incubated with the following antibodies overnight at 4^{o}C. 1:2500 α-MeCP2 (Sigma), 1:5000 α-H3K27me$_3$ (Millipore), 1:2000 α-H3K9me$_2$ (Upstate), 1:10 000 α-H4 (made in-house), 1:4000 α-H4 pan acetylated (Upstate), 1:5000 α-H3K4me$_3$ (Millipore), 1:5000 α-H3K36me$_3$ (made in-house). A number of the antibodies, including α-MeCP2 and α-H4, were tested against their respective purified native or recombinant protein and against non-specific proteins to assess their specificity. The secondary antibodies used were: donkey anti-rabbit IgG HRP-linked whole antibody (GE Healthcare, Amersham) and polyclonal donkey anti-sheep IgG (Abcam). Visualization was done by chemiluminescent detection (PerkinElmer® Western Lightning™ *Plus*-ECL Enhanced Chemiluminescence Substrate).

DNA methylation quantification by scanning densitometry. DNA from the S1 fractions of treated and untreated HeLa S3 cells were obtained through phenol-chloroform extraction. The DNA was then digested in paired, separate reactions using *Hpa*II (New England Biolabs) and *Msp*I (New England Biolabs) at 37^{o}C for 1 hour. Undigested and digested DNA for each reaction were then resolved by 4% native PAGE. The remaining DNA was measured by scanning densitometry using a ChemiImager 4000 scanner and AlphaEase^{TM} Version 3.3d software (AlphaInnotech Corp.) (Ishibashi et al., 2008; Thambirajah et al., 2006). For the purpose of comparison, the digested density values were normalized to their respective undigested values. These values for the normalized *Hpa*II and *Msp*I digestions for each HeLa S3 treatment were used to generate an *Hpa*II/*Msp*I ratio. The relative changes in DNA methylation in the S1 DNA fractions of the treated and untreated HeLa S3 cultures were calculated as: -[(*Hpa*II/*Msp*I)$^{-}$ - (*Hpa*II/*Msp*I)$^{+}$]/ (*Hpa*II/*Msp*I)$^{-}$, where "-" refers to untreated and "+" refers to treated HeLa S3 cells. Each experiment was repeated independently three times with measurements of each taken in triplicate (Ishibashi et al., 2008).

Preparation of cell cultures and tissues samples for real-time quantitative RT-PCR.

Treated HeLa S3 cultures. Treated and untreated adherent HeLa S3 cells were grown to confluency in 10 cm diameter petri dishes and incubated with 10 mM butyrate or 2 mM 3-ABA for 20 hours. Total RNA was extracted from the HeLa S3 cells using a QIAGEN RNeasy preparation kit according to the manufacturer's instructions. QIAshredder columns (QIAGEN) were used to homogenize the cells. RNA from four sets of cells for each treatment condition was prepared.

cDNA synthesis from total RNA. SuperScript^{TM} II reverse transcriptase (Invitrogen) was used to generate cDNA from 1 µg total RNA according to the first strand cDNA synthesis protocol provided by the manufacturer. Total RNA and cDNA quality were confirmed by agarose gel electrophoresis.

Quantitation of MeCP2 transcripts by real-time PCR. The comparative C_t ($2^{-\Delta\Delta Ct}$) method was used to quantify the relative changes in *MeCP2* expression levels between the different treatment conditions (Livak and Schmittgen, 2001; Walzak et al., 2008; Wong and Medrano, 2005). A serial dilution validation assay was performed to assess the appropriateness of the target and reference gene primers for RT-PCR. For all primer sets, when plotting the log cDNA concentration dilution to the ΔC_t value, the slope of the line was less than 0.1 and the efficiencies of the primer sets were greater than 99%.

MeCP2 transcript levels in treated HeLa S3 cultures. The primers used to amplify *MeCP2* produced a ~281 bp amplicon (forward: 5'-AGCCATCAGCCCACCACT, reverse: 5'-CGCAATCAACTCCACTTTAGA). These primers were designed to amplify both *MeCP2* isoforms. *GAPDH* (glyceraldehyde-3-phosphate dehydrogenase) was used as the reference gene and produced a ~300 bp amplicon (forward: 5'-AAGGTCATCCCTGAGCTGAACGGG, reverse: 5'-CCAGGAAATGAGCTTGACAAAGTG). All primers were designed using Primer3 software (Rozen and Skaletsky, 2000) and were made by AlphaDNA Inc. The Invitrogen Platinum® SYBR® Green qPCR SuperMix-UDG with Rox was used in the experiments described. For each reaction, 7.5 µL of the SYBR mix was added to 0.5 µL 10 µM primers, 2 µL 1/20 diluted cDNA and 5 µL of RNase- and DNase-free dH_2O. For each cDNA dilution prepared, the reaction was run in quadruplicate per primer set. A non-

template control was run to test the primers independently as well. The RT-PCR was done using an Agilent Technologies Stratagene Mx3005P instrument and MxPro – Mx3005P v4.10 Build 389, Schema 85 software (©2007 Stratagene). The run parameters were as follows. Segment 1 (1 cycle): denaturation at 94^{o}C - 9 minutes; Segment 2 (40 cycles): denaturation at 95^{o}C – 15 seconds, annealing at 62^{o}C – 30 seconds, and extension at 72^{o}C – 45 seconds; Segment 3 (1 cycle – for dissociation profile): 95^{o}C – 1 minute, 55^{o}C – 30 seconds, 95^{o}C – 30 seconds. Data analysis was done using the $2^{-\Delta\Delta Ct}$ method with the untreated (native) HeLa S3 culture used as the comparator for the 3-ABA- and butyrate-treated cultures in order to determine the relative fold changes in transcript levels.

Results

1. MeCP2 preferentially binds to mononucleosomes having a longer DNA length *in vivo*.

Following the sucrose gradient fractionation of HeLa S3 S1 mononucleosomes, the pooled fractions (A, B, C, D) were normalized according to the total core histone content and verified by SDS-PAGE (Figure 10.A and B). The relative abundance of MeCP2 bound to the separated mononucleosomes was determined by western blotting and compared to the DNA length of each respective fraction. MeCP2 preferentially bound to mononucleosomes having DNA lengths of 146 bp to approximately 160 bp (Figure 10.C and D). This suggested a requirement for a longer linker DNA region to which MeCP2 could bind. This work has been confirmed by *in vitro* reconstitutions that demonstrate that MeCP2 prefers binding within 10 bp of the pseudo-dyad axis of

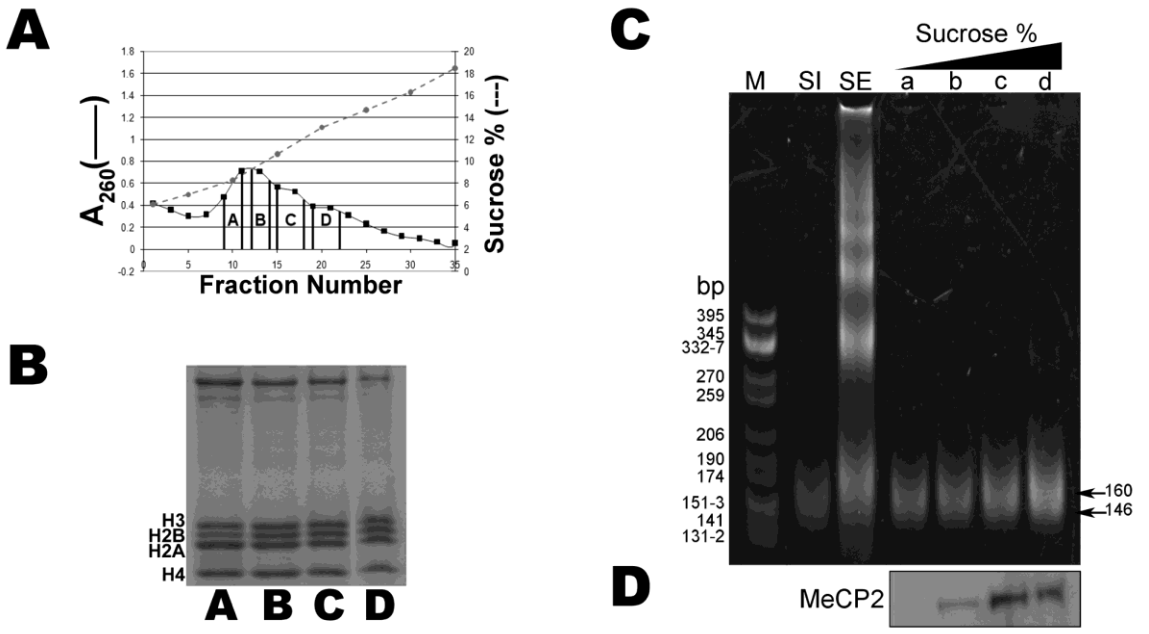

Figure 10. ***MeCP2 associates with HeLa S3 mononucleosomes that contain DNA that is longer than 146 bp.*** **A. Sucrose gradient fractionation of the HeLa S3 S1 mononucleosome population. The absorbance of each 1 mL fraction was measured at A_{260} and this profile is plotted with the corresponding increase in sucrose concentration. The fractions were pooled into four groups as shown: A, B, C, and D. B. The SDS-PAGE showing the normalized loading of the pooled fractions based on the total histone content. C. The DNA composition of the pooled nucleosome fractions (A-D) shown in comparison to the starting S1 and SE chromatin. The DNA was resolved using 4% native PAGE. M refers to the pBR322 – *Cfo*I-digested base pair marker. The arrow heads depict the size range of the S1 nucleosome DNA (146 – 160 bp). D. Western blot of the MeCP2 present in each pooled nucleosome fraction. MeCP2 preferentially binds to nucleosomes having DNA lengths greater than 146 bp to approximately 160 bp.**

symmetry, forming a chromatosome-like particle (Ishibashi et al., 2008).

2. The relative MeCP2 distribution within treated HeLa S3 chromatin is not affected by widespread DNA hypermethylation or histone hyperacetylation.

If MeCP2 acted as an indiscriminate, universal regulator of transcriptional silencing, it would be expected that changes in global chromatin modifications that affect MeCP2 binding sites would influence the distribution of MeCP2 within chromatin. Therefore, to test whether MeCP2 behaved as a global regulator of gene expression, DNA hypermethylation and histone hyperacetylation in HeLa S3 cells were induced and the relative chromatin-based distribution of MeCP2 was characterized. As DNA methylation is a pre-requisite for MeCP2 binding, it was hypothesized that an enrichment of methylated CpG sites may enhance MeCP2 binding within these regions. As MeCP2 is present within heterochromatin regions (Brero et al., 2005), enhanced methylation within these areas may result in a greater association of MeCP2. Under hyperacetylated histone conditions, it was hypothesized that the generally more active chromatin state would result in a rearrangement of MeCP2 to inactive regions if it acted as a global repressor.

The chromatin of treated and untreated HeLa S3 cultures were fractionated following MNase digestion and the DNA of each was resolved using native PAGE (Figure 11.A). The S1 fraction contains the readily-digested, nuclease-accessible portions of chromatin that correlate to regions which are actively transcribed (Henikoff et al., 2009). The S1 is primarily composed of mononucleosomes, and the SE contains mono-, di-, tri- and higher oligonucleosome forms. The SE contains the bulk of the chromatin which includes heterochromatin. The P has a similar composition as the

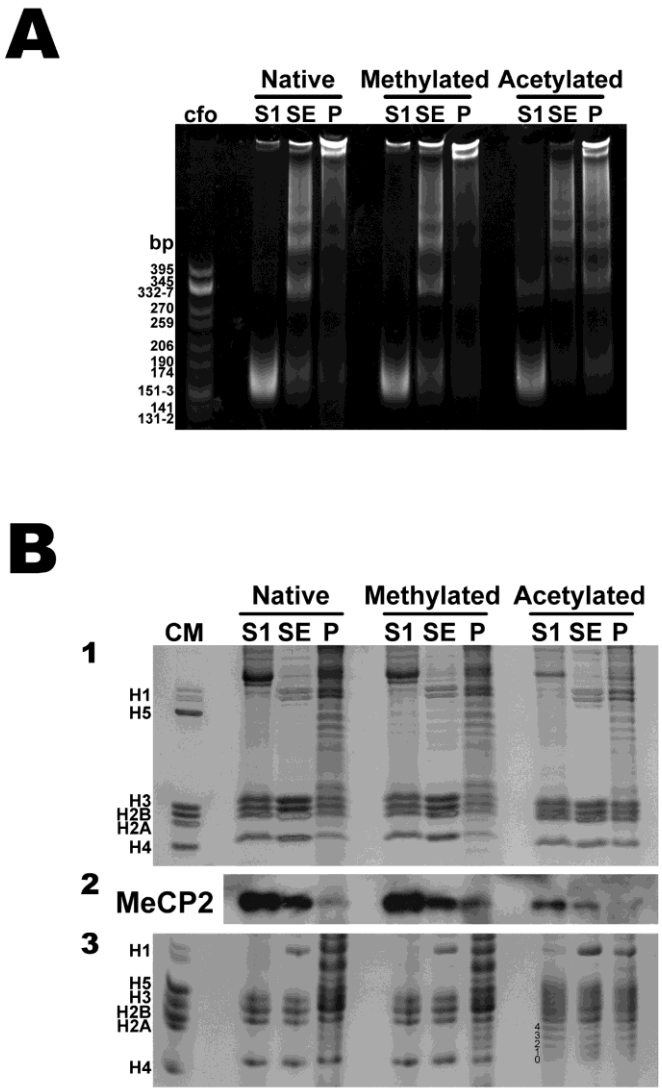

Figure 11. ***Distribution of MeCP2 within fractionated chromatin of treated and untreated HeLa S3 chromatin.*** **A. Native PAGE of DNA extracted from each chromatin fraction of the HeLa S3 nuclei following MNase digestion. Cultures were left untreated or were grown in the presence of 2 mM 3-ABA to induce DNA hypermethylation, or 10 mM butyrate to induce histone hyperacetylation. The base pair marker (cfo) used was a pBR322 – *Cfo*I-digested marker. B. 1. SDS-PAGE of HeLa S3 chromatin separated into the S1, SE, and P fractions. Loading amounts were normalized according to the total histone content. 2. Western blot of normalized chromatin fractions using a Sigma α-MeCP2 antibody. 3. Acetic acid-urea gel of chromatin fractions as loaded for the SDS-PAGE and western. The acetylated forms of H4 are numbered (0-4).**

SE, but typically contains a greater proportion of long DNA strands that are not resolved by native PAGE and remain associated with the wells (Figure 11.A). In addition to containing heterochromatin, the insoluble pellet contains transcriptionally active regions of chromatin which are tethered to large, transcriptional complexes (Henikoff et al., 2009). The proportion of chromatin in each fraction was as follows. For native chromatin, the percent composition for each was: S1 (11%), SE (26%), and P (63%); for the 3-ABA – treated: S1 (13%), SE (28%), and P (59%); and for the butyrate – treated: S1 (15%), SE (13%), and P (72%). Treatment of the cells with 3-ABA or butyrate did not affect the digestion as seen by the similar nucleosome DNA banding patterns (Figure 11.A). Loading amounts were normalized to the total histone content based on both SDS- and AU-PAGE (Figure 11.B.1 and 3). The AU-PAGE clearly shows the acetylated forms of histone H4 in all of the butyrate-treated chromatin fractions.

Interestingly, following DNA hypermethylation, MeCP2 did not show any major qualitative redistribution within the chromatin types and its relative amounts in S1, SE and P fractions were very similar to its native counterparts (Figure 11.B.2). When histone hyperacetylation was induced by butyrate treatment, there was a marked reduction in MeCP2 protein amounts in all chromatin fractions. Despite this, the proportional distribution of MeCP2 within these fractions was primarily conserved. The preparation of cytoplasmic and nuclear fractions showed that there was no change in the cellular localization of MeCP2 in treated cells (data not shown).

Regardless of treatment, most of the MeCP2 was present in the S1. Using sucrose gradient fractionation, approximately 5% of MeCP2 in the S1 was soluble and not chromatin-bound (data not shown). It is perhaps in the P fractions of these three cultures

that subtle differences in the amounts of MeCP2 are observed. In the methylated chromatin, there appears to be a slight enhancement of MeCP2, while in the acetylated fractions, there is a negligible amount of MeCP2 compared to the native control.

To confirm that DNA hypermethylation had occurred subsequent to the 3-ABA treatment, the relative level of DNA methylation was quantified using DNA extracted from both treated and untreated S1 fractions. Paired *Hpa*II and *Msp*I digestions were done according to the protocol previously described in (Ishibashi et al., 2008). The 3-ABA – treated S1 DNA showed an 11% increase in DNA methylation compared to the native control (Figure 12). The butyrate treatment resulted in a 6.7% decrease in DNA methylation in the S1 DNA (Ishibashi et al., 2008). The raw data for the individual *Hpa*II and *Msp*I digestions for both butyrate– and 3-ABA– treated HeLa S3 cells indicated that equivalent levels of digestion were occurring in the butyrate-treated samples for both enzymes (Figure 13). As this enhanced *Hpa*II digestion was greater than that of the native samples, it indicated that there was a rearrangement of CpG regions to the butyrate-treated S1 fraction. Despite this rearrangement, there was still an overall loss of MeCP2 from the butyrate-treated S1 fraction.

The presence of heterochromatin marks within the chromatin fractions was assayed through western blots for H3K9me$_2$ and H3K27me$_3$ (Figure 14). Similarly, the presence of euchromatin PTMs, H3K4me$_3$, H3K36me$_3$, and pan-acetylated H4, were assessed as well (Figure 14) (Santos-Rosa et al., 2002). H3K27me$_3$, a well characterized facultative heterochromatin mark (Peters et al., 2003), was present primarily in the SE fractions, regardless of global DNA hypermethylation or enhanced histone acetylation

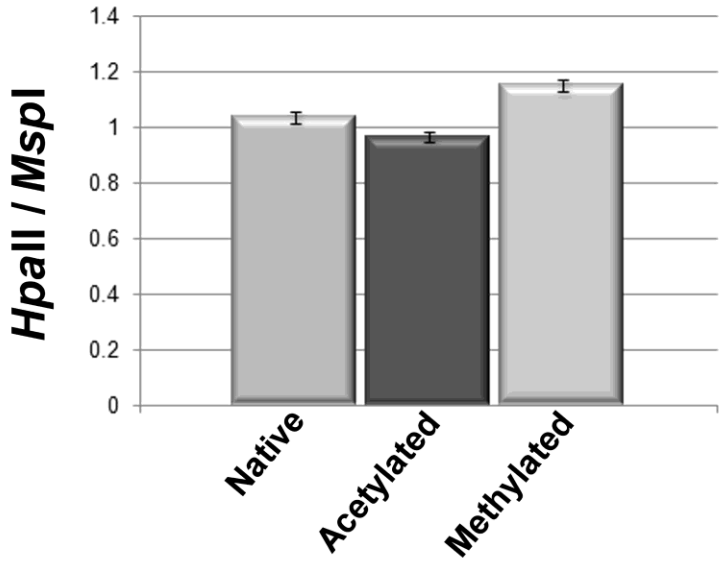

Figure 12. ***Quantification of the relative DNA methylation in S1 chromatin fractions in treated and untreated HeLa S3 cultures.*** **The relative methylation levels of native, hypermethylated, and hyperacetylated chromatin were assessed following paired *Hpa*II and *Msp*I digestions of a single set of cultures. The digested and undigested DNA were subsequently resolved on a 4% native PAGE. Remaining DNA amounts were quantified by scanning densitometry and were normalized to a paired undigested control. *Hpa*II/*Msp*I ratios were calculated and used to determine the relative changes in DNA methylation compared to the control by: -[(*Hpa*II/*Msp*I)$^{-}$ - (*Hpa*II/*Msp*I)$^{+}$]/ (*Hpa*II/*Msp*I)$^{-}$, where "-" refers to untreated and "+" refers to treated HeLa S3 cells. According to the *Hpa*II/*Msp*I ratio, a value equal to 1 would indicate no change in methylation, a value less than 1 would indicate a hypomethylated state and greater than 1, hypermethylation. The standard deviation is depicted by the error bars.**

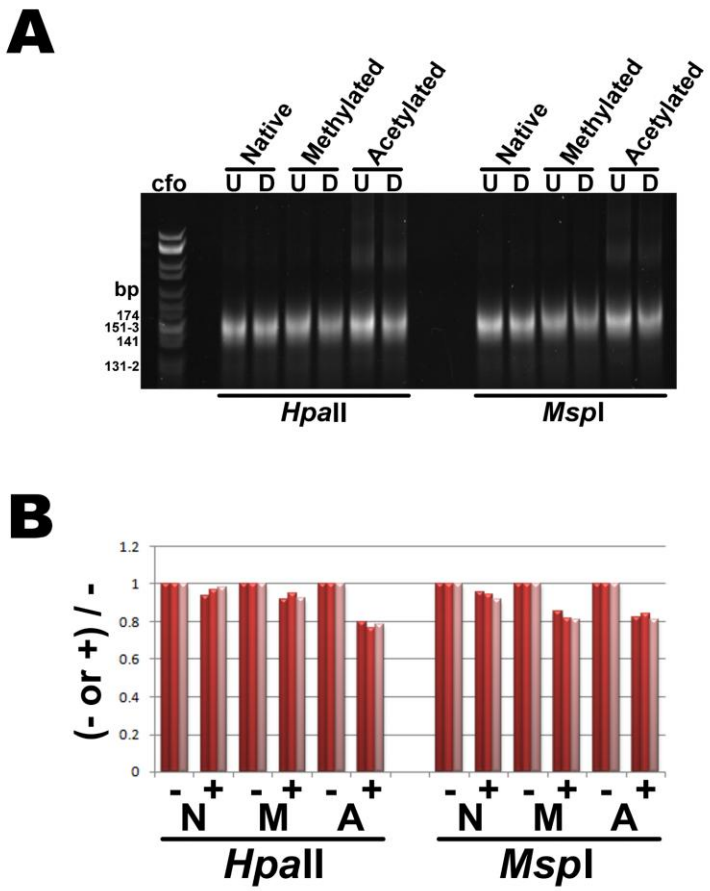

Figure 13. ***Normalized raw data for the quantification of DNA methylation in treated and untreated HeLa S3 cultures.*** **A. Relative methylation in untreated (native, N) and cultures treated with 3-ABA (methylated, M) or butyrate (acetylated, A) were quantified by scanning densitometry following paired *Hpa*II and *Msp*I digestions. The native PAGE is shown in (A) where U = undigested and D = digested. B. Normalization of the input amount of DNA following digestion was done by dividing the density of the remaining DNA by the density of the undigested DNA. For each digestion ('+'), a paired "undigested" ('-') loading control was run without the addition of enzyme. N = native, M = methylated, A = acetylated chromatin preparations. The individual triplicate measurements taken are shown in the plot. The remaining DNA of the acetylated chromatin showed equivalent levels following both *Hpa*II and *Msp*I digestions that were lower than that of the native *Hpa*II digestion. This indicated a potential CpG rearrangement following butyrate treatment.**

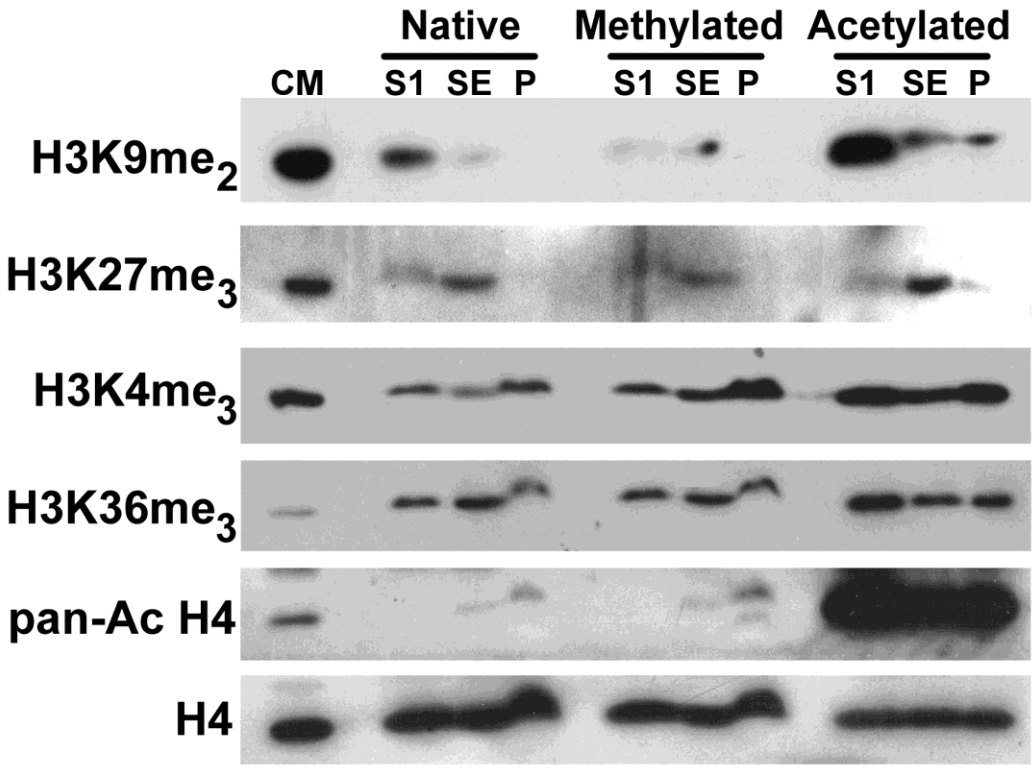

Figure 14. ***Distribution of heterochromatin and euchromatin marks throughout treated and untreated HeLa S3 chromatin.*** **HeLa S3 cultures were either left untreated or treated with 2 mM 3-ABA (DNA hypermethylation) or 10 mM butyrate (histone hyperacetylation) to induce repressive or active chromatin states. Fractions were normalized relative to the total histone content as in Figure 11 and western blotting was performed using the following antibodies separately: α-H3K9me$_2$, α-H3K27me$_3$, α-H3K4me$_3$, α-H3K36me$_3$, α-H4 pan-acetylated and α-H4 to confirm the equivalent loadings. CM refers to the chicken marker histone protein standard.**

(Ishibashi et al., 2009). The H3K9me$_2$ facultative heterochromatin modification was localized primarily within S1 fractions (Figure 14) (Peters et al., 2003). Of note was an inverse correlation between DNA methylation and histone methylation. Particularly for the H3K9me$_2$ PTM, but also for H3K27me$_3$, a loss of these marks was seen in the DNA

hypermethylated fractions compared to the native. In contrast, an increase in the relative amounts of these PTMs was observed in the hyperacetylated chromatin fractions (Figure 14).

H3K4me$_3$, a mark of active genes (Santos-Rosa et al., 2002), was present in all fractions regardless of treatment, but was mostly found in the pellet (Figure 14). The acetylated chromatin, however, showed an increase in this mark in all fractions, but particularly in the S1. H3K36me$_3$ is located within genes, at the 5' end of exons, and is correlated with exon expression (Hon et al., 2009; Kolasinska-Zwierz et al., 2009). H3K36me$_3$ had a broad distribution within native and treated chromatin fractions, and was increased in the S1 of acetylated chromatin (Figure 14). Very faint amounts of reactivity for the pan-acetylated H4 antibody were observed in the SE and P of the native and methylated chromatin. In contrast, every acetylated chromatin fraction showed high levels of pan-acetylated H4 (Figure 14) (Ishibashi et al., 2009).

To ensure that each chemical treatment did not affect the amount of *MeCP2* transcription, real-time RT-PCR was performed for all HeLa S3 cultures (Figure 15). It has previously been shown that butyrate can affect the level of transcription of particular genes, including linker histones (Davie, 2003; Khochbin and Wolffe, 1993). Using the ΔC_t method, no major relative fold increases in the level of *MeCP2* transcripts were observed for either DNA hypermethylated (1.14 ± 0.09 standard deviation, S.D.) or histone hyperacetylated (1.20 ± 0.14 S.D.) HeLa S3 cultures compared to the native control (Figure 15).

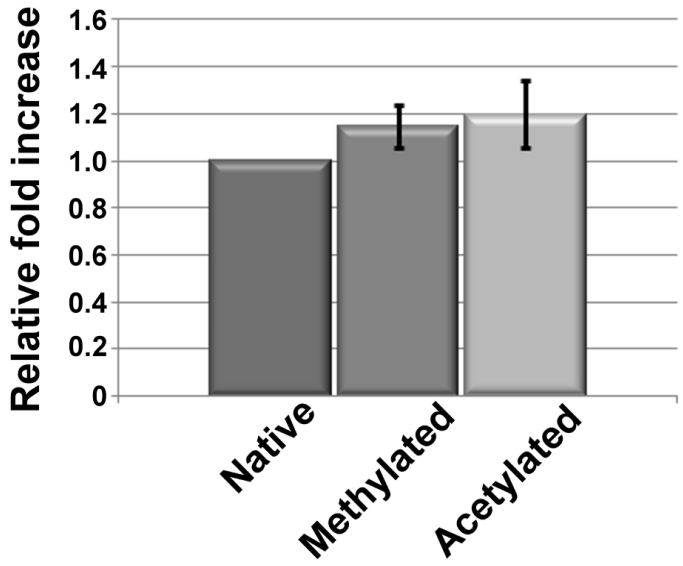

Figure 15. ***Quantification of MeCP2 transcripts by real-time RT-PCR of untreated HeLa S3 cells and cultures treated with 3-ABA (DNA hypermethylation) and butyrate (histone hyperacetylation).*** **The ΔC_t method was used to quantify the fold change in *MeCP2* mRNA following treatment compared to the native culture. *GAPDH* was used as the normalizer control gene in all three treatments. The error bars indicate the standard deviation.**

Discussion

1. MeCP2 binds to nucleosome core particles having a long linker DNA

Much of the early work describing MeCP2 interactions with chromatin involved detailed mechanistic descriptions of *in vitro* reconstitutions. A preference for cruciform-like structures and the ability of MeCP2 to displace the linker histone H1 were supported by *in vivo* studies that showed that MeCP2 formed chromatosome-like structures as it did *in vitro* (Chandler et al., 1999; Galvao and Thomas, 2005; Ishibashi et al., 2008; Nan et

al., 1997; Nikitina et al., 2007a). What had been largely overlooked, however, was how MeCP2 interacted with native chromatin.

The sucrose gradient fractionation of S1 mononucleosomes showed that MeCP2 prefers binding to nucleosomes containing DNA lengths longer than 146 bp to approximately 160 bp (Figure 10). This requirement for a longer linker DNA length was confirmed by *in vitro* studies that demonstrated that the preferential binding site for MeCP2 is within 10 bp of the pseudo-dyad axis of symmetry (Ishibashi et al., 2008).

2. MeCP2 does not act as a universal regulator of transcription

The subsequent studies discussed in this chapter addressed the effects of changes in global chromatin modifications on the distribution of MeCP2 within chromatin. Up until a few years ago, it was largely debated whether MeCP2 behaved as a global silencer of transcription or as a specific one (Nan et al., 1997; Tudor et al., 2002; Yasui et al., 2007). Because MeCP2 interacts with HDACs, it was thought that mutations or deficiencies of MeCP2 would cause changes in widespread histone acetylation, if it were a global regulator. But the results were inconclusive and did not show any consistent effect of MeCP2 mutations on histone acetylation (Urdinguio et al., 2007).

I hypothesized that wide-scale changes to chromatin modifications through DNA hypermethylation or histone hyperacetylation would affect the distribution of MeCP2 within chromatin if it were a global repressor. It was assumed that the existing chromatin modifications would be more important in directing MeCP2 deposition. If the previously considered heterochromatin-binding MeCP2 did act as a non-specific regulator of transcription, it was predicted that the increased DNA methylation would result in the

enhanced accumulation of MeCP2 within heterochromatin regions. Conversely, the increase in histone acetylation would result in a potential loss of MeCP2 from euchromatin regions and a redistribution of MeCP2. However, neither situation occurred. Treatment of HeLa S3 cells with 3-ABA to induce DNA hypermethylation did not result in a qualitative rearrangement of MeCP2 within chromatin. Rather, its distribution was similar to that of untreated HeLa S3 cells (Figure 11). The majority of MeCP2 still partitioned within the nuclease-accessible S1 fraction. Even with the increase in DNA methylation observed in the S1, there were no major qualitative differences in the relative MeCP2 amounts in the SE and P fractions compared to native chromatin (Figure 11 and Figure 12).

The widespread histone hyperacetylation following butyrate treatment had the unexpected result of causing a loss in overall MeCP2 amounts in all chromatin fractions. However, the relative distribution of MeCP2 in chromatin was still retained, and like the native chromatin, MeCP2 was primarily present in the S1 (Figure 11.B). Subtle differences in the amounts of MeCP2 in the P fractions of the treated and untreated HeLa S3 chromatin were noticed. The hypermethylated chromatin appeared to have a slight increase in MeCP2 while the hyperacetylated chromatin had barely detectable amounts of MeCP2 compared to the native chromatin. MeCP2 binding may be more susceptible to changes within the affected chromatin environment of certain transcriptionally active regions that it regulates. These combined findings suggest that MeCP2 does not indiscriminately bind chromatin regions as changes in chromatin modifications do not affect the qualitative relative distribution of MeCP2.

As a control, the fractionated chromatin from untreated and treated cultures was assessed for the presence of two different facultative heterochromatin marks: H3K9me$_2$ and H3K27me$_3$ (Peters et al., 2003). Two euchromatin marks, H3K4me$_3$ and H3K36me$_3$, were similarly assessed (Hon et al., 2009; Kolasinska-Zwierz et al., 2009; Santos-Rosa et al., 2002). H3K4me$_3$ predominated in the P fraction of each chromatin preparation and was enhanced in the S1 of the acetylated chromatin (Figure 14). H3K36me$_3$ was broadly distributed in all chromatin fractions, but was increased in the S1 of acetylated chromatin (Figure 14). H3K9me$_2$ was present in the S1 fractions of the native and histone hyperacetylated chromatin, while very little, if any, was present in the S1 or SE of the DNA hypermethylated fractions. H3K27me$_3$, a marker for facultative heterochromatin, was present primarily in the SE fractions and this distribution was not affected by either treatment condition (Figure 14). Interestingly, there appeared to be an inverse relationship between histone methylation and DNA methylation. The acetylated chromatin, which had a 6.7% decrease in S1 DNA methylation (Ishibashi et al., 2008), showed greater amounts of both H3 methylation heterochromatin PTMs compared to the native. In contrast, the methylated chromatin, which had an 11% increase in methylation in the S1 DNA, showed a decrease in these two PTMs (Figure 12).

The mechanism by which 3-ABA mediates DNA hypermethylation is not well understood, but is proposed to occur through the inhibition of poly-ADP ribosylation of linker histone H1e [H1.4 (Happel and Doenecke, 2009)]. 3-ABA, a poly(ADP-ribose) polymerase inhibitor, prevents this modification of H1e that is otherwise refractory to DNA methylation. In the absence of poly-ADP ribosylated H1e, DNA hypermethylation occurs. In 3-ABA-treated L929 mouse fibroblast cells, methyl groups were incorporated

into the DNA at an amount 60% higher than untreated cells (de Capoa et al., 1999; Zardo et al., 1997). Even against this backdrop of broad changes in epigenetic signals, that the relative distribution of MeCP2 within chromatin has not changed, may be indicative of highly specific requirements for MeCP2 to bind to nucleosomes.

It was imperative to confirm that treatment with either 3-ABA or butyrate did not affect the levels of *MeCP2* transcription. Butyrate has been previously shown to enhance or reduce the transcription of specific genes including those of linker histones (Davie, 2003; Khochbin and Wolffe, 1993). The treatment of HeLa S3 cells with butyrate had resulted in an overall reduction in MeCP2 that did not affect its comparative distribution within chromatin (Ishibashi et al., 2008). Quantification of *MeCP2* transcripts by the ΔC_t method showed that there were no major differences in the levels of *MeCP2* in either treated culture compared to the native (Figure 15). This indicated that the chemical treatment had no affect on the induction of *MeCP2* and that the decrease observed in protein levels was not a result of this.

This observation raised some points for consideration regarding the reduction of MeCP2 in the butyrate-treated chromatin. While it is possible that this decrease could be due to diminished protein translation, this may be an unlikely scenario. Another possibility is that under the acetylated conditions, MeCP2 is released from gene regions that have become transcriptionally active. The now unbound MeCP2 may then be degraded through a proteolytic mechanism (Thambirajah et al., 2009a). It has previously been shown that MeCP2 becomes phosphorylated at serine 421 under activating conditions, resulting in MeCP2 being released from its chromatin target (Zhou et al., 2006). What has not been studied is what happens to this released MeCP2. In Chapter 5,

a hypothesis is proposed that MeCP2 may be degraded by the 26S ubiquitin proteasome system based on the presence of two PEST motifs found within the N- and C-terminal ends of MeCP2 (Thambirajah et al., 2009a). If this hypothesis were true, then under hyperacetylated conditions, the MeCP2 that remains bound could correlate to genes that are terminally repressed or possibly intergenic regions. At the very least, these MeCP2-bound regions could include genes whose expression is refractory to activation by histone acetylation or butyrate treatment. It would be of considerable interest to characterize the bound DNA and the binding of MeCP2 and its PTMs in order to understand how MeCP2 differentially associates with and regulates genes. Moreover, understanding what PTMs mark MeCP2 under these different chromatin states would facilitate understanding how MeCP2 mediates variable regulation.

My work with butyrate and 3-ABA treated HeLa S3 cultures supported a growing notion that MeCP2 does not act as a global repressor of transcription, but rather, as a transcriptional regulator of specific genes (Tudor et al., 2002). This shift in perspective away from the paradigm of MeCP2 as a global silencer began perhaps as early as when it was demonstrated that MeCP2 could regulate the expression of *BDNF* in an activity-dependent manner (Chen et al., 2003; Martinowich et al., 2003). In 2005, Horike et al described the formation of silent chromatin loops containing the *Dlx5-Dlx6* gene locus by MeCP2 and the repression of gene expression (Horike et al., 2005). More recently, detailed analyses of MeCP2-bound genes undertaken by two independent groups showed that MeCP2 interacted with specific gene regions and that the majority of MeCP2-bound promoters were active (Chahrour et al., 2008; Yasui et al., 2007). Most of this work was done in the context of understanding MeCP2 regulation in neuron cell systems. As

mutations in MeCP2 cause Rett syndrome, much of the research interest surrounding MeCP2 has focussed on the brain. But MeCP2 is a ubiquitously expressed protein and has been shown to be present in many tissues within the body. The next chapter will discuss work that sought to understand how MeCP2 might differentially regulate genes in various primary tissues *in situ*.

Chapter 4 – The tissue-specific chromatin distribution of MeCP2 is influenced by histone variants and post-translational modifications

This chapter was adapted from a manuscript prepared for publication:

Thambirajah, A.A. and Ausió, J. (2010) The tissue-specific chromatin distribution of MeCP2 is influenced by histone variants and post-translational modifications. (Submitted)

A.A.T. was primarily responsible for the experimental design and performed all of the experimental work described. A.A.T. conceived and wrote the manuscript.

Abstract

MeCP2 is a chromatin binding protein that suppresses transcription of its bound genes. The nature of its binding to reconstituted chromatin templates has been well-characterized *in vitro*. However, how it interacts within native chromatin has, for the most part, been under-studied. MeCP2 has a distinct distribution within fractionated chromatin that is unique to brain, liver and testis. The brain has significantly more MeCP2 and *MECP2* transcripts per unit mass of DNA than testis or liver. Most of the MeCP2 in brain is present within nuclease-accessible chromatin regions. In brain cortex heterochromatin and euchromatin fractions, novel associations of MeCP2 with mononucleosomes containing histone H2AX, H3K9me$_2$, and H3K27me$_3$ are described. The functional compartmentalization of MeCP2 within different chromatin types may be directed by its associations with nucleosomes containing specific histone variants and/or post-translational modifications.

Introduction

The precise and dynamic modulation of chromatin structure is essential for context-specific transcription- or replication-dependent processes. The disruption of such processes has been linked to the etiology of numerous diseases, underscoring the critical importance of proper chromatin regulation. Mutations in MeCP2 have been linked to RTT and other neurological abnormalities (Amir et al., 1999; Rett, 1966).

The majority of work done to characterize MeCP2 interactions with chromatin structures has been done with reconstituted templates. Under these *in vitro* conditions, MeCP2 has been shown to bind to methylated or unmethylated templates with a preference for the former, particularly in the presence of competitor DNA (Ishibashi et al., 2008; Nikitina et al., 2007b). Upon binding to nucleosomes, MeCP2 forms chromatosome-like structures and may facilitate inter-nucleosomal fibre interactions *in vitro* (Nikitina et al., 2007a). MeCP2 can compete with H1 for binding to the linker DNA and can displace approximately 40% of the bound H1 (Nan et al., 1997). In support of this, fractionation of native mononucleosomes showed that MeCP2 bound to (or protected) nucleosomes with approximately 160 bp of DNA (Ishibashi et al., 2008).

What has perhaps been overlooked is how MeCP2 interacts within native chromatin and what factors govern this relationship. *In vitro* reconstitutions allow for a detailed, mechanistic analysis of isolated variables. However, this approach does not address how accurately the *in vitro* constructs recapitulate the heterogeneity of native interactions in chromatin derived from different tissues.

The object of this work was to investigate nucleosomal components that influence the interaction of MeCP2 with native chromatin. The focus of considerable MeCP2

research has been on its neurological implications. But MeCP2 is ubiquitously expressed throughout many tissues (Shahbazian et al., 2002). As proper transcriptional regulation by MeCP2 is critical for normal development (Guy et al., 2007), it is of interest to know whether MeCP2 behaves similarly with chromatin of different tissues when compared to the brain.

MeCP2 is localized to a broad range of chromatin types, supporting observations that there is a potential plurality to MeCP2 function (Ishibashi et al., 2008). The distribution of MeCP2 in chromatin of brain, liver and testis was investigated. Besides the requirement for sequence-specificity and DNA methylation, how does MeCP2 distinguish its regulation of transcription in different chromatin contexts? The possibility that other nucleosomal factors may govern MeCP2 residence or regulation was investigated, particularly with respect to histone variants and PTMs (Thambirajah and Ausió, 2009). MeCP2 has a distinct tissue-specific distribution in fractionated chromatin. As well, novel associations between MeCP2 and mononucleosomes containing H2AX, $H3K27me_3$, or $H3K9me_2$, were observed in heterochromatin and euchromatin. The importance of epigenetic signals such as DNA methylation, histone variants and PTMs in the temporal control of gene expression is becoming better understood in a broad range of contexts including development and regular homeostatic maintenance. MeCP2 may be able to interpret or act upon a broad range of such signals to fine-tune its regulatory roles in a tissue- and/or activity-dependent manner.

Materials and Methods

***Preparation of nuclei*. Rat or sheep brain nuclei preparations.** Lamb brains were kindly provided by Michael Peterson of the Cole Creek Farm Ltd. abattoir in Metchosin, B.C., Canada. Rat or sheep brains were homogenized on ice using a Polytron blender in 3x volumes (per weight) of 0.32 M sucrose, 1 mM $MgCl_2$, 0.5% (w/v) NP-40 and Roche Complete Protease Cocktail Inhibitor (Pearson et al., 1983; Thompson, 1973). The homogenate was centrifuged using a Beckman centrifuge and JA-20 rotor at 10 000 rpm for 15 minutes at 4^{o}C. The resulting pellet was resuspended in 4x volumes of 2.0 M sucrose, 1 mM $MgCl_2$, and protease inhibitor. A subsequent centrifugation was done using a Beckman L8-70M ultracentrifuge and SW28 rotor at 22 000 rpm for 32 minutes at 4^{o}C (deceleration = 7). The resulting nuclei pellets were resuspended in buffer B (50 mM NaCl, 10 mM PIPES pH 6.8, 5 mM $MgCl_2$, 1 mM $CaCl_2$, and Roche Complete Protease Cocktail Inhibitor), to remove sucrose, and centrifuged using a JA-20 rotor at 5000 rpm for 10 minutes at 4^{o}C.

Rat liver and testis nuclei preparations. Rat liver was homogenized in 4x volumes of buffer A (0.25 M sucrose, 60 mM KCl, 15 mM NaCl, 10 mM MES pH 6.5, 5 mM $MgCl_2$, 1 mM $CaCl_2$, 0.5% Triton X-100, Roche Complete Protease Cocktail Inhibitor) and testis tissue in 2x volumes of buffer A (on ice). The homogenate was filtered through 1-2 layers of pre-wet cheesecloth and incubated on ice for 5 minutes. Centrifugation was performed using a JA-20 rotor (and for all future centrifugation steps) at 5000 rpm for 10 minutes at 4^{o}C. The pellets were resuspended in buffer A and

centrifuged again. The pellets were rinsed in buffer B and centrifuged as before (Abbott et al., 2005; Ausió et al., 1989; Wang et al., 2001).

Digestion and fractionation of chromatin. Isolated nuclei were resuspended in buffer B to a final concentration of 4 mg/mL as determined by the A_{260} readings of a nuclear suspension in 0.5% SDS. Chromatin was digested using MNase (Worthington) at a concentration of 30 units/mg of DNA at 37^{o}C for 15 minutes as described previously (Ishibashi et al., 2008). The S1, SE, and pellet (P) fractions were produced according to the protocol described in Chapter 3 (Wang et al., 2001).

Gel electrophoreses. SDS-PAGE (Laemmli, 1970), AUT-PAGE (Abbott et al., 2001), AU-PAGE (Ausió and van Holde, 1986), native-PAGE (Yager and van Holde, 1984), and agarose gels were performed as described in Chapter 3.

Western blotting. Western blotting was done according to the protocol previously described in (Ishibashi et al., 2008). In addition to the antibodies listed in Chapter 3, blots were incubated with the following antibodies and dilutions overnight at 4^{o}C. 1:3333 α-H2AX (Applied Biological Materials Inc., abm), 1:1000 α-γ-H2AX (Millipore), 1:1000 α-H2A.Z (Abcam), and 1:1000 α-H2A.Z acetylated (a generous gift from Dr. Crane-Robinson). The secondary antibodies and the detection methods used are detailed in Chapter 3.

Preparation of cell cultures and tissues samples for real-time quantitative RT-PCR.

Rat brain, liver, and testis total RNA extraction. Tissues were extracted from 4 male rats and stored in RNAlater (QIAGEN) at 4^{o}C until RNA extraction. Tissues were then flash-frozen in liquid nitrogen and ground to a fine powder using a mortar. Approximately 50 – 100 mg of tissue powder was homogenized in 1 mL of Trizol (Invitrogen). Homogenized samples were flash-frozen in liquid nitrogen and stored at -80^{o}C until the RNA was extracted according to the manufacturer's instructions.

cDNA synthesis from total RNA. SuperScript^{TM} II reverse transcriptase (Invitrogen) was used to generate cDNA from 1 µg total RNA as described in Chapter 3.

Quantitation of MECP2 transcripts by real-time PCR. The comparative C_t ($2^{-\Delta\Delta Ct}$) method was used to quantify the relative fold changes in *MECP2* expression levels between the different tissues (Livak and Schmittgen, 2001; Walzak et al., 2008; Wong and Medrano, 2005). Serial dilution validation assays were performed as described in the previous chapter.

Quantitation of MECP2 mRNA in rat brain, liver, and testis. Analysis was done as described for the HeLa S3 cultures (Chapter 3) using the comparative C_t ($2^{-\Delta\Delta Ct}$) method (Livak and Schmittgen, 2001). A mixed cDNA comparator was prepared in which 2 µL of each 1/20 cDNA dilution for every tissue was combined together and run as a separate sample (Walzak et al., 2008). Every tissue cDNA 1/20 dilution was run in triplicate as were non-template (primer) controls. Two reference genes, *GAPDH* and the *GC-rich*

promoter binding protein 1 (*GPBP1*) were used to normalize the target gene (*MECP2*) and to account for any variations that may be present in reference gene levels between the different tissues (Kwon et al., 2009). The primer sequences used for each gene were as follows. *MECP2* primers: forward 5'-GCCTCTGCTTCTCCCAAAC and reverse 5'-CCACCTCCCTCACCCTTAC (485 bp amplicon). *GAPDH* primers: forward 5'-TCAAGAAGGTGGTGAAGCAG and reverse 5'-CCTGTTGTTATGGGGTCTGG (376 bp amplicon). *GPBP1* primers: forward 5'- CTTAGTCCCCAAACCTGCTG and reverse 5'-TGAGAAATCACCGAGGCATT (462 bp amplicon).

Native co-immunoprecipitation of MeCP2-bound mononucleosomes. Sheep neural cortex were used to produce the mononucleosome-containing S1 and SE according to the chromatin fractionation procedure described earlier. Cortices were used as the brain has a greater amount of MeCP2 relative to the nucleosome content compared to other tissues. For the S1 and SE co-immunoprecipitations, an excess of chromatin was used to ensure that the antibody binding was saturated. In paired α-MeCP2 and normal rabbit IgG pull-down reactions, 350 µg of S1 chromatin were added to 50 mM NaCl, 20 mM Tris pH 7.5 to a final volume of 1.0 mL. In similarly paired pull-down reactions, 250 µg of SE chromatin were added to 100 mM NaCl, 20 mM Tris pH 7.5 and brought to a final concentration of 50 mM NaCl in a total volume of 1.0 mL. 5.0 µg of salmon sperm DNA (Invitrogen) were added to block any non-specific interactions. The samples were pre-cleared for 5 minutes at 4^{o}C with tumbling using 15 µL of a 50:50 slurry of Pierce protein A/G agarose beads. This was initially done to reduce any non-specific binding to the beads (Spencer et al., 2003). Following a brief centrifugation to remove the beads (3000

rpm, 3 minutes, 4°C), 12 µL of each precleared input supernatant were kept for later analysis. To the MeCP2 pull-downs, 15 µL of 0.6 mg/mL α-MeCP2 antibody (Sigma) were added to the remaining supernatant. 9 µL of a 1 mg/mL normal rabbit IgG (Sigma) were added to the non-specific pull-down control. Reactions were tumbled at 4°C overnight. 100 µL of the protein A/G bead slurry were added to all of the reactions and tumbled at 4°C for 2 hours. Centrifugation was performed as above and the unbound supernatant was retained. Pull-down beads were subsequently washed by inversion in 1.0 mL each of 5 mM NaCl, 50 mM NaCl, and 100 mM NaCl, all in the presence of 20 mM Tris pH 7.5. The supernatants were kept after each wash step. The recovered bound beads were then resuspended in 20 µL 2X SDS sample buffer and heated at 100°C for 3 minutes. Analysis of the bound fractions was performed by SDS-PAGE followed by western blotting.

Reverse-phase HPLC analysis of the histone content in rat brain, liver and testis.

Nuclei from each of the three tissues were isolated as described above. Histones (and other basic proteins) were extracted by homogenization of the nuclei in a final concentration of 0.4 N HCl as described in (Ausió and Moore, 1998). Proteins (200 µg) from each tissue were resuspended in dH_2O and loaded onto a Varian C4 column (250 mm X 4.6 mm) and eluted under an increasing gradient of acetonitrile in 0.1% TFA. A flow rate of 1.0 mL/minute was used and the protein elution was monitored at a wavelength of 230 nm (Ausió and Moore, 1998; Moore et al., 1997). The acetonitrile gradient was as follows: 0-5% - 1 minute, 5-25% - 10 minutes, 25-30% - 15 minutes, 30-35% - 20 minutes, 35-40% - 20 minutes, 40-43% - 10 minutes, 43-55% - 50 minutes, 55-

90% - 5 minutes, 90-100% - 20 minutes, 100-100% - 5 minutes, 100-0% - 10 minutes, and 0-0% - 1 minute.

Results

1. Comparison of chromatin variation within different tissues

As MeCP2 does not act as a global transcriptional regulator in cultured cells, it was of interest to characterize how MeCP2 behaved in tissues. Furthermore, we sought to determine what other nucleosomal factors might specify MeCP2 localization within different chromatin domains. Prior to characterizing variations in MeCP2 distribution within rat tissues or the dependence of MeCP2 binding on specific histone variants or PTMs, it was important to establish the background histone variability in chromatin composition in brain, liver and testis (Figure 16).

Many of the functional studies of MeCP2 have focussed on its role in development of brain or in regulating neural genes (such as *BDNF*). However, the distribution of MeCP2 in all chromatin types in brain is not understood. Liver was used as a somatic tissue comparison. It was thought that the regulatory functions of MeCP2 in the liver would not be the same as in the brain, and hence, this could possibly be reflected in differences in its chromatin distribution. And finally, the use of testis served as a germline or non-somatic comparison. Although a mix of developmental cell types is present in testis, mature sperm is typically transcriptionally inactive. If any MeCP2 is present, it may show a broad chromatin distribution.

Testis is well known to have several testis-specific histone variants, and this is apparent when comparing acid-extracted histones from the nuclei of testis to either liver

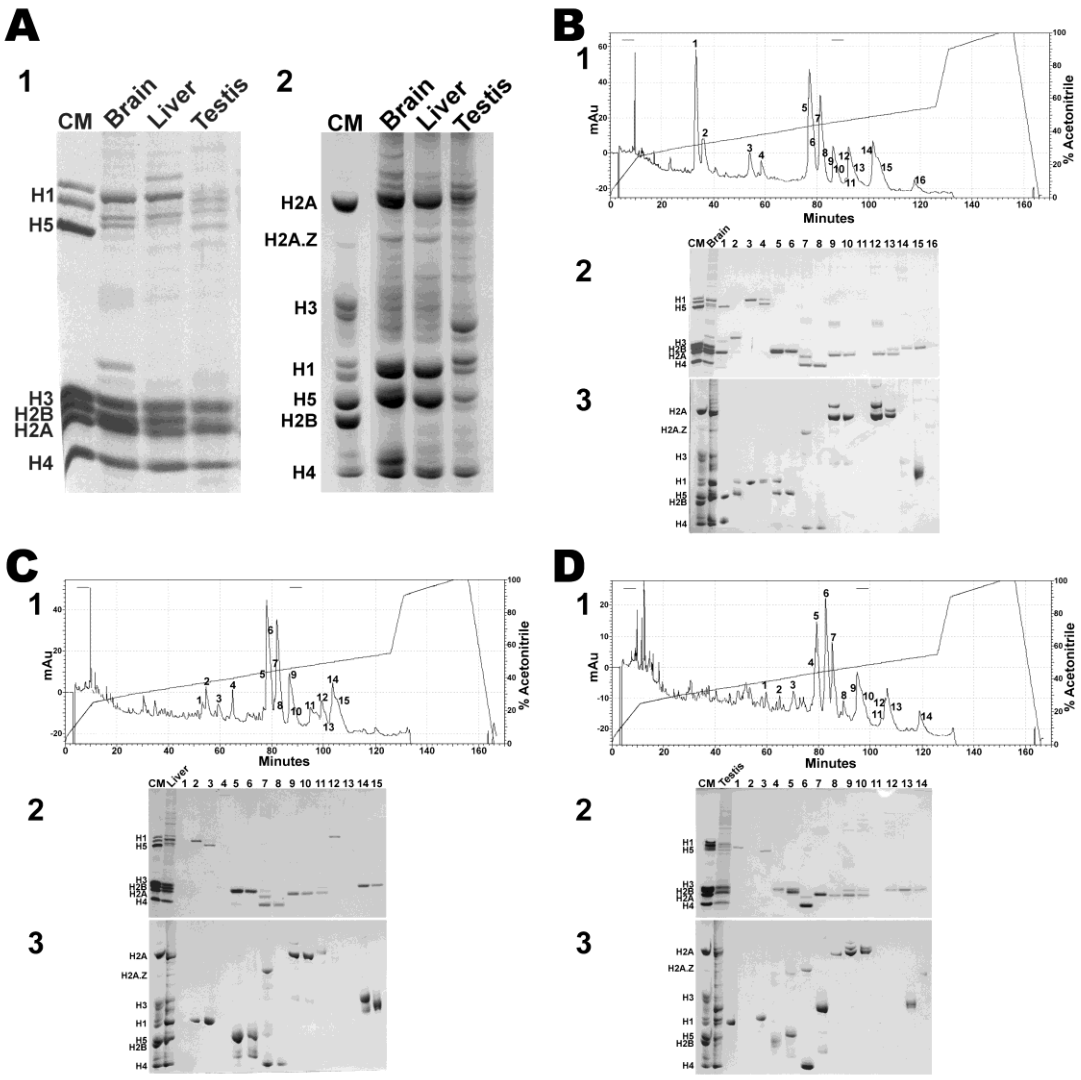

Figure 16. ***Histone composition variability in different rat tissues.*** **Nuclei were separately obtained from rat (whole) brain, liver, and testis and acid-extracted to obtain the histones free of contaminating DNA. A. 1. SDS-PAGE of histones obtained from rat tissues. 2. Acetic acid – urea – triton (AUT) PAGE analysis of rat tissue histones. B. HPLC separation of rat brain histones. C. HPLC separation of rat liver histones. D. HPLC separation of rat testis histones. For B, C, and D, the component figures numbered 1, 2, and 3 are correspondingly the same for each tissue. 1. HPLC chromatogram of the elution profile of histones under an increasing acetonitrile gradient. 2. SDS-PAGE analysis of selected fractions as numbered in 1. 3. AUT analysis of histones as per the SDS-PAGE. CM refers to the chicken marker histone protein standard.**

or brain by SDS-PAGE or AUT-PAGE (Figure 16.A) and also following RP-HPLC separation (Figure 16.B, C, D). Though both somatic tissues, the subtle differences in the histone variant and PTM content between liver and brain are better visualized following RP-HPLC separation. For instance, the brain appears to have a different proportion of H2A isoforms, which may also include modified forms (Figure 16.B) (Bosch and Suau, 1995). Furthermore, as seen by SDS-PAGE, the H2B complement in brain has a faster electrophoretic mobility than the liver H2B (Figure 16.A).

Following MNase digestion, the percent composition of the fractionated chromatin in each tissue was: brain- S1 (14%), SE (24%), and P (62%); liver- S1 (27%), SE (38%), and P (35%); and testis- S1 (14%), SE (27%), and P (59%). The histone compositional differences are enhanced when chromatin from the different tissues is fractionated into the S1, SE, and P (Figure 17). In brain, H2A.Z is present in nearly equivalent amounts to H2A in the S1 fraction, whereas all other tissues and fractions display a lower amount of this variant (Figure 17.A). H2AX was present in equal amounts in the S1, SE, and P fractions of brain and testis, although the testis overall had a significantly higher amount of H2AX. Very little H2AX was observed in the liver and was mostly located within the SE (Figure 17.B). γ-H2AX was present in greater amounts in all testis fractions compared to the other tissues. The P contained the most γ-H2AX in testis. In the brain, γ-H2AX was mainly present in the S1. In the liver and the brain, H3K9me$_2$ was broadly distributed in all fractions in equivalent amounts, whereas only the S1 and SE of testis contained H3K9me$_2$. Interestingly, the S1 testis fraction showed a doublet which may be due to a modified testis-specific H3 isoform (Figure 17.B). No H3K27me$_3$ was observed in the testis, but H3K27me$_3$ was present in the SE of brain in

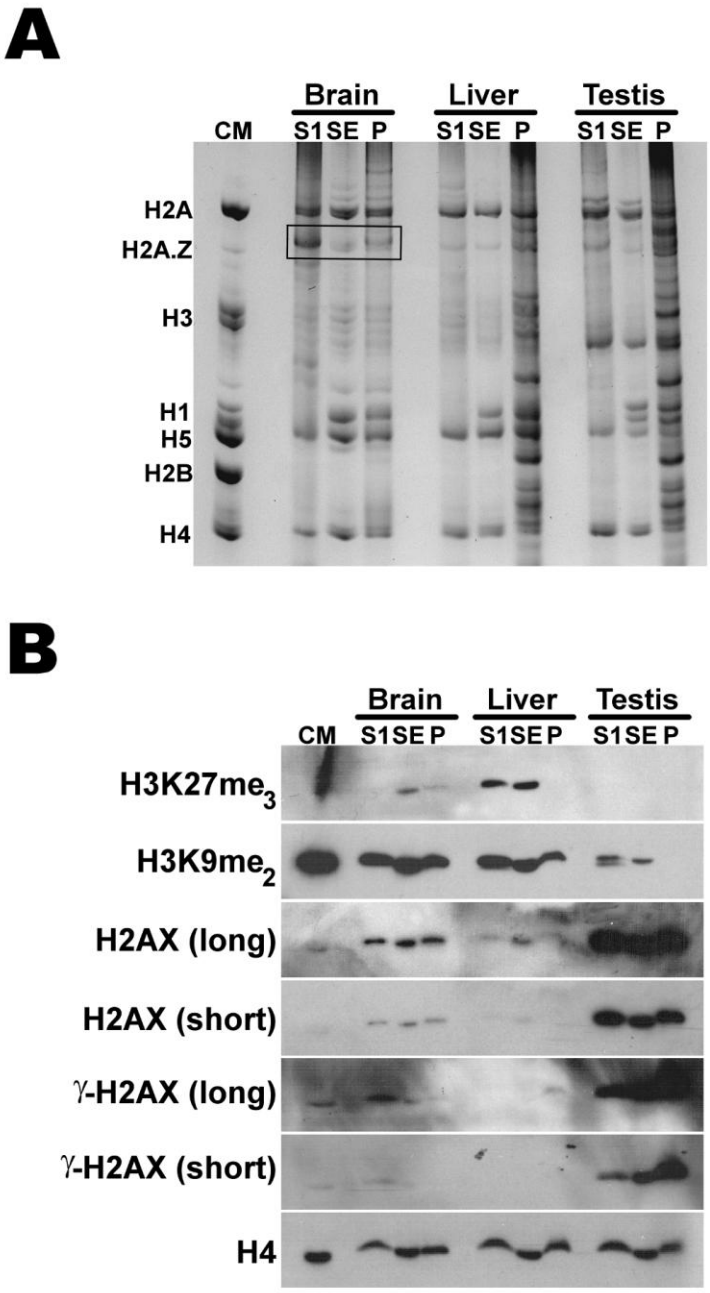

Figure 17. ***Variation in histone variant and PTM distribution in fractionated chromatin of rat brain, liver, and testis tissues.*** **A. AUT-PAGE analysis of the S1, SE, and P chromatin fractions of each tissue. The AUT-PAGE is ideal for visualizing different variant forms, in particular, H2A.Z (see box). B. Western blot analysis of the histone variant and PTM distribution within the different chromatin fractions obtained. Loading in (A) and (B) were done according to the total histone content, with western blotting for H4 done as a confirmation.**

lower amounts compared to the S1 and SE of liver. The liver S1 and SE had equivalent levels of H3K27me$_3$ (Figure 17.B). Given the chromatin composition heterogeneity among these tissues, it is conceivable that this variability could influence the deposition and function of MeCP2, which is ubiquitously expressed in all of them.

MeCP2 differentially distributes within fractionated chromatin in a way that is dependent upon tissue type

The chromatin from whole brain, liver, and testis were fractionated into the S1, SE, and P components following MNase digestion. The associated DNA in each chromatin fraction was analyzed by native PAGE (Figure 18.A). Each tissue displayed a consistent nucleosome patterning, similar to that of Figure 11.A. An SDS-PAGE analysis of the normalized total histones in each fraction is shown in Figure 18.B. Relative amounts of MeCP2 were qualitatively determined following western blot analysis. Compared to the liver or testis, the brain contained the greatest amounts of MeCP2 (Figure 18.C). The vast majority of MeCP2 was within the S1 fraction and correspondingly lesser amounts were present in the SE and P fractions. Interestingly, the liver has equivalent amounts of MeCP2 within the S1 and P fractions, and a similar amount was seen in the testis S1. The S1 contained the greatest amount of MeCP2 in the testis (Figure 18.C). Following a longer exposure, a small amount of MeCP2 was observed in the SE of the liver, and in the testis, the SE and P had equivalent amounts of MeCP2 that were less than that of the S1 (Figure 18.C).

To ensure that the distribution of MeCP2 in the brain chromatin was not influenced by the length of digestion time, a time-course digestion of isolated nuclei was

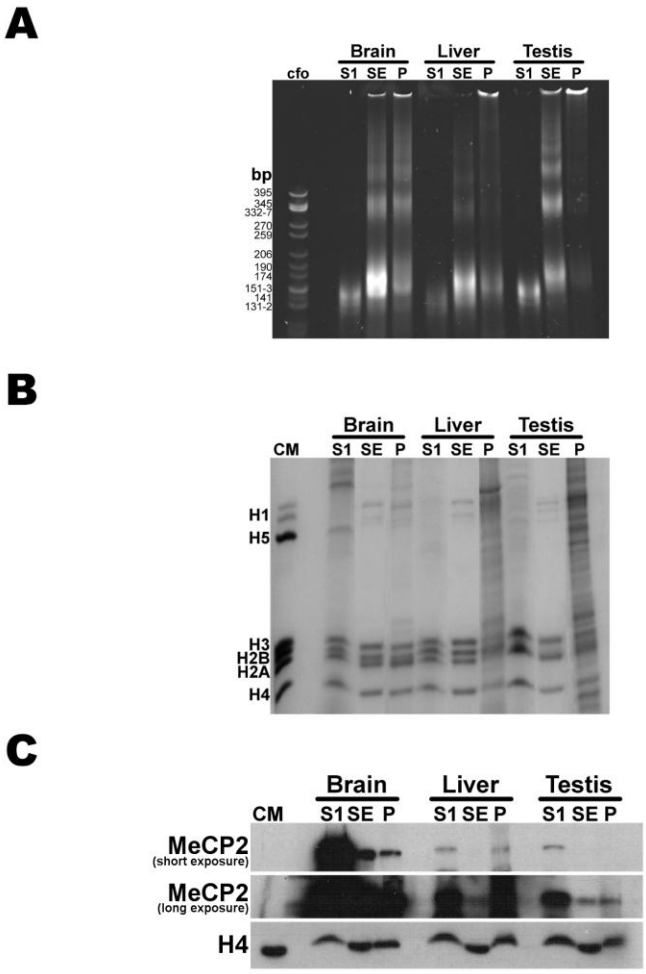

Figure 18. ***Distribution of MeCP2 within fractionated tissue chromatin.*** **A. Native PAGE analysis of the DNA present in the S1, SE, and P chromatin fractions of rat brain, liver and testis. A pBR322 – CfoI-digested marker was used for a base pair size comparison. In all tissues, the S1 contains primarily mononucleosomes, while the SE, in addition to mononucleosomes, contain di-, tri-, and higher oligonucleosome forms. The P chromatin composition is typically quite similar to the SE, but additionally contains longer chromatin strands which do not resolve in the native PAGE. B. SDS-PAGE analysis of the histones present in each chromatin fraction. C. Variation in MeCP2 distribution in the fractionated chromatin of rat brain, liver and testis. Two differently timed exposures (short and long) of the MeCP2 western blot were taken to highlight the differences in MeCP2 deposition within the chromatin fractions of the different tissues. The H4 western blot shows the equivalent loading of each respective fraction.**

done using MNase (Figure 19.A). Nuclei were digested for 5, 10, and 15 minutes and fractionated into the S1, SE, and P as described before. As seen in Figure 19.A., at the 5 minute digestion time, the majority of the MeCP2 is already within the S1 and less within the SE and P. Even though there was insufficient material for the normalization of H4 for the 5 minute S1, the distribution of MeCP2 within the S1, SE, and P reflects what is seen with longer digestion times. The only subtle variation is the release of more MeCP2 from the insoluble P into the SE (and possibly the S1) with increased digestion times (Figure 19.B).

In order to ascertain whether the higher MeCP2 protein levels in the brain were the result of enhanced translation or correlated to a greater amount of *MECP2* transcripts, *MECP2* in each tissue was quantified by real-time RT-PCR (Figure 20). Analysis was done using the ΔC_t method and normalized to a mixed cDNA comparator with both *GAPDH* and *GPBP1* used as internal controls. The brain had a relative fold difference of 19.47 ± 0.504 (S.D.) times more *MECP2* than the mixed cDNA comparator (Figure 20). The liver had a relative fold difference of 0.328 ± 0.108 (S.D.) while the testis showed a difference of 0.851 ± 0.02 (S.D.) (Figure 20). By this analysis, the brain had greater than 22 times more *MECP2* mRNA compared to testis, and more than 59 times the amount in liver. This relative overabundance of *MECP2* mRNA in the brain could certainly account for the differences in protein amounts observed by western blotting.

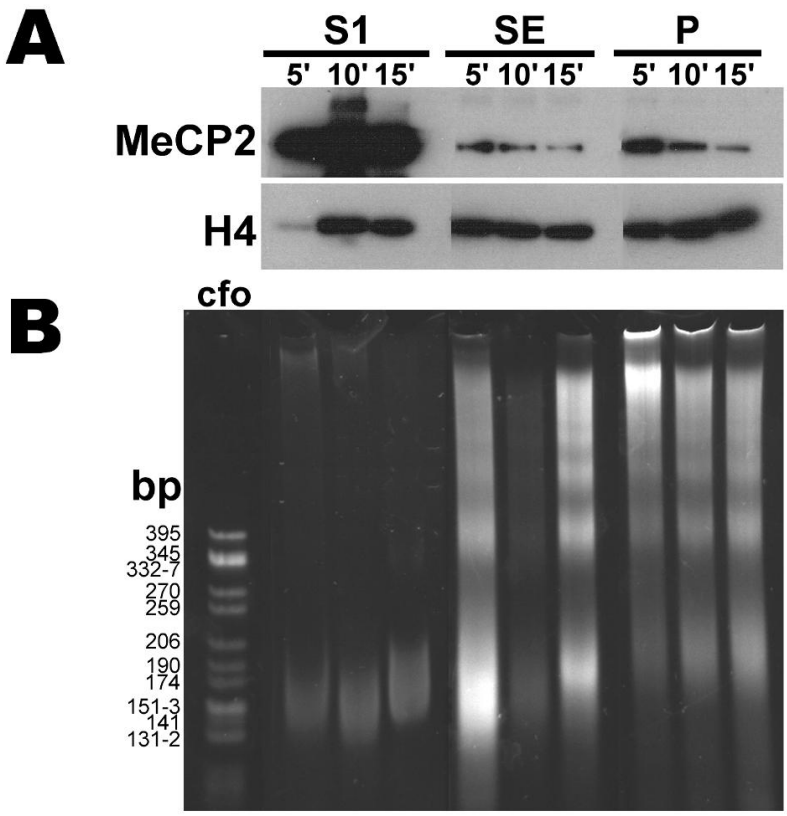

Figure 19. ***Micrococcal nuclease time course digestion of rat brain chromatin.*** **This assay was done to control for the effects of the length of digestion (5, 10 and 15 minutes) on the partitioning of MeCP2 between the S1, SE and P fractions. A. The top two panels are of western blots for MeCP2 and H4 (to control for loading), respectively. B. The native PAGE shows the corresponding DNA of each chromatin fraction at the different time points. A pBR322 – *Cfo*I-digested marker served as the base pair ladder.**

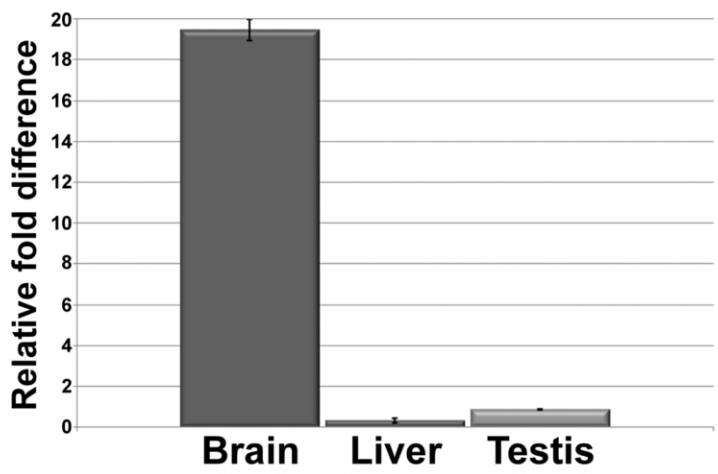

Figure 20. ***Quantitative real-time RT-PCR of MECP2 transcripts in rat brain, liver and testis.*** **The ΔC_t method was used to determine the relative fold difference of *MECP2* in each tissue compared to a comparator comprised of a mixed pool of all the cDNA samples prepared from each tissue tested. *GAPDH* and *GPBP1* were used as the normalizer reference genes. The standard deviation is indicated by the error bars.**

2. MeCP2 binds to nucleosomes containing the histone variant H2AX and methylated H3, respectively

In order to identify what may influence MeCP2 localization to specific nucleosomes in different chromatin environments, potential nucleosomal factors were investigated (Figure 21). These included specific histone variants or histone PTMs which could serve as epigenetic signals to distinguish MeCP2 binding between heterochromatin and euchromatin. Native co-immunoprecipitations of mononucleosomes obtained from S1 or SE chromatin fractions were performed using an α-MeCP2 antibody and were then probed by western blot for the respective histone variant or PTM. Cross-linking was not

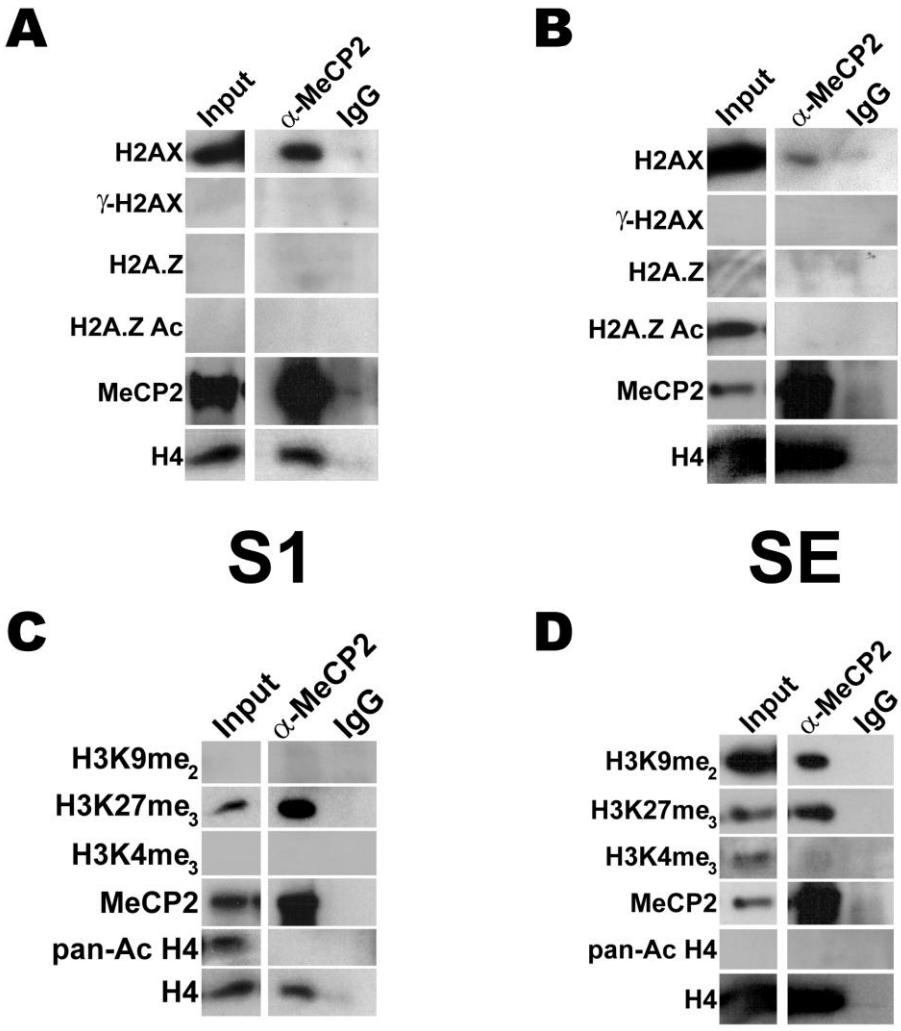

Figure 21. ***The histone variant and PTM nucleosomal interacting partners of MeCP2 within S1 and SE chromatin obtained from sheep cortex.*** **Mononucleosomes from S1 and SE fractions were co-immunoprecipitated under native conditions using an α-MeCP2 antibody. Any potential interactions between MeCP2 and nucleosomes containing specific histone variants or histone PTMs were assessed by western blotting. Normal rabbit IgG was used as a non-specific control and the pull-downs for both α-MeCP2 and IgG were compared to a normalized sample input used in the co-immunoprecipitations. A and B. Co-immunoprecipitated mononucleosomes were probed by western blotting for specific H2A variants and PTMs in the S1 (A) and SE (B) chromatin fractions. C and D. Interactions between MeCP2 and mononucleosomes containing H3 PTMs were assessed by western blotting pull-downs of both S1 (C) and SE (D) chromatin fractions.**

utilized to preserve the S1 and SE fractionation. In the S1, a strong interaction was observed for MeCP2 with H2AX-containing mononuclesomes. No associations, however, were observed for nucleosomes with γ-H2AX, H2A.Z, or acetylated H2A.Z (Figure 21.A). Co-immunoprecipitated mononucleosomes were probed for H4 and MeCP2 by western blotting as a control. In the SE, a weaker interaction was seen for MeCP2 and H2AX-containing mononucleosomes, but no interactions were seen for γ-H2AX, H2A.Z or acetylated H2A.Z (Figure 21.B).

Interactions of MeCP2 with mononucleosomes containing specific H3 PTMs were investigated as well. In the SE, MeCP2 associated with mononucleosomes containing H3K9me$_2$ and in a separate pull-down, with H3K27me$_3$. No interactions were observed for either H3K4me$_3$ or pan-acetylated H4 (Figure 21.D). Similar interactions were observed in the S1 of MeCP2 pull-downs of mononucleosomes; however, no interactions were observed with H3K9me$_2$ (Figure 21.C). Interestingly, the H3K27me$_3$ association was greatly enriched above the background S1 input levels (Figure 21.C).

Discussion

1. MeCP2 is unevenly distributed and expressed across different tissues

How MeCP2 interacts with the chromatin of different tissues and cell types, while having been largely ignored, has tremendous relevance for understanding the breadth of roles MeCP2 undertakes. Furthermore, it was of key interest to determine whether there were specific nucleosomal cues that might distinguish or facilitate the association of MeCP2 with different chromatin types (*i.e.*, euchromatin and heterochromatin).

When the chromatin composition of these tissues is considered, it is evident that a diverse heterogeneity exists between the brain, liver, and testis simply in terms of the general histone composition (Figure 16 and Figure 17). When overlaid with variable DNA methylation and the activities of other non-histone *trans*-acting factors, it is not implausible to conjecture that this histone variability permits the tissues or specific cell types to modulate their unique transcriptional needs. And it is against these very different chromatin canvases that MeCP2 is binding to and directing the transcription requirements of particular genes in a potentially temporal-dependent manner.

There was a differential distribution of MeCP2 between the brain, liver and testis (Figure 18). MeCP2 was most abundant in the brain compared to the liver and the testis. In the individual tissues, the majority of the MeCP2 was located within the S1 of the brain and testis, whereas in liver, MeCP2 was present in roughly equivalent amounts in the S1 and insoluble P (Figure 18.C). This variability in MeCP2 deposition may indicate that MeCP2 has distinct regulatory roles in these different tissues.

Real-time RT-PCR quantification of *MECP2* transcripts correlated with the qualitative protein levels visualized by western blotting. Using the ΔC_t method, the brain had more than 22 times the amount of *MECP2* mRNA compared to the testis and 59 times more than the liver (Figure 20). A previous study assessed the amounts of MeCP2 in various tissues by western blotting and *MeCP2* transcripts by northern blotting, but using different approaches to normalization (Shahbazian et al., 2002). In sharp contrast to our results, no correlation between protein and mRNA expression was found (Shahbazian et al., 2002). In the ΔC_t method described here, two internal controls, *GAPDH* and *GPBP1*, were utilized to account for variations in these normalizing genes

in the different tissues. It has been reported that the mRNA levels of housekeeping genes used as internal controls can vary between tissues and even disease states (Kwon et al., 2009).

2. MeCP2 interacts with nucleosomes containing specific histone variants and post-translational modifications

Having established that MeCP2 is present in a broad range of chromatin environments, it was of interest to determine what nucleosomal factors may be involved in its distribution. Other studies have shown that MeCP2 not only associates with promoter regions, but also with intergenic regions and other regions outside genes (Chahrour et al., 2008; Yasui et al., 2007). DNA methylation within a sequence specific context has been shown to direct MeCP2 binding, but even the requirement for DNA methylation is not an absolute. At least 4 adenine or thymine residues within an 11 base pair region are required for MeCP2 to bind to the methylated 5'-CpG (Klose et al., 2005). This requirement may not be exclusive to MeCP2 when one considers that the periodic placement of certain dinucleotides (*i.e.* CG, AA or TT, depending on the organism) can facilitate nucleosome positioning (Bettecken and Trifonov, 2009). Is a simple binary mechanism of DNA methylation sufficient to account for the plurality of MeCP2 binding within chromatin?

Given all of this, I decided to check for the presence of other nucleosomal factors that could influence and distinguish MeCP2 binding (Thambirajah and Ausió, 2009). As the H2A C-terminal tail and the H3 N-terminal tail exit the nucleosome (Luger et al., 1997) close to the site where MeCP2 has been proposed to bind (Ishibashi et al., 2008;

Nikitina et al., 2007a), candidate variants and PTMs of these two core histones were investigated.

The histone variant H2A.Z has been shown to mark the 5' end of promoters and upon activation, become acetylated. Structural studies of native H2A.Z showed that it associated with stable chromatin structures, but this effect was reduced when it and the chromatin environment were acetylated (Thambirajah et al., 2006). This variant also demarcates the borders between euchromatin and heterochromatin and seemed a likely candidate for MeCP2 which also is present at promoter regions that are primed for activation (Chen et al., 2003; Martinowich et al., 2003; Meneghini et al., 2003). In addition, like MeCP2, H2A.Z is very abundant in the S1 fraction in brain (Figure 17.A box). Despite this, co-immunoprecipitation of MeCP2 with nucleosomes did not show any association with either H2A.Z or acetylated H2A.Z in either the S1 or SE chromatin fractions (Figure 21.A and B). It has recently been shown in *Arabidopsis thaliana* that H2A.Z and DNA methylation are antagonistic marks that prevent the other from occupying the same chromatin region (Kobor and Lorincz, 2009; Zilberman et al., 2008). This observation may account for the lack of association between MeCP2 and H2A.Z nucleosomes.

A novel and strong association was observed between MeCP2 and H2AX-containing mononucleosomes in S1 chromatin (Figure 21.A). To a lesser extent, MeCP2 was also similarly associated with H2AX in the SE (Figure 21.B). MeCP2 interacts with the Brahma subunit of the SWI/SNF remodelling complex (Harikrishnan et al., 2005) and both MeCP2 and SWI/SNF have been shown to cyclically associate with an inducible promoter undergoing transcriptional activation (Metivier et al., 2008). This latter

association is coupled to the demethylation of the promoter DNA through base excision (Metivier et al., 2008). The SWI/SNF complex has been shown to facilitate the phosphorylation of H2AX through the recruitment of kinases in response to DNA damage (Ray et al., 2009; Wuebbles and Jones, 2004). The binding of MeCP2 to H2AX nucleosomes may be functionally linked through SWI/SNF or the need for DNA repair mechanisms. A putative model discussing the functional relevance of MeCP2 – H2AX-nucleosome interactions is discussed in Figure 22.A. No associations were observed between MeCP2 and γ-H2AX in either the S1 or SE fractions (Figure 21.A and B). However, if any interactions were weak or transient, the native co-immunoprecipitation method may not have been sensitive enough to ascertain this association and fixed conditions may be required.

MeCP2 has been shown to interact with the KMT responsible for mediating H3K9 methylation, a mark associated with repressed transcription (Fuks et al., 2003b). Such methyltransferase activity was also linked to Dnmt3a (Fuks et al., 2003a). H3K9me$_2$ was observed to have a broad chromatin distribution throughout the whole brain, although it was not observed in the cortex S1 fraction (Figure 17.B and Figure 21.C). MeCP2 interacted with mononucleosomes containing this PTM in the SE fraction, but not in the S1 fraction (Figure 21.C). The association of MeCP2 with H3K9 methylation has been described in the IL-6 gene region (Dandrea et al., 2009). A direct correlation between the binding of MeCP2 and the presence of H3K9me$_2$ in promoter 1 of the *BDNF* gene and the *IκBα* gene has been reported as well (Mann et al., 2007; Tian et al., 2009). Through these co-immunoprecipitations, it is shown for the first time that MeCP2 not only directly interacts with nucleosomes containing H3K9me$_2$, but that this

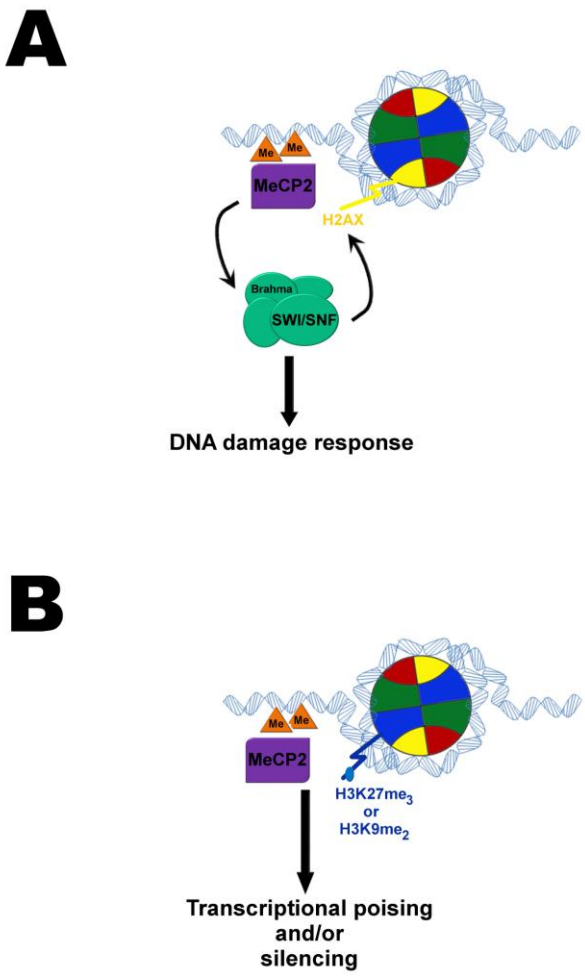

Figure 22. ***Putative models for the context-specific regulation of MeCP2 activity.*** **A. Role of H2AX. The association of MeCP2 with H2AX – containing nucleosomes may be functionally linked through the SWI/SNF remodelling complex. MeCP2 has been shown to interact with the Brahma subunit of the SWI/SNF complex (Harikrishnan et al., 2005). Independent studies have demonstrated that the SWI/SNF complex is able recruit kinases to the site of DNA damage, resulting in the phosphorylation of H2AX (Ray et al., 2009). It is possible that MeCP2 may be an intermediate link between SWI/SNF and H2AX that is required for the repair of promoter regions undergoing DNA demethylation. As demethylation of MeCP2-bound sites occurs through base excision (Metivier et al., 2008), it may be that H2AX is involved in the repair process. B. Role of $H3K9me_2$/$H3K27me_3$. The interaction of MeCP2 with nucleosomes containing $H3K27me_3$ or $H3K9me_2$ may either poise the associated gene regions for transcriptional repression or for**

terminal silencing. H3K27me$_3$ is a facultative heterochromatin mark, which in concert with H3K4me$_3$, has been shown to poise inducible gene regions for transcriptional repression (Delcuve et al., 2009). H3K9me$_2$ is another heterochromatin mark and methylation of this histone residue is recognized by HP1 which can result in the heterochromatinization of the chromatin region (Lachner et al., 2001). It is possible that the association of MeCP2 with this PTM may correlate to a terminally repressed chromatin state in the SE of the cortex. It is important to note that interactions with these three different PTMs and variant were shown individually. It is possible that synergistic combinations of them (or other yet-to-be identified PTMs) may delineate highly specialized transcriptional states.

interaction is dependent upon the chromatin organization in the cortex. This specific interaction could facilitate distinguishing between transient and permanent transcriptional silencing as mediated by MeCP2 in different chromatin states (Figure 22.B).

The presence of divalent PTMs, H3K27me$_3$ and H3K4me$_3$, on the same histone tail has been reported to poise the associated gene regions for either transcriptional activation or silencing (Delcuve et al., 2009; Gan et al., 2007; Soshnikova and Duboule, 2008). If activation is triggered, then the H3K27me$_3$ mark is lost while the H3K4me$_3$ PTM is perpetuated. The opposite scenario proceeds in the case of a repressive signal. H3K27me$_3$, a mark of facultative heterochromatin, was present in MeCP2-bound nucleosomes in both the S1 and SE (Figure 21.C and D). What was rather surprising is that H3K27me$_3$ was present in the SE, and to a lesser extent, the P of whole brain, but was barely detectable by western blotting in the S1 (Figure 17.B). However, a strong enrichment for this signal was observed in the S1 pull-downs of the sheep cortex (Figure 21.C). This could indicate that a major portion of MeCP2-bound nucleosomes contain

H3K27me$_3$ in this particular brain fraction. A suggested model for this interaction is proposed in Figure 22.B.

MeCP2 has been shown to positively regulate the expression of the H3K27 methyltransferase, EZH2 (Mann et al., 2009). However, the resulting enhanced H3K27me$_2$ modification within the *PPARγ* gene did not coincide with the binding of MeCP2 within this gene (Mann et al., 2009). This demonstrates that the highly specific nature of MeCP2 binding to nucleosomes can distinguish the subtle differences between di- and tri-methylation PTMs.

No associations with the H3K4me$_3$ mark were observed in MeCP2 pull-downs of either S1 or SE mononucleosomes (Figure 21.C and D). It may be that MeCP2 is not strongly associated with nucleosomes containing this PTM under activating conditions and that the native co-immunoprecipitation method is not sensitive enough for the detection of weak interactions. No interactions with nucleosomes containing pan-acetylated H4 were observed in either the S1 or SE (Figure 21.C and D).

Besides the newly described nature of the *in situ* chromatin environment of MeCP2, this work raises some interesting issues. For instance, if MeCP2 has sequence requirements for binding, by corollary, is there some sequence-specificity to the deposition of particular histone variants or PTMs (or combinations of both) that MeCP2 associates with? Are there other histone variants or PTMs that MeCP2 additionally associates with? Is there a direct interaction between MeCP2 and these histone tails? Are there combinations of PTMs or variants within nucleosomes that specialize the transcriptional role that MeCP2 adopts within different tissue and/or chromatin fractions? Does MeCP2 have an indirect role in DNA excision or repair mechanisms? Does H2AX

have a role in regulating inducible gene expression and possibly the methylation state of active gene promoters? Would these possible new roles be defined by sequence requirements which determine H2AX deposition and/or by the simultaneous presence of other H3 PTMs within the same nucleosome?

There is a growing body of evidence that MeCP2 does not act as a global repressor of transcription (Tudor et al., 2002). MeCP2, although ubiquitously expressed, associates with chromatin in a unique manner that is dependent on the type of tissue. Furthermore, MeCP2 binds to nucleosomes comprised of specific histone variants and PTMs in different chromatin fractions. It is of future interest to elucidate how MeCP2 responds to unique epigenetic signatures to modulate transcriptional regulation in different chromatin and tissue types. Another key point of investigation would be to understand if MeCP2 is involved in the deposition of histone variants or PTMs within associated nucleosomes. This becomes increasingly pertinent when considering that the vast majority of Rett syndrome cases are derived from mutations in MeCP2. Perhaps because it manifests as a neurodevelopmental disorder, the effects of mutated MeCP2 forms on transcriptional regulation in other tissues has not been thoroughly explored. It is possible that some of the symptom pathology may be due to localized dysfunction in certain tissues or organs. Indeed, it has been recently shown that MeCP2 plays a key role in hepatic fibrogenesis in response to damage (Mann et al., 2009). The implications for understanding disease states are tremendous and provide new areas of query and investigation.

Chapter 5 – MeCP2 Post-Translational Regulation through PEST Domains: Two Novel Hypotheses. Potential Relevance and Implications for Rett Syndrome

This chapter was adapted from the following publication:

Thambirajah, A.A., Eubanks, J., and Ausió, J. (2009) MeCP2 Post-Translational Regulation through PEST domains: Two Novel Hypotheses. Bioessays. **31**:561-9.

A.A.T. developed the hypotheses and wrote the original manuscript. All three authors participated in the extensive editorial revisions made to the manuscript.

Abstract

Mutations in MeCP2 cause Rett syndrome, a severe neurodevelopmental disease that causes ataxia and other post-natal symptoms similar to autism. Much research interest has focussed on its implications in disease and neural physiology. However, little or no attention has been paid to how MeCP2 turnover is regulated. The post-translational control of MeCP2 is of critical importance, particularly as subtle increases or decreases in MeCP2 amounts can affect neural morphology and function. The latter point is relevant to gene therapeutic approaches in which exogenous wild-type MeCP2 is being introduced into (RTT) diseased neurons. Further to this, we propose two hypotheses. Two PEST motifs were discovered within the N- and C-termini of MeCP2. These motifs typically predispose the protein containing them for proteolytic degradation following poly-ubiquitination of lysine residues flanking the PEST sites. I hypothesize that MeCP2 turnover is regulated through poly-ubiquitin mediated proteasome degradation. The second hypothesis proposes the use of histone deacetylase inhibitors to modulate the amounts of MeCP2 expressed in conjunction with potential gene therapies to be used to treat Rett syndrome.

Introduction

The importance of epigenetic marks in regulatory and developmental processes is becoming increasingly better understood. Not only limited to DNA methylation, such marks also include post-translational modifications of proteins. DNA methylation, particularly 5' methylation of CpG dinucleotides, is recognized by MBD proteins, which, through the recruitment of other *trans*-acting factors, can mediate changes to the local chromatin structure. In doing so, MBD proteins can positively or negatively affect gene transcription.

Besides its roles in transcriptional regulation, the levels of MeCP2 must be critically maintained. Too little or too much MeCP2 can result in an abnormal neuronal phenotype (Armstrong et al., 1998; Jugloff et al., 2005), altered neuronal function (Asaka et al., 2006; Chao et al., 2007; Dani et al., 2005; Moretti and Zoghbi, 2006), and impaired behavioural performance (Collins et al., 2004; Jugloff et al., 2008; Kerr et al., 2008; Luikenhuis et al., 2004; Samaco et al., 2008). Considering the essential role of MeCP2, particularly during development, it is imperative to understand how MeCP2 protein levels and stability are maintained. In this chapter, I propose two hypotheses regarding the regulation of MeCP2 amounts and draw on supporting evidence that has been produced in recent years.

Proteolytic degradation is one common mechanism for regulating protein amounts. Protein turnover through the 26S ubiquitin proteasome system (26S UPS) is one such well-studied mechanism (Schwartz and Ciechanover, 2008). Consensus sequences enriched in proline, glutamate, serine, and threonine residues (PEST) have been identified to predispose proteins containing them for rapid proteolytic degradation

(Rechsteiner and Rogers, 1996; Rogers et al., 1986) by the 26S UPS. Using the PESTfinder algorithm, we demonstrate here that MeCP2 contains two strong PEST sequences; one at the N-terminal end and the other at the C-terminus. Additionally, HDACs have been suggested to have a therapeutic potential for RTT (Kazantsev and Thompson, 2008). Indeed, it has been shown that HDACs can reduce the amount of MeCP2 in treated cells (Ishibashi et al., 2008; Kundakovic et al., 2008). Based on all this information, two hypotheses are put forward. 1) I propose that the PEST sequences of MeCP2 provide the mechanism by which MeCP2 protein turnover is regulated *in vivo*, thereby permitting a cell to achieve the critical protein balance required, and 2) I hypothesize that HDAC inhibitors may be good therapeutic candidates to adjust the MeCP2 imbalance resulting from protein replacement therapies.

MeCP2 and chromatin: The shift in dogma

At the chromatin level, MeCP2 has been shown to compete for binding with histone H1 (Nan et al., 1997), a global repressor of gene activity (Weintraub, 1984). In fact, MeCP2 can to bind to the nucleosome in ways that are reminiscent of linker histones (Chandler et al., 1999; Nan et al., 1997), but in contrast to the latter, binding occurs in a DNA-methylation dependent manner (Ishibashi et al., 2008; Nikitina et al., 2007a). There is *in vitro* evidence suggesting that MeCP2 can also bind unmethylated DNA (Georgel et al., 2003), yet has a higher affinity for methylated targets (Georgel et al., 2003; Ishibashi et al., 2008). The repressive properties of MeCP2 led to the implicit belief that it would operate as a global repressor (and likely to be present in heterochromatin regions of the genome) (Nan et al., 1996).

It was not until several years later when a major shift in this manner of thinking occurred. At the end of 2007 and the beginning of 2008, using chromatin immunoprecipitation (ChIP) approaches, two groups independently showed that the majority of MeCP2 is bound to active genes in neurons (Chahrour et al., 2008; Yasui et al., 2007). In one study, utilizing SH-SY5Y human neuronal cells, 63% of promoters bound by MeCP2 were transcriptionally active (Yasui et al., 2007). A second group showed that approximately 85% of genes associated with MeCP2 were active in the mouse hypothalamus (Chahrour et al., 2008). It was also shown through chromatin fractionations that the majority of MeCP2 associated with nucleosomes of transcriptionally active, nuclease-accessible chromatin (Ishibashi et al., 2008). It could be argued that in many instances, the ChIP experiments are unable to distinguish genes belonging to the active and silenced allelic forms in tissues comprised of heterogeneous cell types (Chahrour et al., 2008). However, the chromatin fractionation approach, although technically simpler, clearly dispels this criticism. Furthermore, while the ChIP experiments permit a more detailed analysis of potential MeCP2 – gene interactions, it underestimates the total number of MeCP2 gene targets due to chromatin being lost to insoluble fractions which are refractory to MNase digestion (Ishibashi et al., 2008).

The association of MeCP2 with actively transcribed regions of the genome, as suggested by these converging data, does not necessarily alter the primary repressor function of the protein. However, it suggests that MeCP2 functions more as a specific, transient transcriptional regulator rather than as a global permanent transcriptional repressor as was initially conceived (Wade, 2001). In this role, MeCP2 still retains its

intrinsic repressive chromatin binding activity, but operates as a regulatory switch for transcription.

MeCP2 Structure and Post-Translational Modifications

MeCP2 consists of two isoforms, MeCP2e1 (MeCP2B in humans) and MeCP2e2 (MeCP2A), which are generated through an alternative splicing between exons 1 and 2 as the nomenclature implies (Kriaucionis and Bird, 2004; Mnatzakanian et al., 2004). MeCP2e1 is the longer of the two proteins, and contains an additional 12 N-terminal amino acids. The first 21 amino acids of MeCP2e1 are distinct from MeCP2e2 and are enriched in acidic and hydrophobic residues (Figure 23.A). This difference aside, the remainder of the sequence is conserved between these isoforms. In general, the primary structure of MeCP2 is highly conserved among vertebrates and especially so in mammals (Figure 23.A). At the secondary and tertiary structural levels, the protein exhibits a substantial amount of disordered organization (Adams et al., 2007) (Figure 23.B and C). However, it has several structured motifs that include a nuclear localization signal (NLS) the methyl-CpG binding domain (MBD) and a transcriptional repressor domain (TRD) that interacts with other *trans*-acting factors. The presence of a Group II WW binding domain may endow MeCP2 with mRNA splicing related functions (Buschdorf and Stratling, 2004) (Figure 23.A). The tertiary structure of the MBD has been determined (Figure 23.C) (Wakefield et al., 1999).

Using the PESTfinder algorithm (*http://www.at.embnet.org/toolbox/pestfind/*), I identified two strong PEST sequences in MeCP2 (Figure 23.A). Using the MeCP2e1 sequence, the first PEST domain is located within the N-terminal region (amino acid

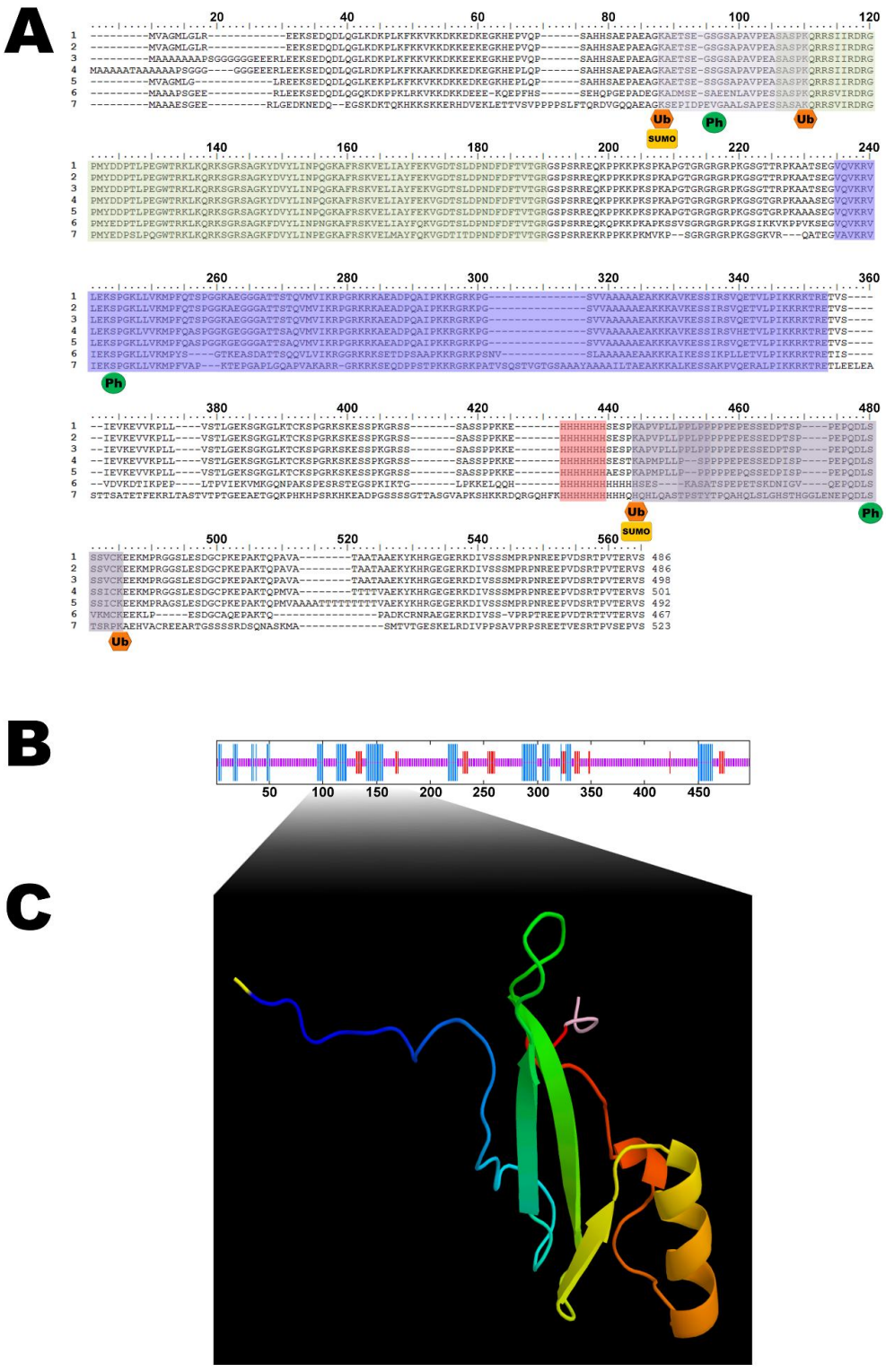

Figure 23. ***MeCP2 primary, secondary and tertiary structures and sites of known and predicted PTMs.*** **A. A ClustalW alignment of MeCP2 primary sequences with**

accession numbers given in parentheses (Larkin et al., 2007). The alignment was formatted using BioEdit. (1) *Macaca fascicularis* (AAK97131.1); (2) *Homo sapiens* (*MeCP2e2*, NP_004983.1); (3) *Homo sapiens* (*MeCP2e1*, NP_001104262.1); (4) *Mus musculus* (CAM18742.1); (5) *Rattus norvegicus* (NP_073164.2); (6) *Xenopus laevis* (AAD02651.1); and (7) *Danio rerio* (CAQ14978.1). Sequence motifs and domains are highlighted in coloured boxes: N- and C-terminal PEST domains (purple), MBD (green; overlaps with the N-terminal PEST domain), central TRD (blue), and a stretch of seven histidine residues (red). A Group II WW binding domain found within the C-terminal PEST domain is shown with a darker purple box. Known phosphorylation sites are denoted by green circles beneath the modified serine residue (Zhou et al., 2006). Putative ubiquitination and SUMOylation sites within PEST sequences are depicted using orange hexagons and yellow rectangles, respectively. B. MeCP2 secondary structure prediction based on the human MeCP2e1 isoform and determined using the Hierarchical Neural Network analysis (Combet et al., 2000). The longer blue lines indicate the presence of α-helices, the intermediate length red lines, β-sheets, and the short purple lines, random coil. C. Tertiary structure of the human MeCP2 MBD (NP_001104262.1, residues 94-176) modelled using Phyre software (Bennett-Lovsey et al., 2008) based on the PDB structure 1QK9 (Wakefield et al., 1999). The yellow residue at the N-terminal end indicates the lysine residue that is shared by both the PEST and MBD motifs. At the C-terminal end, four residues that are not a part of the MBD are highlighted in pink.

residues 73-94) and has a PESTfind score of +8.45. The second, and the stronger of the two sequences, is located within the C-terminus between residues 389-426 and has a PESTfind score of +17.30. Any PEST sequence with an ascribed value ranging from +0 to +50 is considered to be a potential PEST sequence candidate, and any score above +5 is of strong interest. As shown in Figure 23.A, the PEST sequences of MeCP2 display a

high level of sequence conservation. While each of the other MBD family members had predicted weak PEST sequences, only MBD1 was found to have a strong PEST sequence which is located centrally (residues 283-304). The PESTfind score for MBD1 was +17.48, which is approximately equal to the score for the second sequence in MeCP2.

PEST sequences possess both α-helical and poly-proline type II (PII) structures which become destabilized upon phosphorylation. It is this alteration in conformational stability, not the recognition of the phosphorylation, that mediates the rapid proteolytic degradation of the modified protein (Garcia-Alai et al., 2006).

The first documented PTM of MeCP2 is its phosphorylation following membrane depolarization (Chen et al., 2003; Martinowich et al., 2003). This phosphorylation of MeCP2 was shown to facilitate its release from promoter III of the *BDNF* gene. Since then, additional sites of phosphorylation (S80, S229, S421) have been determined (Zhou et al., 2006) (Figure 23.A) and work continues towards identifying the specific kinases that target MeCP2 (Mari et al., 2005; Zhou et al., 2006). It is worth noting that a critical phosphorylation site of MeCP2 in neurons following depolarization is serine 421, a site residing within the C-terminal PEST sequence.

In addition to phosphorylation, the PEST sequences allow for the identification of several potential ubiquitination sites at lysine residues flanking the PEST domains (see Figure 23.A). As well, the modification of MeCP2 by SUMO has recently been described (Miyake and Nagai, 2007) and may potentially modify the same residues.

MeCP2: More than Just a Regulator in the Brain?

Although MeCP2 is most often viewed as a neuronal modulator, it is a ubiquitously expressed protein (Shahbazian et al., 2002). Additionally, the distribution of the two isoforms between different tissues varies as well. In the brain, MeCP2e1 predominates over its shorter counterpart (Kriaucionis and Bird, 2004). MeCP2 regulates the transcription of brain-specific genes in neurons, but how is this activity affected in other tissues that do not require such transcripts? What other genes are being regulated by MeCP2 in non-neuronal tissues? Is the mechanism similar? This is particularly important when considering mutations to MeCP2 that result in its dysfunction. It is possible that the regulatory behaviour of MeCP2 can be fine-tuned through differential PTMs to MeCP2 itself or through changes to the local chromatin environment. As discussed above, MeCP2 is subject to different PTMs (Figure 23.A). Their specific relevance remains a hot topic of investigation and each of these PTMs may influence protein stability and lifespan either individually or in combination.

PEST Domain – mediated proteolysis

In 2004, Irwin Rose, Aaron Ciechanover, and Avram Hershko were awarded the Nobel prize in Chemistry for their pioneering work describing the mechanism of proteolytic degradation by the 26S UPS. Through the concerted action of activating and conjugating enzymes, a single ubiquitin monomer is convalently linked to lysine residues typically flanking PEST regions of the target protein substrate. The initial ubiquitination is often preceded by phosphorylation within the PEST domain, although this is not an absolute requirement. This ubiquitin modification is then transformed into a poly-

ubiquitin chain through the subsequent covalent attachment of additional ubiquitin moieties (Schwartz and Ciechanover, 2008). Depending on which ubiquitin lysine residue is linked to the C-terminal lysine of the preceding ubiquitin monomer, the functionality of the poly-ubiquitin chain is thus determined.

Although the poly-ubiquitin modification of PEST sequences is best known for leading to rapid proteolytic degradation, such modifications can also signal for trafficking and other endosomal processing activities. Once marked for degradation, proteolysis occurs *via* the 26S UPS. A large, multipartite complex, the 26S UPS is composed of a 20S complex which is flanked by two 19S complexes. The two end 19S macromolecules contain an ATP-dependent unfolding activity, which primes the target protein for degradation by the 20S particle. The 20S particle, also composed of several protein subunits, contains chymotrypsin and trypsin digestive functions. The 26S UPS provides one of the most prevalent mechanisms for protein turnover and maintenance of protein levels. Based on the occurrence of PEST sequences within MeCP2 and the above discussion, the following hypothesis is proposed.

Hypothesis 1. PEST Domain – mediated degradation of MeCP2

MeCP2 turnover is regulated by proteolytic degradation through the 26S UPS and mediated via its two PEST domains. Furthermore, PTMs that are associated with the modification of these domains, phosphorylation and ubiquitination, are proposed to differentially regulate the functional activity of MeCP2.

This mechanism of post-translational control could be pivotal during development when MeCP2 levels are in flux and when mutations in MeCP2 most profoundly exhibit their deleterious effects as seen in RTT. It has been shown that the rate of protein turnover by proteolytic degradation is much faster in infants and children compared to adults (Schwartz and Ciechanover, 2008; Van Goudoever et al., 1995). As will be discussed, additional PTMs potentially associated with ubiquitination could also be involved in diversifying the functions of MeCP2.

Phosphorylation often precedes ubiquitination of lysine residues flanking the PEST sites, although phosphorylation is not a prerequisite for ubiquitination. Mass spectrometric analyses showed that MeCP2 is multiply phosphorylated, and that some of these PTMs are critical to MeCP2 function at molecular to physiological levels (Figure 23.A) (Kazantsev and Thompson, 2008). Phosphorylation of S421 of MeCP2e1 regulates the activity-dependent transcription of the *BDNF* gene and additionally, the maturation of dendritic patterning and spine morphogenesis. S80 and S229 were also identified to be sites for phosphorylation, although upon SDS-PAGE analysis, only phosphorylation of S421 resulted in the formation of a slower-migrating MeCP2 species (Zhou et al., 2006). It is of considerable interest to note that S80 and S421 lie within the N-terminal and C-terminal PEST sequences, respectively (Figure 23.A). As the C-terminal PEST region is the strongest candidate, and S421 phosphorylation results in a higher molecular weight species, it is tempting to speculate that this modification, if not S80 as well, could be a precursor to ubiquitination.

Higher molecular weight forms of MeCP2 have been reported that could correlate to poly-ubiquitination or a similarly large PTM. In 2003, Jarrar *et al* described the

appearance of low-mobility electrophoretic MeCP2 bands in extranuclear, post-synaptic fractions in the cerebral cortex (Jarrar et al., 2003). In SDS-PAGE, MeCP2 typically shows an electrophoretic mobility corresponding to an apparent molecular mass of 75 kDa. In this work, MeCP2 additionally showed an immunoreactive band at 100 kDa, with an intermediate ladder banding pattern observed in between (Jarrar et al., 2003). The 100 kDa MeCP2 species could potentially be attributed to a tri-ubiquitin chain motif (ubiquitin monomers have a molecular mass of approximately 8 kDa). Although this is speculative, this is one of the first reports of higher molecular weight MeCP2 species having an unidentified PTM.

I have initiated studies to address whether MeCP2 turnover is regulated through poly-ubiquitination and 26S UPS – mediated proteolytic turnover. I have observed higher molecular mass species (~95 kDa) of MeCP2 in brain chromatin extracts (Figure 19.A). Efforts were made to purify MeCP2 from brain extracts by RP-HPLC; however, MeCP2 had a broad elution through a <35% - 45% acetonitrile gradient.

I treated HeLa S3 cells with the Roche complete protease inhibitor to see if *in situ*, higher molecular forms of MeCP2 (presumably poly-ubiquitinated) could be induced or if MeCP2 would accumulate. Indeed, faint higher molecular mass forms of MeCP2 were observed. Due to a lack of time, I was not able to recapitulate these findings in SH-SY5Y neuroblastoma cells treated with the 26S UPS inhibitor MG132.

In regard to future studies, I would certainly like to continue the cell culture studies to test if MG132 treatment of SH-SY5Y cells does result in an accumulation of MeCP2 and possibly modified forms of MeCP2. This will likely be a much better culture system to work with than HeLa S3 cells as MeCP2 expression can be induced to higher

levels with chemical treatment. To ensure that MeCP2 turnover is regulated through the PEST domains, point mutations of critical lysine or serine residues should be made to see which PEST domain (or both) is responsible for turnover. Mass spectrometry could be used to characterize post-translationally modified forms of MeCP2 purified by HPLC and to confirm any potential ubiquitination. There are certainly many directions that these studies could take.

Functional relevance and implications of MeCP2 poly-ubiquitination

When considering how MeCP2 exerts its regulatory effects at the molecular level and particularly how its dysfunction contributes to RTT pathophysiology, little is known about how the turnover of MeCP2 *itself* is regulated. What controls the regulator? The current understanding of MeCP2 molecular function at the chromatin level is continuously expanding, yet less attention has been paid to what role MeCP2 may play in the cytoplasm or in post-synaptic fractions. No doubt there is much to be learned and revealed about the multiplicity of potentially diverse roles MeCP2 undertakes. For example, a recent publication has described the association of MBD2, MBD3 and MeCP2 at the promoter of the oestrogen-inducible *pS2* gene (Metivier et al., 2008) (Figure 24).

Based on this and on the previous section, a model for the regulatory behaviour of MeCP2 is proposed (Figure 24). As has been shown with the *BDNF* gene regulation, upon induction of transcription, MeCP2 becomes phosphorylated and is released from its

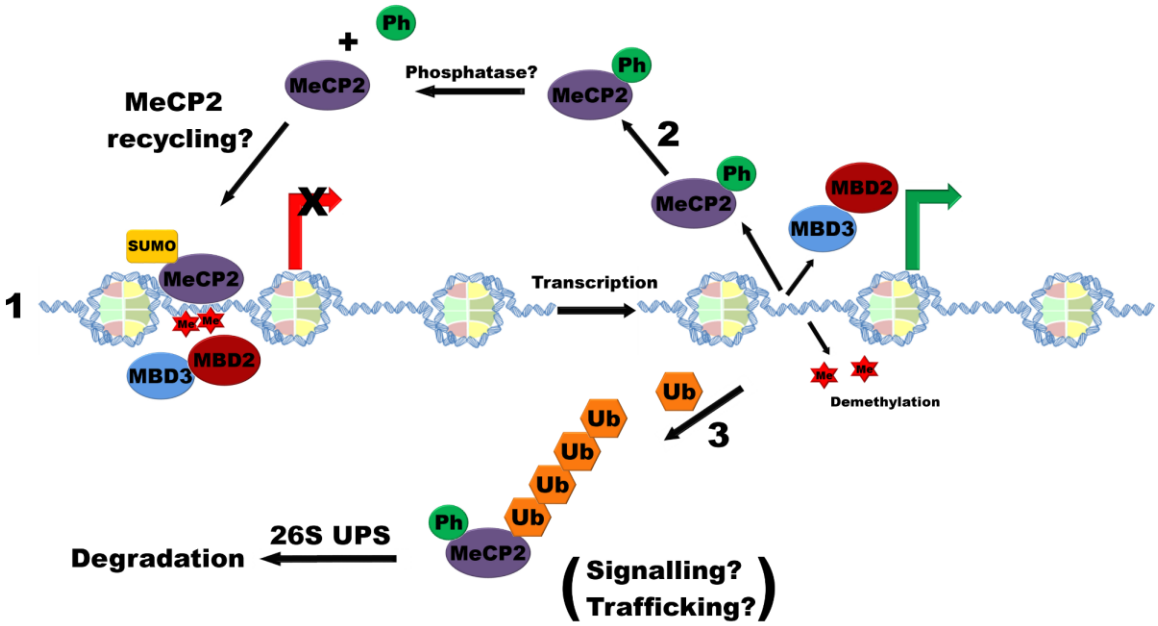

Figure 24. ***Proposed model for MeCP2 regulation and turnover by PTMs (phosphorylation, SUMOylation and ubiquitination).*** **(1) MeCP2 has recently been shown to be a transcriptional regulator (Chahrour et al., 2008; Yasui et al., 2007) rather than a terminal repressor of global gene expression (Wade, 2001). It can cycle around gene promoters in a way that is dependent on the particular gene involved (Ooi and Wood, 2008). A cycling between MeCP2 and MBD2/MBD3 binding has also been shown at the promoter of a steroid inducible gene, *pS2* (Metivier et al., 2008). Note that this cycling may occur concurrently with DNA demethylation by Dnmt3 proteins (Metivier et al., 2008) or by other demethylases yet to be identified. SUMOylation may confer stability to MeCP2 (Miyake and Nagai, 2007). (2) Phosphorylation of S421 plays a critical role in MeCP2 release upon induction of transcription, as seen with the *BDNF* gene (Chen et al., 2003; Zhou et al., 2006). Interestingly, two of the experimentally identified phosphorylation sites co-localize within the N- and C-terminal PEST sequences of MeCP2. The phosphate moieties of MeCP2 could be removed by phosphatases and MeCP2 may potentially be recycled. (3) Alternatively, if present at PEST sequences, phosphorylation could mediate MeCP2 poly-ubiquitination which could target the protein for degradation by the 26S UPS. Such rapid proteolytic degradation would**

ensure that no aberrant repression would occur when long-term transcriptional activity is required. However, it cannot be excluded that the poly-ubiquitination could serve other functions such as signalling or trafficking by the modified MeCP2. Note that in this model, MeCP2 operates as a chromatin bound repressor molecule. Transcription repression (indicated by thick red arrow) can only be relieved (green thick arrow) upon MeCP2 release by phosphorylation, or other yet unknown mechanisms.

target sequence (Chen et al., 2003; Martinowich et al., 2003) (Figure 24.1). However, the question remains: what happens to MeCP2 once it is released? We propose two possible modes of regulation for MeCP2. First, depending on the site of phosphorylation, MeCP2 may only be transiently modified until acted upon by a phosphatase (none described as yet) at which point, MeCP2 may regain its basal regulatory activities (Figure 24.2). Alternatively, a different route could involve further modification within phosphorylated PEST regions by (a) poly-ubiquitin chain(s). Depending on the type of lysine linkage generated within the poly-ubiquitin chain, this PTM could signal for the degradation of MeCP2 via the 26S UPS (Figure 24.3) (Pickart and Fushman, 2004). It is also worth noting that other degradative pathways, such as caspases and calpains, also recognize PEST domains (Barnes and Gomes, 1995; Belizario et al., 2008), raising the possibility that non-proteasome degradation of MeCP2 could also occur.

Regulation of MeCP2 protein levels through rapid proteolytic degradation could be useful for several reasons. The removal of MeCP2 would ensure that no accidental or deleterious transcriptional aberrations would occur once induction-dependent activation had commenced (Figure 24.3). Such rapid clearance could extend the pro-activity

configuration of target genes for a longer period of time, and thereby potentiate transcriptional signals. The latter requirement may be particularly critical during developmental processes or even homeostatic responses to stress. Thus, it is possible that MeCP2 regulation could occur in a cyclical fashion. MeCP2 could initially be phosphorylated and then subsequently ubiquitinated, leading to its eventual degradation. Newly translated MeCP2, or a fraction of phosphorylated MeCP2 that is recycled by phosphatase activity (Figure 24.2), would subsequently restore basal MeCP2 function to target sequences. Additional PTMs, such as SUMOylation, may stabilize portions of the translated MeCP2 pool depending upon the context of the signal received.

In consideration of this hypothetical model, it would be possible to envisage that in those instances where MeCP2 mutations do not affect its binding to chromatin (Ghosh et al., 2008; Kumar et al., 2008), dysfunctional regulation could arise from the inability to properly modulate transcription. In this regard, it is of interest to note that approximately 10% of RTT MeCP2 mutations involve a truncation of the C-terminal tail which includes the stronger PEST domain. Is it possible that the resulting dysfunction is due to the inability to fully release MeCP2 from its target in this particular subset of mutations?

Hypothesis 2. Maintaining MeCP2 balance using HDAC inhibitors

Independent of the cellular localization of MeCP2, it is imperative that the levels of MeCP2 be tightly balanced; too little MeCP2 results in abnormal dendritic branching, whereas superfluous dendritic branching follows from an overexpression of MeCP2 (Jugloff et al., 2005). Maintaining the proper amount of MeCP2 is not only important for normal cell functioning, but it has important implications for replacement therapies. The

latter instance involves the ectopic expression of wild-type MeCP2 that is introduced into brain tissues that produce a deleterious mutant form of MeCP2 (Giacometti et al., 2007; Guy et al., 2007; Jugloff et al., 2008; Luikenhuis et al., 2004). These experimental strategies have been carried out in mutant MeCP2 mice with the long-term translational goal of developing therapies to ameliorate RTT symptom pathology and eventually even designing a cure for RTT. While it is a promising approach, one of the main problems encountered involves the ectopic over-expression of MeCP2 (Jugloff et al., 2008) which, in the worst-case scenario, could exacerbate the existing RTT phenotype.

It has been shown that treatment of HeLa cells with butyrate under conditions (5-10 mM) that inhibit HDACs and enhance the overall levels of global histone acetylation, reduced the total amount of MeCP2 *in situ*. This decrease did not affect the relative distribution of MeCP2 within chromatin fractions (Ishibashi et al., 2008). A subsequent study also demonstrated the reduction in MeCP2 protein amounts following treatment with various HDAC inhibitors (MS-275 showed a 33% decrease, trichostatin A, 49%, and valproic acid, 55%) (Kundakovic et al., 2008). The decrease in expression of MeCP2 is not surprising as there are as many examples of genes whose activity is down-regulated as up-regulated by this drug and by other HDAC inhibitors (Rada-Iglesias et al., 2007). Although the molecular mechanism involved in the butyrate-induced down-regulation of MeCP2 still needs to be unravelled, it may be possible to use different HDAC inhibitor dosages *in vivo* to correct the adverse over-expression phenotypes that result from the gene therapies described above. Based on this, we propose the following hypothesis:

Clinical administration of HDAC inhibitors in conjunction with genetic therapeutic approaches could be used to control the overall amounts of ectopic MeCP2 being translated.

While it is uncertain whether the endogenous or exogenous MeCP2 products would be more susceptible to HDAC inhibitor treatment, the use of HDAC inhibitors could prove a useful and powerful method of fine-tuning MeCP2 levels. As the lysine deacetylase activities of HDACs are not limited to histones, but apply to other non-histone proteins as well, it is not known what specifically causes the change in MeCP2 levels (Sweatt, 2007). This may be a concern when considering possible toxic side-effects that may arise from a potentially long-term, chronic administration of a therapeutic HDAC inhibitor. While such considerations are beyond the scope of this proposed hypothesis, it is nonetheless encouraging to note that HDAC inhibitors have been tested in clinical trials and have shown low toxicity (Santini et al., 2007). HDAC inhibitors have already been used as clinical therapeutics for cancer and their possible use in the treatment of neurodegenerative disorders such as Alzheimer's is being explored as well (Kazantsev and Thompson, 2008; Sigalotti et al., 2007; Takizawa and Meshorer, 2008). Furthermore, the use of HDAC inhibitors in mouse models of Rubinstein-Taybi syndrome, a human chromatin remodelling disease, showed improvements in memory function (Alarcon et al., 2004).

Interestingly, a recent review suggested the potential use of HDAC inhibitors as a RTT therapeutic (Kazantsev and Thompson, 2008). However, no indication was provided as to how this might work. Of additional interest is the observation that

dendritic sprouting and synaptogenesis was enhanced in a neurodegenerative mouse model when treated with HDAC inhibitors (Fischer et al., 2007; Takizawa and Meshorer, 2008). It is unknown whether the reduction in MeCP2 protein amounts and the enhanced neuron morphology upon treatment with HDAC inhibitors are a direct result of histone hyperacetylation or another affected process. Furthermore, there is no evidence to suggest that the two phenomena are related. It is likely that this beneficial change in neuron morphology is extrinsic to modulation of MeCP2 levels based on previous studies (Jugloff et al., 2005). However decreased MeCP2 levels may potentially correlate to improved dendritic and synapse formation following HDAC inhibitor treatment, combined they may provide a synergistic benefit in mitigating the RTT phenotype.

Concluding Remarks

I propose a novel model for the regulation of MeCP2 based on a well-studied mechanism, something that has not been thoroughly explored at present. Accordingly, the role of known PTMs, such as phosphorylation and SUMOylation, and predicted PTMs (ubiquitination) are expected to strongly influence the maintenance of MeCP2 levels during critical developmental times. Such a mechanism fits well with the concept of MeCP2 operating as a transcriptional regulatory switch. In this regard, MeCP2 would lose its intrinsic chromatin binding repressor activity upon phosphorylation and would subsequently be removed by poly-ubiquitination, or recycled by phosphatase activity (Figure 24).

The consideration of a system of turnover for MeCP2 not only has pivotal implications for disease pathology (RTT and other disorders related to MeCP2

dysfunction), but also for the delivery of potential genetic therapeutics. To this end, we propose that the clinical administration of HDAC inhibitors may be useful in fine-tuning translated amounts of MeCP2. The possible ramifications for this proposal on expanding the understanding of fundamental molecular mechanisms of MeCP2 are quite exciting. This proposal could offer a new perspective in the study of how molecular events precipitate long-range physiological effects, not only in the brain, but elsewhere in other tissues. In addition, insight gained from elucidating the turnover of MeCP2 could be an important variable to consider in the successful development and implementation of promising therapeutics for RTT. It cannot be underestimated that the maintenance of proper chromatin plasticity is intrinsically linked to healthy brain plasticity. What may prove important to this modulation of plasticity is the regulation of MeCP2 during development through proteolytic turnover.

Chapter 6 – Summary

It is essential that the plasticity of chromatin structures be maintained in order to permit the proper genetic response to regulatory requirements. Functional and structural variability can be introduced into chromatin through the incorporation of histone variants, post-translational modification of histones (and non-histone) proteins, DNA methylation, and the activities of *trans*-acting factors, among others. The focus of this dissertation was to understand the contribution of two of these factors to the organization of native chromatin structures. In Chapter 2, the effects of the histone variant H2A.Z on the successive organization of chromatin forms were investigated. The bulk of the research presented, however, focussed on the MBD protein MeCP2 and the constraints on its chromatin interactions. Chapter 3 tested the early and prevalent assumption that MeCP2 acted as a global transcriptional repressor. In Chapter 4, the tissue-specific nature of MeCP2 binding to chromatin and the requirement for specific histone variants and PTMs were explored. And finally, Chapter 5 discussed two hypotheses regarding the regulation of MeCP2 turnover through PEST domains and proteolytic degradation.

H2A.Z stabilizes octamer, nucleosome and chromatin fibre structures

The H2A.Z nucleosome was crystallized in 2000 and it was predicted that the presence of this histone variant would result in a destabilized chromatin structure (Suto et al., 2000). However, subsequent biophysical studies of recombinant H2A.Z-containing chromatin structures produced opposing results (Abbott et al., 2001; Fan et al., 2002). This work was performed by two independent groups and it was considered that the use

of a prokaryotic recombinant system may preclude any necessary PTMs or folding requirements. To avoid these potential difficulties, the chromatin structures containing H2A.Z used in the present studies were obtained from native sources. The chromatin and histones used were obtained from either chicken erythrocytes or liver tissues.

The dissociation of native octamers was studied using gel filtration chromatography under decreasing pH conditions. At physiological pH (7.5), H2A.Z was present primarily within stabilized octamer forms. However, with a decrease in pH (6.0), stable octamers began to dissociate and H2A.Z was present within octamer, hexamer, tetramer and dimer forms. At pH 5.5, H2A.Z was primarily present in dimer forms. In contrast, characterization of the H2A.Z-H2B dimer folding by circular dichroism showed that the variant dimer was largely unfolded compared to the canonical dimer. The instability of the H2A.Z-H2B dimer may indicate the necessity of a chaperone to maintain folding.

Sedimentation analysis of nucleosome core particles under increasing NaCl concentrations indicated that as nucleosomes dissociated, H2A.Z was preferentially localized within more stabilized forms. The association of H2A.Z within chromatin fibres was assessed by HAP chromatography. Histones were eluted from adsorbed chromatin under an increasing NaCl gradient. Regardless of the chromatin type or tissue source, H2A.Z had a late elution with H3 and H4 that came after H2A. This could indicate a stronger interaction with the H3-H4 tetramer, the DNA, or both. The HAP chromatography and the KCl fractionation of chromatin also showed that the deposition of H2A.Z occurred independently of linker histones.

MeCP2 does not act as a global repressor of transcription

Shortly after the discovery of MeCP2, it was postulated to act as a global repressor of gene activity (Meehan et al., 1992). However, despite the emergence of experimental findings that challenged this notion, the debate persisted (Tudor et al., 2002). If MeCP2 did act as an indiscriminate repressor of transcription, it was hypothesized that changes in global chromatin modifications would affect the relative distribution of MeCP2 within different chromatin regions. HeLa S3 cells were left untreated or treated with 3-ABA or butyrate to induce DNA hypermethylation and histone hyperacetylation, respectively. Regardless of treatment, the majority of the chromatin-associated MeCP2 was present within the nuclease-accessible S1 fraction. The amount of MeCP2 decreased correspondingly in the SE and P fractions. Approximately 5% of MeCP2 in the S1 was not chromatin-bound. The relative chromatin distribution of MeCP2 was conserved regardless of treatment. The hypermethylation of the DNA did not affect the amount of MeCP2 in each fraction compared to the untreated chromatin. However, the butyrate treatment resulted in concomitant decreases in MeCP2 in all chromatin fractions. Neither chemical treatment affected the level of *MeCP2* transcription, and was therefore not responsible for this reduction. These results suggested that MeCP2 did not act as a global repressor, but more likely as a specific regulator of transcription. Converging data produced by independent groups support this latter model (Chahrour et al., 2008; Yasui et al., 2007).

Changes in DNA methylation were quantified by paired *Hpa*II and *Msp*I digestions of the S1 DNA of each chromatin treatment. Compared to the native culture, the 3-ABA – treated S1 had an 11% increase in DNA methylation, whereas the butyrate-

treated S1 had a 6.7% decrease. A comparison of the *Hpa*II and *Msp*I digestions for the butyrate-treated S1 showed roughly equivalent levels of digestion, indicating that a CpG rearrangement had occurred.

Histone H3 PTMs associated with heterochromatin and euchromatin were used to characterize the chromatin fractions for each HeLa S3 treatment. Interestingly, an inverse correlation was observed between the levels of DNA methylation and the comparative abundance of the heterochromatin PTMs in particular.

MeCP2 interacts with chromatin in a tissue-specific manner and with nucleosomes containing certain histone variants and PTMs

Having established that MeCP2 does not act as a global repressor, it was of interest to understand how this ubiquitously expressed protein behaves in different primary tissues. Given the unique roles that MeCP2 plays in neuron maturation, it is not implausible that it may differentially regulate genes in other tissues. If this were the case, it is possible that such differences may manifest in a distinct, tissue-specific chromatin distribution of MeCP2. Moreover, it was also of interest to understand what nucleosomal factors may influence the localization of MeCP2 within different chromatin types. It has already been shown that MeCP2 has a broad distribution within heterochromatin and euchromatin, but is MeCP2 binding simply defined by sequence specificity and DNA methylation alone? If there was a further specialization of MeCP2 binding by the local chromatin environment, then the presence of histone variants or PTMs may play a role.

Tissue comparisons were conducted using rat brain, liver and testis tissues. An initial characterization of the chromatin environments of each tissue was performed. It is

well known that the testis contains testis-specific isoforms, and for the brain and liver, variations in the relative amount and distribution of histone variants and PTMs were observed.

MeCP2 exhibited a unique distribution within the fractionated chromatin of each of these tissues. The brain had substantially more MeCP2 than either the liver or testis and most of it was present in the S1 fraction. Prorportionally less MeCP2 was present in the SE and P, respectively. The liver S1 and P had approximately equivalent amounts of MeCP2, with much less in the SE. Most of the MeCP2 in testis was present in the S1, and decreased, similar amounts were observed in the SE and P. It is possible that MeCP2 differentially regulates a distinct set of genes or gene regions in these individual tissues. This distribution of MeCP2 in (brain) chromatin occurred independently of the duration of digestion by MNase. The relative overabundance of MeCP2 in the brain compared to the liver or testis was reflected in the quantification of *MECP2* transcripts in each tissue. The brain had approximately 59 times more *MECP2* than the liver and 22 times more *MECP2* than the testis.

Native co-immunoprecipitation of MeCP2 with mononucleosomes revealed a number of novel nucleosomal interacting partners of MeCP2 in the sheep cortex. In the S1, MeCP2 interacted strongly with nucleosomes containing H2AX, while in the SE, an attenuated interaction was observed with these variant nucleosomes. No interactions were observed with γ-H2AX, H2A.Z, or acetylated H2A.Z in either the S1 or the SE. In the S1 fraction, a strongly enhanced interaction was observed between MeCP2 and nucleosomes containing H3K27me$_3$. This interaction with H3K27me$_3$ nucleosomes was also observed in the SE. Interestingly, MeCP2 was observed to associate with

mononucleosomes containing H3K9me$_2$ in the SE of sheep cortex, but not in the S1. MeCP2 has previously been shown to interact with the HMT responsible for methylating H3K9 (Fuks et al., 2003b). No interactions were observed in either chromatin fraction between MeCP2 and nucleosomes containing H3K4me$_3$ or acetylated H4 forms.

Two potential models for the interaction of MeCP2 with nucleosomes containing H2AX, H3K27me$_3$, or H3K9me$_2$ were proposed. It may be that MeCP2 is in close association with nucleosomes containing H2AX for DNA repair purposes. It has previously been described that the demethylation of promoter regions bound by MeCP2 occurs through base excision. It is possible that the close proximity of H2AX to these regions may play a unique role in facilitating a repair process. In the other scenario, the placement of H3K27me$_3$ in nucleosomes adjacent to MeCP2 binding sites may have a role in poising transcribed regions for activation or silencing. Similarly, the presence of H3K9me$_2$ in MeCP2-bound nucleosomes may signify a transcriptionally quiescent state. While these models are independently proposed, it is possible that any combination of this variant or these PTMs may synergistically co-habit the same nucleosome (or with other yet-to-be identified variants or PTMs).

It is of considerable interest to elucidate the functional significance of the association of MeCP2 with nucleosomes containing H2AX, H3K27me$_3$, or H3K9me$_2$. Chromatin immunoprecipitation (ChIP) – sequencing could be used to identify what genes are associated with MeCP2 and these variants or PTMs and if there is any co-localization between them at the same gene sites. Under induced activation, ChIP could be used to assess the presence of variants, PTMs, or MeCP2 at the sites of identified genes in order to understand the dynamic deposition of these different proteins during

transcriptional activation. Such an analysis could show how MeCP2 differentially associates with different genomic locales (*i.e.*, promoters, intergenic regions) in relation to the local chromatin composition. Moreover, such experiments could also show how chromatin composition (in particular, histone and non-histone proteins) changes at specific gene sites under activation conditions. A similar ChIP analysis could be used to ascertain whether MeCP2-bound H2AX nucleosomes are involved in repair processes. Such investigations would provide an exciting platform from which to further understand the basis of chromatin regulation by MeCP2.

The regulation of MeCP2 turnover through PEST domains

Phosphorylation of MeCP2 coincides with the release of MeCP2 from its bound promoter, thereby permitting transcription (Chen et al., 2003; Martinowich et al., 2003). But what happens to this released MeCP2? Is it recycled for further use as a transcriptional regulator or does it become degraded? In Chapter 5, the identification of two PEST sequences within the N- and C-termini of MeCP2 is described. PEST sequences typically predispose the protein containing them for proteolytic degradation by the 26S UPS. A hypothesis was proposed that the turnover of MeCP2 is regulated through the poly-ubiquitination of these two PEST sequences, with potentially important consequences for MeCP2 function. Efforts have been made to experimentally test this hypothesis and potential future studies are explored further in Chapter 5. A second hypothesis was discussed regarding the regulation of MeCP2 levels through the use of HDAC inhibitors in conjunction with replacement therapeutics for RTT.

Concluding Comments

This research provides a springboard from which to further investigate how MeCP2-bound chromatin environments are specialized to respond to a broad range of unique transcription- (or replication-) dependent requirements and stimuli. The native chromatin environment with which MeCP2 interacts is more diverse than previously anticipated. This information is certainly relevant to understanding the etiology of diseases such as Rett syndrome and also how MeCP2 mediates its regulation in a temporal and tissue-specific manner.

Bibliography

Abbott, D.W., Chadwick, B.P., Thambirajah, A.A. and Ausió, J. 2005. Beyond the Xi: macroH2A chromatin distribution and post-translational modification in an avian system. J Biol Chem **280**(16): 16437-45.

Abbott, D.W., Ivanova, V.S., Wang, X., Bonner, W.M. and Ausió, J. 2001. Characterization of the stability and folding of H2A.Z chromatin particles: implications for transcriptional activation. J Biol Chem **276**(45): 41945-9.

Abbott, D.W., Laszczak, M., Lewis, J.D., Su, H., Moore, S.C., Hills, M., Dimitrov, S. and Ausió, J. 2004. Structural characterization of macroH2A containing chromatin. Biochemistry **43**(5): 1352-9.

Adam, M., Robert, F., Larochelle, M. and Gaudreau, L. 2001. H2A.Z is required for global chromatin integrity and for recruitment of RNA polymerase II under specific conditions. Mol Cell Biol **21**(18): 6270-9.

Adams, V.H., McBryant, S.J., Wade, P.A., Woodcock, C.L. and Hansen, J.C. 2007. Intrinsic disorder and autonomous domain function in the multifunctional nuclear protein, MeCP2. J Biol Chem **282**(20): 15057-64.

Agarwal, N., Hardt, T., Brero, A., Nowak, D., Rothbauer, U., Becker, A., Leonhardt, H. and Cardoso, M.C. 2007. MeCP2 interacts with HP1 and modulates its heterochromatin association during myogenic differentiation. Nucleic Acids Res **35**(16): 5402-8.

Agger, K., Christensen, J., Cloos, P.A. and Helin, K. 2008. The emerging functions of histone demethylases. Curr Opin Genet Dev **18**(2): 159-68.

Alarcon, J.M., Malleret, G., Touzani, K., Vronskaya, S., Ishii, S., Kandel, E.R. and Barco, A. 2004. Chromatin acetylation, memory, and LTP are impaired in CBP+/- mice: a model for the cognitive deficit in Rubinstein-Taybi syndrome and its amelioration. Neuron **42**(6): 947-59.

Albig, W. and Doenecke, D. 1997. The human histone gene cluster at the D6S105 locus. Hum Genet **101**(3): 284-94.

Alexandrow, M.G. and Hamlin, J.L. 2005. Chromatin decondensation in S-phase involves recruitment of Cdk2 by Cdc45 and histone H1 phosphorylation. J Cell Biol **168**(6): 875-86.

Altaf, M., Auger, A., Covic, M. and Cote, J. 2009. Connection between histone H2A variants and chromatin remodeling complexes. Biochem Cell Biol **87**(1): 35-50.

Amir, R.E., Van den Veyver, I.B., Wan, M., Tran, C.Q., Francke, U. and Zoghbi, H.Y. 1999. Rett syndrome is caused by mutations in X-linked MECP2, encoding methyl-CpG-binding protein 2. Nat Genet **23**(2): 185-8.

Arents, G. and Moudrianakis, E.N. 1993. Topography of the histone octamer surface: repeating structural motifs utilized in the docking of nucleosomal DNA. Proc Natl Acad Sci U S A **90**(22): 10489-93.

Arents, G. and Moudrianakis, E.N. 1995. The histone fold: a ubiquitous architectural motif utilized in DNA compaction and protein dimerization. Proc Natl Acad Sci U S A **92**(24): 11170-4.

Armstrong, D.D., Dunn, K. and Antalffy, B. 1998. Decreased dendritic branching in frontal, motor and limbic cortex in Rett syndrome compared with trisomy 21. J Neuropathol Exp Neurol **57**(11): 1013-7.

Asaka, Y., Jugloff, D.G., Zhang, L., Eubanks, J.H. and Fitzsimonds, R.M. 2006. Hippocampal synaptic plasticity is impaired in the Mecp2-null mouse model of Rett syndrome. Neurobiol Dis **21**(1): 217-27.

Ausió, J. 2006. Histone variants--the structure behind the function. Brief Funct Genomic Proteomic **5**(3): 228-43.

Ausió, J., Abbott, D.W., Wang, X. and Moore, S.C. 2001. Histone variants and histone modifications: a structural perspective. Biochem Cell Biol **79**(6): 693-708.

Ausió, J., Dong, F. and van Holde, K.E. 1989. Use of selectively trypsinized nucleosome core particles to analyze the role of the histone "tails" in the stabilization of the nucleosome. J Mol Biol **206**(3): 451-63.

Ausió, J., Levin, D.B., De Amorim, G.V., Bakker, S. and Macleod, P.M. 2003. Syndromes of disordered chromatin remodeling. Clin Genet **64**(2): 83-95.

Ausió, J. and Moore, S.C. 1998. Reconstitution of chromatin complexes from high-performance liquid chromatography-purified histones. Methods **15**(4): 333-42.

Ausió, J. and van Holde, K.E. 1986. Histone hyperacetylation: its effects on nucleosome conformation and stability. Biochemistry **25**(6): 1421-8.

Baatout, S. and Derradji, H. 2006. About histone H1 phosphorylation during mitosis. Cell Biochem Funct **24**(2): 93-4.

Ballas, N., Lioy, D.T., Grunseich, C. and Mandel, G. 2009. Non-cell autonomous influence of MeCP2-deficient glia on neuronal dendritic morphology. Nat Neurosci **12**(3): 311-7.

Balmer, D., Arredondo, J., Samaco, R.C. and LaSalle, J.M. 2002. MECP2 mutations in Rett syndrome adversely affect lymphocyte growth, but do not affect imprinted gene expression in blood or brain. Hum Genet **110**(6): 545-52.

Barnes, J.A. and Gomes, A.V. 1995. PEST sequences in calmodulin-binding proteins. Mol Cell Biochem **149-150**(17-27.

Baxevanis, A.D., Arents, G., Moudrianakis, E.N. and Landsman, D. 1995. A variety of DNA-binding and multimeric proteins contain the histone fold motif. Nucleic Acids Res **23**(14): 2685-91.

Belizario, J.E., Alves, J., Garay-Malpartida, M. and Occhiucci, J.M. 2008. Coupling caspase cleavage and proteasomal degradation of proteins carrying PEST motif. Curr Protein Pept Sci **9**(3): 210-20.

Benevolenskaya, E.V. 2007. Histone H3K4 demethylases are essential in development and differentiation. Biochem Cell Biol **85**(4): 435-43.

Bennett-Lovsey, R.M., Herbert, A.D., Sternberg, M.J. and Kelley, L.A. 2008. Exploring the extremes of sequence/structure space with ensemble fold recognition in the program Phyre. Proteins **70**(3): 611-25.

Bernstein, E., Muratore-Schroeder, T.L., Diaz, R.L., Chow, J.C., Changolkar, L.N., Shabanowitz, J., Heard, E., Pehrson, J.R., Hunt, D.F. and Allis, C.D. 2008. A phosphorylated subpopulation of the histone variant macroH2A1 is excluded from the inactive X chromosome and enriched during mitosis. Proc Natl Acad Sci U S A **105**(5): 1533-8.

Bertani, I., Rusconi, L., Bolognese, F., Forlani, G., Conca, B., De Monte, L., Badaracco, G., Landsberger, N. and Kilstrup-Nielsen, C. 2006. Functional consequences of mutations in CDKL5, an X-linked gene involved in infantile spasms and mental retardation. J Biol Chem **281**(42): 32048-56.

Bettecken, T. and Trifonov, E.N. 2009. Repertoires of the nucleosome-positioning dinucleotides. PLoS One **4**(11): e7654.

Bird, A., Taggart, M., Frommer, M., Miller, O.J. and Macleod, D. 1985. A fraction of the mouse genome that is derived from islands of nonmethylated, CpG-rich DNA. Cell **40**(1): 91-9.

Bogdanovic, O. and Veenstra, G.J. 2009. DNA methylation and methyl-CpG binding proteins: developmental requirements and function. Chromosoma **118**(5): 549-65.

Bonenfant, D., Coulot, M., Towbin, H., Schindler, P. and van Oostrum, J. 2006. Characterization of histone H2A and H2B variants and their post-translational modifications by mass spectrometry. Mol Cell Proteomics **5**(3): 541-52.

Bonenfant, D., Towbin, H., Coulot, M., Schindler, P., Mueller, D.R. and van Oostrum, J. 2007. Analysis of dynamic changes in post-translational modifications of human histones during cell cycle by mass spectrometry. Mol Cell Proteomics **6**(11): 1917-32.

Bosch, A. and Suau, P. 1995. Changes in core histone variant composition in differentiating neurons: the roles of differential turnover and synthesis rates. Eur J Cell Biol **68**(3): 220-5.

Bradbury, E.M. 1992. Reversible histone modifications and the chromosome cell cycle. Bioessays **14**(1): 9-16.

Brero, A., Easwaran, H.P., Nowak, D., Grunewald, I., Cremer, T., Leonhardt, H. and Cardoso, M.C. 2005. Methyl CpG-binding proteins induce large-scale chromatin reorganization during terminal differentiation. J Cell Biol **169**(5): 733-43.

Brown, C.J., Ballabio, A., Rupert, J.L., Lafreniere, R.G., Grompe, M., Tonlorenzi, R. and Willard, H.F. 1991. A gene from the region of the human X inactivation centre is expressed exclusively from the inactive X chromosome. Nature **349**(6304): 38-44.

Bruce, K., Myers, F.A., Mantouvalou, E., Lefevre, P., Greaves, I., Bonifer, C., Tremethick, D.J., Thorne, A.W. and Crane-Robinson, C. 2005. The replacement histone H2A.Z in a hyperacetylated form is a feature of active genes in the chicken. Nucleic Acids Res **33**(17): 5633-9.

Buschdorf, J.P. and Stratling, W.H. 2004. A WW domain binding region in methyl-CpG-binding protein MeCP2: impact on Rett syndrome. J Mol Med **82**(2): 135-43.

Calestagne-Morelli, A. and Ausió, J. 2006. Long-range histone acetylation: biological significance, structural implications, and mechanisms. Biochem Cell Biol **84**(4): 518-27.

Catez, F., Ueda, T. and Bustin, M. 2006. Determinants of histone H1 mobility and chromatin binding in living cells. Nat Struct Mol Biol **13**(4): 305-10.

Chahrour, M., Jung, S.Y., Shaw, C., Zhou, X., Wong, S.T., Qin, J. and Zoghbi, H.Y. 2008. MeCP2, a key contributor to neurological disease, activates and represses transcription. Science **320**(5880): 1224-9.

Chahrour, M. and Zoghbi, H.Y. 2007. The story of Rett syndrome: from clinic to neurobiology. Neuron **56**(3): 422-37.

Chandler, S.P., Guschin, D., Landsberger, N. and Wolffe, A.P. 1999. The methyl-CpG binding transcriptional repressor MeCP2 stably associates with nucleosomal DNA. Biochemistry **38**(22): 7008-18.

Chao, H.T., Zoghbi, H.Y. and Rosenmund, C. 2007. MeCP2 controls excitatory synaptic strength by regulating glutamatergic synapse number. Neuron **56**(1): 58-65.

Chen, H.Y., Sun, J.M., Zhang, Y., Davie, J.R. and Meistrich, M.L. 1998. Ubiquitination of histone H3 in elongating spermatids of rat testes. J Biol Chem **273**(21): 13165-9.

Chen, W.G., Chang, Q., Lin, Y., Meissner, A., West, A.E., Griffith, E.C., Jaenisch, R. and Greenberg, M.E. 2003. Derepression of BDNF transcription involves calcium-dependent phosphorylation of MeCP2. Science **302**(5646): 885-9.

Christodoulou, J., Grimm, A., Maher, T. and Bennetts, B. 2003. RettBASE: The IRSA MECP2 variation database-a new mutation database in evolution. Hum Mutat **21**(5): 466-72.

Christodoulou, J. and Weaving, L.S. 2003. MECP2 and beyond: phenotype-genotype correlations in Rett syndrome. J Child Neurol **18**(10): 669-74.

Clark, K.L., Halay, E.D., Lai, E. and Burley, S.K. 1993. Co-crystal structure of the HNF-3/fork head DNA-recognition motif resembles histone H5. Nature **364**(6436): 412-20.

Clarkson, M.J., Wells, J.R., Gibson, F., Saint, R. and Tremethick, D.J. 1999. Regions of variant histone His2AvD required for Drosophila development. Nature **399**(6737): 694-7.

Clouaire, T. and Stancheva, I. 2008. Methyl-CpG binding proteins: specialized transcriptional repressors or structural components of chromatin? Cell Mol Life Sci **65**(10): 1509-22.

Collins, A.L., Levenson, J.M., Vilaythong, A.P., Richman, R., Armstrong, D.L., Noebels, J.L., David Sweatt, J. and Zoghbi, H.Y. 2004. Mild overexpression of MeCP2 causes a progressive neurological disorder in mice. Hum Mol Genet **13**(21): 2679-89.

Combet, C., Blanchet, C., Geourjon, C. and Deleage, G. 2000. NPS@: network protein sequence analysis. Trends Biochem Sci **25**(3): 147-50.

Coon, J.J., Ueberheide, B., Syka, J.E., Dryhurst, D.D., Ausió, J., Shabanowitz, J. and Hunt, D.F. 2005. Protein identification using sequential ion/ion reactions and tandem mass spectrometry. Proc Natl Acad Sci U S A **102**(27): 9463-8.

Crowe, S.L., Movsesyan, V.A., Jorgensen, T.J. and Kondratyev, A. 2006. Rapid phosphorylation of histone H2A.X following ionotropic glutamate receptor activation. Eur J Neurosci **23**(9): 2351-61.

Dandrea, M., Donadelli, M., Costanzo, C., Scarpa, A. and Palmieri, M. 2009. MeCP2/H3meK9 are involved in IL-6 gene silencing in pancreatic adenocarcinoma cell lines. Nucleic Acids Res **37**(20): 6681-90.

Dani, V.S., Chang, Q., Maffei, A., Turrigiano, G.G., Jaenisch, R. and Nelson, S.B. 2005. Reduced cortical activity due to a shift in the balance between excitation and inhibition in a mouse model of Rett syndrome. Proc Natl Acad Sci U S A **102**(35): 12560-5.

Davey, C.A., Sargent, D.F., Luger, K., Maeder, A.W. and Richmond, T.J. 2002. Solvent mediated interactions in the structure of the nucleosome core particle at 1.9 a resolution. J Mol Biol **319**(5): 1097-113.

Davie, J.R. 2003. Inhibition of histone deacetylase activity by butyrate. J Nutr **133**(7 Suppl): 2485S-2493S.

de Capoa, A., Febbo, F.R., Giovannelli, F., Niveleau, A., Zardo, G., Marenzi, S. and Caiafa, P. 1999. Reduced levels of poly(ADP-ribosyl)ation result in chromatin compaction and hypermethylation as shown by cell-by-cell computer-assisted quantitative analysis. FASEB J **13**(1): 89-93.

DeLano, W.L. 2002. The PyMOL Molecular Graphics System. DeLano Scientific, Palo Alto, California. Available from http://www.pymol.org

Delcuve, G.P., Rastegar, M. and Davie, J.R. 2009. Epigenetic control. J Cell Physiol **219**(2): 243-50.

Dhillon, N. and Kamakaka, R.T. 2000. A histone variant, Htz1p, and a Sir1p-like protein, Esc2p, mediate silencing at HMR. Mol Cell **6**(4): 769-80.

Doenecke, D. and Tonjes, R. 1986. Differential distribution of lysine and arginine residues in the closely related histones H1 and H5. Analysis of a human H1 gene. J Mol Biol **187**(3): 461-4.

Dryhurst, D., Thambirajah, A.A. and Ausió, J. 2004. New twists on H2A.Z: a histone variant with a controversial structural and functional past. Biochem Cell Biol **82**(4): 490-7.

Eickbush, T.H. and Moudrianakis, E.N. 1978. The histone core complex: an octamer assembled by two sets of protein-protein interactions. Biochemistry **17**(23): 4955-64.

Eirin-Lopez, J.M. and Ausió, J. 2009. Origin and evolution of chromosomal sperm proteins. Bioessays **31**(10): 1062-70.

Evans, S.V. 1993. SETOR: hardware-lighted three-dimensional solid model representations of macromolecules. J Mol Graph **11**(2): 134-8, 127-8.

Faast, R., Thonglairoam, V., Schulz, T.C., Beall, J., Wells, J.R., Taylor, H., Matthaei, K., Rathjen, P.D., Tremethick, D.J. and Lyons, I. 2001. Histone variant H2A.Z is required for early mammalian development. Curr Biol **11**(15): 1183-7.

Fan, J.Y., Gordon, F., Luger, K., Hansen, J.C. and Tremethick, D.J. 2002. The essential histone variant H2A.Z regulates the equilibrium between different chromatin conformational states. Nat Struct Biol **9**(3): 172-6.

Fan, J.Y., Rangasamy, D., Luger, K. and Tremethick, D.J. 2004. H2A.Z alters the nucleosome surface to promote HP1alpha-mediated chromatin fiber folding. Mol Cell **16**(4): 655-61.

Farris, S.D., Rubio, E.D., Moon, J.J., Gombert, W.M., Nelson, B.H. and Krumm, A. 2005. Transcription-induced chromatin remodeling at the c-myc gene involves the local exchange of histone H2A.Z. J Biol Chem **280**(26): 25298-303.

Faulhaber, I. and Bernardi, G. 1967. Chromatography of calf-thymus nucleoprotein on hydroxyapatite columns. Biochim Biophys Acta **140**(3): 561-4.

Fischer, A., Sananbenesi, F., Wang, X., Dobbin, M. and Tsai, L.H. 2007. Recovery of learning and memory is associated with chromatin remodelling. Nature **447**(7141): 178-82.

Fischle, W. 2008. Talk is cheap--cross-talk in establishment, maintenance, and readout of chromatin modifications. Genes Dev **22**(24): 3375-82.

Francis, N.J. and Kingston, R.E. 2001. Mechanisms of transcriptional memory. Nat Rev Mol Cell Biol **2**(6): 409-21.

Fuks, F., Hurd, P.J., Deplus, R. and Kouzarides, T. 2003a. The DNA methyltransferases associate with HP1 and the SUV39H1 histone methyltransferase. Nucleic Acids Res **31**(9): 2305-12.

Fuks, F., Hurd, P.J., Wolf, D., Nan, X., Bird, A.P. and Kouzarides, T. 2003b. The methyl-CpG-binding protein MeCP2 links DNA methylation to histone methylation. J Biol Chem **278**(6): 4035-40.

Galvao, T.C. and Thomas, J.O. 2005. Structure-specific binding of MeCP2 to four-way junction DNA through its methyl CpG-binding domain. Nucleic Acids Res **33**(20): 6603-9.

Gan, Q., Yoshida, T., McDonald, O.G. and Owens, G.K. 2007. Concise review: epigenetic mechanisms contribute to pluripotency and cell lineage determination of embryonic stem cells. Stem Cells **25**(1): 2-9.

Garcia-Alai, M.M., Gallo, M., Salame, M., Wetzler, D.E., McBride, A.A., Paci, M., Cicero, D.O. and de Prat-Gay, G. 2006. Molecular basis for phosphorylation-dependent, PEST-mediated protein turnover. Structure **14**(2): 309-19.

Garcia-Ramirez, M., Rocchini, C. and Ausió, J. 1995. Modulation of chromatin folding by histone acetylation. J Biol Chem **270**(30): 17923-8.

Georgel, P.T., Horowitz-Scherer, R.A., Adkins, N., Woodcock, C.L., Wade, P.A. and Hansen, J.C. 2003. Chromatin compaction by human MeCP2. Assembly of novel

secondary chromatin structures in the absence of DNA methylation. J Biol Chem **278**(34): 32181-8.

Ghosh, R.P., Horowitz-Scherer, R.A., Nikitina, T., Gierasch, L.M. and Woodcock, C.L. 2008. Rett syndrome-causing mutations in human MeCP2 result in diverse structural changes that impact folding and DNA interactions. J Biol Chem **283**(29): 20523-34.

Giacometti, E., Luikenhuis, S., Beard, C. and Jaenisch, R. 2007. Partial rescue of MeCP2 deficiency by postnatal activation of MeCP2. Proc Natl Acad Sci U S A **104**(6): 1931-6.

Gloss, L.M. and Placek, B.J. 2002. The effect of salts on the stability of the H2A-H2B histone dimer. Biochemistry **41**(50): 14951-9.

Guillemette, B., Bataille, A.R., Gevry, N., Adam, M., Blanchette, M., Robert, F. and Gaudreau, L. 2005. Variant histone H2A.Z is globally localized to the promoters of inactive yeast genes and regulates nucleosome positioning. PLoS Biol **3**(12): e384.

Guy, J., Gan, J., Selfridge, J., Cobb, S. and Bird, A. 2007. Reversal of neurological defects in a mouse model of Rett syndrome. Science **315**(5815): 1143-7.

Hagberg, B., Aicardi, J., Dias, K. and Ramos, O. 1983. A progressive syndrome of autism, dementia, ataxia, and loss of purposeful hand use in girls: Rett's syndrome: report of 35 cases. Ann Neurol **14**(4): 471-9.

Happel, N. and Doenecke, D. 2009. Histone H1 and its isoforms: contribution to chromatin structure and function. Gene **431**(1-2): 1-12.

Harikrishnan, K.N., Chow, M.Z., Baker, E.K., Pal, S., Bassal, S., Brasacchio, D., Wang, L., Craig, J.M., Jones, P.L., Sif, S. and El-Osta, A. 2005. Brahma links the SWI/SNF chromatin-remodeling complex with MeCP2-dependent transcriptional silencing. Nat Genet **37**(3): 254-64.

Hatch, C.L. and Bonner, W.M. 1990. The human histone H2A.Z gene. Sequence and regulation. J Biol Chem **265**(25): 15211-8.

Hatch, C.L. and Bonner, W.M. 1995. Characterization of the proximal promoter of the human histone H2A.Z gene. DNA Cell Biol **14**(3): 257-66.

Hay, R.T. 2007. SUMO-specific proteases: a twist in the tail. Trends Cell Biol **17**(8): 370-6.

Heitmann, B., Maurer, T., Weitzel, J.M., Stratling, W.H., Kalbitzer, H.R. and Brunner, E. 2003. Solution structure of the matrix attachment region-binding domain of chicken MeCP2. Eur J Biochem **270**(15): 3263-70.

Hendrich, B. and Bird, A. 1998. Identification and characterization of a family of mammalian methyl-CpG binding proteins. Mol Cell Biol **18**(11): 6538-47.

Hendrich, B., Hardeland, U., Ng, H.H., Jiricny, J. and Bird, A. 1999. The thymine glycosylase MBD4 can bind to the product of deamination at methylated CpG sites. Nature **401**(6750): 301-4.

Hendrich, B. and Tweedie, S. 2003. The methyl-CpG binding domain and the evolving role of DNA methylation in animals. Trends Genet **19**(5): 269-77.

Henikoff, S., Henikoff, J.G., Sakai, A., Loeb, G.B. and Ahmad, K. 2009. Genome-wide profiling of salt fractions maps physical properties of chromatin. Genome Res **19**(3): 460-9.

Hirose, M. 1988. Effects of histone acetylation on nucleosome properties as evaluated by polyacrylamide gel electrophoresis and hydroxylapatite dissociation chromatography. J Biochem **103**(1): 31-5.

Ho, K.L., McNae, I.W., Schmiedeberg, L., Klose, R.J., Bird, A.P. and Walkinshaw, M.D. 2008. MeCP2 binding to DNA depends upon hydration at methyl-CpG. Mol Cell **29**(4): 525-31.

Hon, G., Wang, W. and Ren, B. 2009. Discovery and annotation of functional chromatin signatures in the human genome. PLoS Comput Biol **5**(11): e1000566.

Horike, S., Cai, S., Miyano, M., Cheng, J.F. and Kohwi-Shigematsu, T. 2005. Loss of silent-chromatin looping and impaired imprinting of DLX5 in Rett syndrome. Nat Genet **37**(1): 31-40.

Hu, K., Nan, X., Bird, A. and Wang, W. 2006. Testing for association between MeCP2 and the brahma-associated SWI/SNF chromatin-remodeling complex. Nat Genet **38**(9): 962-4; author reply 964-7.

Illingworth, R.S. and Bird, A.P. 2009. CpG islands--'a rough guide'. FEBS Lett **583**(11): 1713-20.

Isaacs, J.S., Murdock, M., Lane, J. and Percy, A.K. 2003. Eating difficulties in girls with Rett syndrome compared with other developmental disabilities. J Am Diet Assoc **103**(2): 224-30.

Ishibashi, T., Dryhurst, D., Rose, K.L., Shabanowitz, J., Hunt, D.F. and Ausió, J. 2009. Acetylation of vertebrate H2A.Z and its effect on the structure of the nucleosome. Biochemistry **48**(22): 5007-17.

Ishibashi, T., Thambirajah, A.A. and Ausió, J. 2008. MeCP2 preferentially binds to methylated linker DNA in the absence of the terminal tail of histone H3 and independently of histone acetylation. FEBS Lett **582**(7): 1157-62.

Jackson, J.D. and Gorovsky, M.A. 2000. Histone H2A.Z has a conserved function that is distinct from that of the major H2A sequence variants. Nucleic Acids Res **28**(19): 3811-6.

Jarrar, M.H., Danko, C.G., Reddy, S., Lee, Y.J., Bibat, G. and Kaufmann, W.E. 2003. MeCP2 expression in human cerebral cortex and lymphoid cells: immunochemical characterization of a novel higher-molecular-weight form. J Child Neurol **18**(10): 675-82.

Jason, L.J., Moore, S.C., Lewis, J.D., Lindsey, G. and Ausió, J. 2002. Histone ubiquitination: a tagging tail unfolds? Bioessays **24**(2): 166-74.

Jenuwein, T. and Allis, C.D. 2001. Translating the histone code. Science **293**(5532): 1074-80.

Jiang, T., Zhou, X., Taghizadeh, K., Dong, M. and Dedon, P.C. 2007. N-formylation of lysine in histone proteins as a secondary modification arising from oxidative DNA damage. Proc Natl Acad Sci U S A **104**(1): 60-5.

Jiang, Y., Langley, B., Lubin, F.D., Renthal, W., Wood, M.A., Yasui, D.H., Kumar, A., Nestler, E.J., Akbarian, S. and Beckel-Mitchener, A.C. 2008. Epigenetics in the nervous system. J Neurosci **28**(46): 11753-9.

Jones, P.L., Veenstra, G.J., Wade, P.A., Vermaak, D., Kass, S.U., Landsberger, N., Strouboulis, J. and Wolffe, A.P. 1998. Methylated DNA and MeCP2 recruit histone deacetylase to repress transcription. Nat Genet **19**(2): 187-91.

Jugloff, D.G., Jung, B.P., Purushotham, D., Logan, R. and Eubanks, J.H. 2005. Increased dendritic complexity and axonal length in cultured mouse cortical neurons overexpressing methyl-CpG-binding protein MeCP2. Neurobiol Dis **19**(1-2): 18-27.

Jugloff, D.G., Vandamme, K., Logan, R., Visanji, N.P., Brotchie, J.M. and Eubanks, J.H. 2008. Targeted delivery of an Mecp2 transgene to forebrain neurons improves the behavior of female Mecp2-deficient mice. Hum Mol Genet **17**(10): 1386-96.

Kalantry, S., Purushothaman, S., Bowen, R.B., Starmer, J. and Magnuson, T. 2009. Evidence of Xist RNA-independent initiation of mouse imprinted X-chromosome inactivation. Nature **460**(7255): 647-51.

Karantza, V., Baxevanis, A.D., Freire, E. and Moudrianakis, E.N. 1995. Thermodynamic studies of the core histones: ionic strength and pH dependence of H2A-H2B dimer stability. Biochemistry **34**(17): 5988-96.

Karantza, V., Freire, E. and Moudrianakis, E.N. 1996. Thermodynamic studies of the core histones: pH and ionic strength effects on the stability of the (H3-H4)/(H3-H4)2 system. Biochemistry **35**(6): 2037-46.

Karantza, V., Freire, E. and Moudrianakis, E.N. 2001. Thermodynamic studies of the core histones: stability of the octamer subunits is not altered by removal of their terminal domains. Biochemistry **40**(43): 13114-23.

Kaufmann, W.E., Jarrar, M.H., Wang, J.S., Lee, Y.J., Reddy, S., Bibat, G. and Naidu, S. 2005. Histone modifications in Rett syndrome lymphocytes: a preliminary evaluation. Brain Dev **27**(5): 331-9.

Kazantsev, A.G. and Thompson, L.M. 2008. Therapeutic application of histone deacetylase inhibitors for central nervous system disorders. Nat Rev Drug Discov **7**(10): 854-68.

Kerr, B., Alvarez-Saavedra, M., Saez, M.A., Saona, A. and Young, J.I. 2008. Defective body-weight regulation, motor control and abnormal social interactions in Mecp2 hypomorphic mice. Hum Mol Genet **17**(12): 1707-17.

Khochbin, S. and Wolffe, A.P. 1993. Developmental regulation and butyrate-inducible transcription of the Xenopus histone H1(0) promoter. Gene **128**(2): 173-80.

Kim, H.S., Vanoosthuyse, V., Fillingham, J., Roguev, A., Watt, S., Kislinger, T., Treyer, A., Carpenter, L.R., Bennett, C.S., Emili, A., Greenblatt, J.F., Hardwick, K.G., Krogan, N.J., Bahler, J. and Keogh, M.C. 2009. An acetylated form of histone H2A.Z regulates chromosome architecture in Schizosaccharomyces pombe. Nat Struct Mol Biol

Klose, R.J., Sarraf, S.A., Schmiedeberg, L., McDermott, S.M., Stancheva, I. and Bird, A.P. 2005. DNA binding selectivity of MeCP2 due to a requirement for A/T sequences adjacent to methyl-CpG. Mol Cell **19**(5): 667-78.

Kobor, M.S. and Lorincz, M.C. 2009. H2A.Z and DNA methylation: irreconcilable differences. Trends Biochem Sci **34**(4): 158-61.

Kobor, M.S., Venkatasubrahmanyam, S., Meneghini, M.D., Gin, J.W., Jennings, J.L., Link, A.J., Madhani, H.D. and Rine, J. 2004. A protein complex containing the conserved Swi2/Snf2-related ATPase Swr1p deposits histone variant H2A.Z into euchromatin. PLoS Biol **2**(5): E131.

Koch, C. and Stratling, W.H. 2004. DNA binding of methyl-CpG-binding protein MeCP2 in human MCF7 cells. Biochemistry **43**(17): 5011-21.

Kokura, K., Kaul, S.C., Wadhwa, R., Nomura, T., Khan, M.M., Shinagawa, T., Yasukawa, T., Colmenares, C. and Ishii, S. 2001. The Ski protein family is required for MeCP2-mediated transcriptional repression. J Biol Chem **276**(36): 34115-21.

Kolasinska-Zwierz, P., Down, T., Latorre, I., Liu, T., Liu, X.S. and Ahringer, J. 2009. Differential chromatin marking of introns and expressed exons by H3K36me3. Nat Genet **41**(3): 376-81.

Korber, P. and Horz, W. 2004. SWRred not shaken; mixing the histones. Cell **117**(1): 5-7.

Kornberg, R.D. and Thomas, J.O. 1974. Chromatin structure; oligomers of the histones. Science **184**(139): 865-8.

Kouzarides, T. 2007. Chromatin modifications and their function. Cell **128**(4): 693-705.
Kriaucionis, S. and Bird, A. 2004. The major form of MeCP2 has a novel N-terminus generated by alternative splicing. Nucleic Acids Res **32**(5): 1818-23.

Krogan, N.J., Keogh, M.C., Datta, N., Sawa, C., Ryan, O.W., Ding, H., Haw, R.A., Pootoolal, J., Tong, A., Canadien, V., Richards, D.P., Wu, X., Emili, A., Hughes, T.R., Buratowski, S. and Greenblatt, J.F. 2003. A Snf2 family ATPase complex required for recruitment of the histone H2A variant Htz1. Mol Cell **12**(6): 1565-76.

Kumar, A., Kamboj, S., Malone, B.M., Kudo, S., Twiss, J.L., Czymmek, K.J., LaSalle, J.M. and Schanen, N.C. 2008. Analysis of protein domains and Rett syndrome mutations indicate that multiple regions influence chromatin-binding dynamics of the chromatin-associated protein MECP2 in vivo. J Cell Sci **121**(Pt 7): 1128-37.

Kundakovic, M., Chen, Y., Guidotti, A. and Grayson, D.R. 2008. The reelin and GAD67 promoters are activated by epigenetic drugs that facilitate the disruption of local repressor complexes. Mol Pharmacol

Kwon, M.J., Oh, E., Lee, S., Roh, M.R., Kim, S.E., Lee, Y., Choi, Y.L., In, Y.H., Park, T., Koh, S.S. and Shin, Y.K. 2009. Identification of novel reference genes using multiplatform expression data and their validation for quantitative gene expression analysis. PLoS One **4**(7): e6162.

Lachner, M., O'Carroll, D., Rea, S., Mechtler, K. and Jenuwein, T. 2001. Methylation of histone H3 lysine 9 creates a binding site for HP1 proteins. Nature **410**(6824): 116-20.

Laemmli, U.K. 1970. Cleavage of structural proteins during the assembly of the head of bacteriophage T4. Nature **227**(5259): 680-5.

Larkin, M.A., Blackshields, G., Brown, N.P., Chenna, R., McGettigan, P.A., McWilliam, H., Valentin, F., Wallace, I.M., Wilm, A., Lopez, R., Thompson, J.D., Gibson, T.J. and Higgins, D.G. 2007. Clustal W and Clustal X version 2.0. Bioinformatics **23**(21): 2947-8.

Larochelle, M. and Gaudreau, L. 2003. H2A.Z has a function reminiscent of an activator required for preferential binding to intergenic DNA. EMBO J **22**(17): 4512-22.

Leach, T.J., Mazzeo, M., Chotkowski, H.L., Madigan, J.P., Wotring, M.G. and Glaser, R.L. 2000. Histone H2A.Z is widely but nonrandomly distributed in chromosomes of Drosophila melanogaster. J Biol Chem **275**(30): 23267-72.

Lee, K.M. and Hayes, J.J. 1997. The N-terminal tail of histone H2A binds to two distinct sites within the nucleosome core. Proc Natl Acad Sci U S A **94**(17): 8959-64.

Leuba, S.H., Bustamante, C., van Holde, K. and Zlatanova, J. 1998. Linker histone tails and N-tails of histone H3 are redundant: scanning force microscopy studies of reconstituted fibers. Biophys J **74**(6): 2830-9.

Lewis, J.D., Meehan, R.R., Henzel, W.J., Maurer-Fogy, I., Jeppesen, P., Klein, F. and Bird, A. 1992. Purification, sequence, and cellular localization of a novel chromosomal protein that binds to methylated DNA. Cell **69**(6): 905-14.

Li, W., Nagaraja, S., Delcuve, G.P., Hendzel, M.J. and Davie, J.R. 1993. Effects of histone acetylation, ubiquitination and variants on nucleosome stability. Biochem J **296 (Pt 3)**(737-44.

Liu, X., Bowen, J. and Gorovsky, M.A. 1996. Either of the major H2A genes but not an evolutionarily conserved H2A.F/Z variant of Tetrahymena thermophila can function as the sole H2A gene in the yeast Saccharomyces cerevisiae. Mol Cell Biol **16**(6): 2878-87.

Livak, K.J. and Schmittgen, T.D. 2001. Analysis of relative gene expression data using real-time quantitative PCR and the 2(-Delta Delta C(T)) Method. Methods **25**(4): 402-8.

Lomen-Hoerth, C. and Shooter, E.M. 1995. Widespread neurotrophin receptor expression in the immune system and other nonneuronal rat tissues. J Neurochem **64**(4): 1780-9.

Lowell, J.E., Kaiser, F., Janzen, C.J. and Cross, G.A. 2005. Histone H2AZ dimerizes with a novel variant H2B and is enriched at repetitive DNA in Trypanosoma brucei. J Cell Sci **118**(Pt 24): 5721-30.

Lu, X. and Hansen, J.C. 2004. Identification of specific functional subdomains within the linker histone H10 C-terminal domain. J Biol Chem **279**(10): 8701-7.

Luger, K., Mader, A.W., Richmond, R.K., Sargent, D.F. and Richmond, T.J. 1997. Crystal structure of the nucleosome core particle at 2.8 A resolution. Nature **389**(6648): 251-60.

Luijsterburg, M.S., White, M.F., van Driel, R. and Dame, R.T. 2008. The major architects of chromatin: architectural proteins in bacteria, archaea and eukaryotes. Crit Rev Biochem Mol Biol **43**(6): 393-418.

Luikenhuis, S., Giacometti, E., Beard, C.F. and Jaenisch, R. 2004. Expression of MeCP2 in postmitotic neurons rescues Rett syndrome in mice. Proc Natl Acad Sci U S A **101**(16): 6033-8.

Luk, E., Vu, N.D., Patteson, K., Mizuguchi, G., Wu, W.H., Ranjan, A., Backus, J., Sen, S., Lewis, M., Bai, Y. and Wu, C. 2007. Chz1, a nuclear chaperone for histone H2AZ. Mol Cell **25**(3): 357-68.

Mann, J., Chu, D.C., Maxwell, A., Oakley, F., Zhu, N.L., Tsukamoto, H. and Mann, D.A. 2009. MeCP2 controls an epigenetic pathway that promotes myofibroblast transdifferentiation and fibrosis. Gastroenterology

Mann, J., Oakley, F., Akiboye, F., Elsharkawy, A., Thorne, A.W. and Mann, D.A. 2007. Regulation of myofibroblast transdifferentiation by DNA methylation and MeCP2: implications for wound healing and fibrogenesis. Cell Death Differ **14**(2): 275-85.

Marchi, M., Guarda, A., Bergo, A., Landsberger, N., Kilstrup-Nielsen, C., Ratto, G.M. and Costa, M. 2007. Spatio-temporal dynamics and localization of MeCP2 and pathological mutants in living cells. Epigenetics **2**(3): 187-97.

Mari, F., Azimonti, S., Bertani, I., Bolognese, F., Colombo, E., Caselli, R., Scala, E., Longo, I., Grosso, S., Pescucci, C., Ariani, F., Hayek, G., Balestri, P., Bergo, A., Badaracco, G., Zappella, M., Broccoli, V., Renieri, A., Kilstrup-Nielsen, C. and Landsberger, N. 2005. CDKL5 belongs to the same molecular pathway of MeCP2 and it is responsible for the early-onset seizure variant of Rett syndrome. Hum Mol Genet **14**(14): 1935-46.

Marino-Ramirez, L., Kann, M.G., Shoemaker, B.A. and Landsman, D. 2005. Histone structure and nucleosome stability. Expert Rev Proteomics **2**(5): 719-29.

Martinowich, K., Hattori, D., Wu, H., Fouse, S., He, F., Hu, Y., Fan, G. and Sun, Y.E. 2003. DNA methylation-related chromatin remodeling in activity-dependent BDNF gene regulation. Science **302**(5646): 890-3.

Meehan, R.R., Lewis, J.D. and Bird, A.P. 1992. Characterization of MeCP2, a vertebrate DNA binding protein with affinity for methylated DNA. Nucleic Acids Res **20**(19): 5085-92.

Meneghini, M.D., Wu, M. and Madhani, H.D. 2003. Conserved histone variant H2A.Z protects euchromatin from the ectopic spread of silent heterochromatin. Cell **112**(5): 725-36.

Metivier, R., Gallais, R., Tiffoche, C., Le Peron, C., Jurkowska, R.Z., Carmouche, R.P., Ibberson, D., Barath, P., Demay, F., Reid, G., Benes, V., Jeltsch, A., Gannon, F. and Salbert, G. 2008. Cyclical DNA methylation of a transcriptionally active promoter. Nature **452**(7183): 45-50.

Miyake, K. and Nagai, K. 2007. Phosphorylation of methyl-CpG binding protein 2 (MeCP2) regulates the intracellular localization during neuronal cell differentiation. Neurochem Int **50**(1): 264-70.

Mizuguchi, G., Shen, X., Landry, J., Wu, W.H., Sen, S. and Wu, C. 2004. ATP-driven exchange of histone H2AZ variant catalyzed by SWR1 chromatin remodeling complex. Science **303**(5656): 343-8.

Mnatzakanian, G.N., Lohi, H., Munteanu, I., Alfred, S.E., Yamada, T., MacLeod, P.J., Jones, J.R., Scherer, S.W., Schanen, N.C., Friez, M.J., Vincent, J.B. and Minassian, B.A. 2004. A previously unidentified MECP2 open reading frame defines a new protein isoform relevant to Rett syndrome. Nat Genet **36**(4): 339-41.

Moore, S.C., Rice, P., Iskandar, M. and Ausió, J. 1997. Reconstitution of native-like nucleosome core particles from reversed-phase-HPLC-fractionated histones. Biochem J **328 (Pt 2)**(409-14.

Moretti, P. and Zoghbi, H.Y. 2006. MeCP2 dysfunction in Rett syndrome and related disorders. Curr Opin Genet Dev **16**(3): 276-81.

Moudrianakis, E.N. and Arents, G. 1993. Structure of the histone octamer core of the nucleosome and its potential interactions with DNA. Cold Spring Harb Symp Quant Biol **58**(273-9.

Myers, F.A., Chong, W., Evans, D.R., Thorne, A.W. and Crane-Robinson, C. 2003. Acetylation of histone H2B mirrors that of H4 and H3 at the chicken beta-globin locus but not at housekeeping genes. J Biol Chem **278**(38): 36315-22.

Myers, F.A., Evans, D.R., Clayton, A.L., Thorne, A.W. and Crane-Robinson, C. 2001. Targeted and extended acetylation of histones H4 and H3 at active and inactive genes in chicken embryo erythrocytes. J Biol Chem **276**(23): 20197-205.

Nan, X., Campoy, F.J. and Bird, A. 1997. MeCP2 is a transcriptional repressor with abundant binding sites in genomic chromatin. Cell **88**(4): 471-81.

Nan, X., Meehan, R.R. and Bird, A. 1993. Dissection of the methyl-CpG binding domain from the chromosomal protein MeCP2. Nucleic Acids Res **21**(21): 4886-92.

Nan, X., Ng, H.H., Johnson, C.A., Laherty, C.D., Turner, B.M., Eisenman, R.N. and Bird, A. 1998. Transcriptional repression by the methyl-CpG-binding protein MeCP2 involves a histone deacetylase complex. Nature **393**(6683): 386-9.

Nan, X., Tate, P., Li, E. and Bird, A. 1996. DNA methylation specifies chromosomal localization of MeCP2. Mol Cell Biol **16**(1): 414-21.

Nathan, D., Ingvarsdottir, K., Sterner, D.E., Bylebyl, G.R., Dokmanovic, M., Dorsey, J.A., Whelan, K.A., Krsmanovic, M., Lane, W.S., Meluh, P.B., Johnson, E.S. and Berger, S.L. 2006. Histone sumoylation is a negative regulator in Saccharomyces cerevisiae and shows dynamic interplay with positive-acting histone modifications. Genes Dev **20**(8): 966-76.

Neelin, J.M., Callahan, P.X., Lamb, D.C. and Murray, K. 1964. The Histones of Chicken Erythrocyte Nuclei. Can J Biochem Physiol **42**(1743-52.

Nikitina, T., Ghosh, R.P., Horowitz-Scherer, R.A., Hansen, J.C., Grigoryev, S.A. and Woodcock, C.L. 2007a. MeCP2-chromatin interactions include the formation of chromatosome-like structures and are altered in mutations causing Rett syndrome. J Biol Chem **282**(38): 28237-45.

Nikitina, T., Shi, X., Ghosh, R.P., Horowitz-Scherer, R.A., Hansen, J.C. and Woodcock, C.L. 2007b. Multiple modes of interaction between the methylated DNA binding protein MeCP2 and chromatin. Mol Cell Biol **27**(3): 864-77.

Norton, V.G., Imai, B.S., Yau, P. and Bradbury, E.M. 1989. Histone acetylation reduces nucleosome core particle linking number change. Cell **57**(3): 449-57.

Ogata, N., Ueda, K. and Hayaishi, O. 1980. ADP-ribosylation of histone H2B. Identification of glutamic acid residue 2 as the modification site. J Biol Chem **255**(16): 7610-5.

Olins, A.L., Carlson, R.D., Wright, E.B. and Olins, D.E. 1976. Chromatin nu bodies: isolation, subfractionation and physical characterization. Nucleic Acids Res **3**(12): 3271-91.

Olins, A.L. and Olins, D.E. 1974. Spheroid chromatin units (v bodies). Science **183**(4122): 330-2.

Ooi, L. and Wood, I.C. 2008. Regulation of gene expression in the nervous system. Biochem J **414**(3): 327-41.

Oudet, P., Gross-Bellard, M. and Chambon, P. 1975. Electron microscopic and biochemical evidence that chromatin structure is a repeating unit. Cell **4**(4): 281-300.

Park, Y.J., Dyer, P.N., Tremethick, D.J. and Luger, K. 2004. A new fluorescence resonance energy transfer approach demonstrates that the histone variant H2AZ stabilizes the histone octamer within the nucleosome. J Biol Chem **279**(23): 24274-82.

Pearson, E.C., Butler, P.J. and Thomas, J.O. 1983. Higher-order structure of nucleosome oligomers from short-repeat chromatin. EMBO J **2**(8): 1367-72.

Pehrson, J.R. and Fried, V.A. 1992. MacroH2A, a core histone containing a large nonhistone region. Science **257**(5075): 1398-400.

Perry, M. and Chalkley, R. 1981. The effect of histone hyperacetylation on the nuclease sensitivity and the solubility of chromatin. J Biol Chem **256**(7): 3313-8.

Perry, M. and Chalkley, R. 1982. Histone acetylation increases the solubility of chromatin and occurs sequentially over most of the chromatin. A novel model for the biological role of histone acetylation. J Biol Chem **257**(13): 7336-47.

Peters, A.H., Kubicek, S., Mechtler, K., O'Sullivan, R.J., Derijck, A.A., Perez-Burgos, L., Kohlmaier, A., Opravil, S., Tachibana, M., Shinkai, Y., Martens, J.H. and Jenuwein, T. 2003. Partitioning and plasticity of repressive histone methylation states in mammalian chromatin. Mol Cell **12**(6): 1577-89.

Pham, A.D. and Sauer, F. 2000. Ubiquitin-activating/conjugating activity of TAFII250, a mediator of activation of gene expression in Drosophila. Science **289**(5488): 2357-60.

Pickart, C.M. and Fushman, D. 2004. Polyubiquitin chains: polymeric protein signals. Curr Opin Chem Biol **8**(6): 610-6.

Placek, B.J. and Gloss, L.M. 2002. The N-terminal tails of the H2A-H2B histones affect dimer structure and stability. Biochemistry **41**(50): 14960-8.

Placek, B.J., Harrison, L.N., Villers, B.M. and Gloss, L.M. 2005. The H2A.Z/H2B dimer is unstable compared to the dimer containing the major H2A isoform. Protein Sci **14**(2): 514-22.

Prakash, Y.S., Thompson, M.A. and Pabelick, C.M. 2009. Brain Derived Neurotrophic Factor in TNF{alpha} Modulation of Ca2+ in Human Airway Smooth Muscle. Am J Respir Cell Mol Biol

Probst, A.V., Dunleavy, E. and Almouzni, G. 2009. Epigenetic inheritance during the cell cycle. Nat Rev Mol Cell Biol **10**(3): 192-206.

Rabbani, A., Iskandar, M. and Ausió, J. 1999. Daunomycin-induced unfolding and aggregation of chromatin. J Biol Chem **274**(26): 18401-6.

Rada-Iglesias, A., Enroth, S., Ameur, A., Koch, C.M., Clelland, G.K., Respuela-Alonso, P., Wilcox, S., Dovey, O.M., Ellis, P.D., Langford, C.F., Dunham, I., Komorowski, J. and Wadelius, C. 2007. Butyrate mediates decrease of histone acetylation centered on transcription start sites and down-regulation of associated genes. Genome Res **17**(6): 708-19.

Rai, K., Huggins, I.J., James, S.R., Karpf, A.R., Jones, D.A. and Cairns, B.R. 2008. DNA demethylation in zebrafish involves the coupling of a deaminase, a glycosylase, and gadd45. Cell **135**(7): 1201-12.

Raisner, R.M., Hartley, P.D., Meneghini, M.D., Bao, M.Z., Liu, C.L., Schreiber, S.L., Rando, O.J. and Madhani, H.D. 2005. Histone variant H2A.Z marks the 5' ends of both active and inactive genes in euchromatin. Cell **123**(2): 233-48.

Ramakrishnan, V., Finch, J.T., Graziano, V., Lee, P.L. and Sweet, R.M. 1993. Crystal structure of globular domain of histone H5 and its implications for nucleosome binding. Nature **362**(6417): 219-23.

Rangasamy, D., Berven, L., Ridgway, P. and Tremethick, D.J. 2003. Pericentric heterochromatin becomes enriched with H2A.Z during early mammalian development. EMBO J **22**(7): 1599-607.

Ray, A., Mir, S.N., Wani, G., Zhao, Q., Battu, A., Zhu, Q., Wang, Q.E. and Wani, A.A. 2009. Human SNF5/INI1, a component of the human SWI/SNF chromatin remodeling complex, promotes nucleotide excision repair by influencing ATM recruitment and downstream H2AX phosphorylation. Mol Cell Biol **29**(23): 6206-19.

Rechsteiner, M. and Rogers, S.W. 1996. PEST sequences and regulation by proteolysis. Trends Biochem Sci **21**(7): 267-71.

Ren, Q. and Gorovsky, M.A. 2001. Histone H2A.Z acetylation modulates an essential charge patch. Mol Cell **7**(6): 1329-35.

Ren, Q. and Gorovsky, M.A. 2003. The nonessential H2A N-terminal tail can function as an essential charge patch on the H2A.Z variant N-terminal tail. Mol Cell Biol **23**(8): 2778-89.

Rett, A. 1966. [On a unusual brain atrophy syndrome in hyperammonemia in childhood]. Wien Med Wochenschr **116**(37): 723-6.

Richmond, T.J. and Davey, C.A. 2003. The structure of DNA in the nucleosome core. Nature **423**(6936): 145-50.

Roberts, R.J. and Cheng, X. 1998. Base flipping. Annu Rev Biochem **67**(181-98.
Rogakou, E.P., Pilch, D.R., Orr, A.H., Ivanova, V.S. and Bonner, W.M. 1998. DNA double-stranded breaks induce histone H2AX phosphorylation on serine 139. J Biol Chem **273**(10): 5858-68.

Rogers, S., Wells, R. and Rechsteiner, M. 1986. Amino acid sequences common to rapidly degraded proteins: the PEST hypothesis. Science **234**(4774): 364-8.

Rozen, S. and Skaletsky, H. 2000. Primer3 on the WWW for general users and for biologist programmers. Methods Mol Biol **132**(365-86.

Samaco, R.C., Fryer, J.D., Ren, J., Fyffe, S., Chao, H.T., Sun, Y., Greer, J.J., Zoghbi, H.Y. and Neul, J.L. 2008. A partial loss of function allele of methyl-CpG-binding protein 2 predicts a human neurodevelopmental syndrome. Hum Mol Genet **17**(12): 1718-27.

Sansom, O.J., Maddison, K. and Clarke, A.R. 2007. Mechanisms of disease: methyl-binding domain proteins as potential therapeutic targets in cancer. Nat Clin Pract Oncol **4**(5): 305-15.

Santini, V., Gozzini, A. and Ferrari, G. 2007. Histone deacetylase inhibitors: molecular and biological activity as a premise to clinical application. Curr Drug Metab **8**(4): 383-93.

Santisteban, M.S., Kalashnikova, T. and Smith, M.M. 2000. Histone H2A.Z regulates transcription and is partially redundant with nucleosome remodeling complexes. Cell **103**(3): 411-22.

Santos-Rosa, H., Schneider, R., Bannister, A.J., Sherriff, J., Bernstein, B.E., Emre, N.C., Schreiber, S.L., Mellor, J. and Kouzarides, T. 2002. Active genes are tri-methylated at K4 of histone H3. Nature **419**(6905): 407-11.

Schwartz, A.L. and Ciechanover, A. 2008. Targeting Proteins for Destruction by the Ubiquitin System: Implications for Human Pathobiology. Annu Rev Pharmacol Toxicol

Shahbazian, M.D., Antalffy, B., Armstrong, D.L. and Zoghbi, H.Y. 2002. Insight into Rett syndrome: MeCP2 levels display tissue- and cell-specific differences and correlate with neuronal maturation. Hum Mol Genet **11**(2): 115-24.

Shahbazian, M.D. and Zoghbi, H.Y. 2001. Molecular genetics of Rett syndrome and clinical spectrum of MECP2 mutations. Curr Opin Neurol **14**(2): 171-6.

Shi, Y., Lan, F., Matson, C., Mulligan, P., Whetstine, J.R., Cole, P.A. and Casero, R.A. 2004. Histone demethylation mediated by the nuclear amine oxidase homolog LSD1. Cell **119**(7): 941-53.

Shogren-Knaak, M., Ishii, H., Sun, J.M., Pazin, M.J., Davie, J.R. and Peterson, C.L. 2006. Histone H4-K16 acetylation controls chromatin structure and protein interactions. Science **311**(5762): 844-7.

Shukla, A., Chaurasia, P. and Bhaumik, S.R. 2009. Histone methylation and ubiquitination with their cross-talk and roles in gene expression and stability. Cell Mol Life Sci **66**(8): 1419-33.

Sigalotti, L., Fratta, E., Coral, S., Cortini, E., Covre, A., Nicolay, H.J., Anzalone, L., Pezzani, L., Di Giacomo, A.M., Fonsatti, E., Colizzi, F., Altomonte, M., Calabro, L. and Maio, M. 2007. Epigenetic drugs as pleiotropic agents in cancer treatment: biomolecular aspects and clinical applications. J Cell Physiol **212**(2): 330-44.

Simpson, R.T. 1978. Structure of the chromatosome, a chromatin particle containing 160 base pairs of DNA and all the histones. Biochemistry **17**(25): 5524-31.

Soshnikova, N. and Duboule, D. 2008. Epigenetic regulation of Hox gene activation: the waltz of methyls. Bioessays **30**(3): 199-202.

Spencer, V.A., Sun, J.M., Li, L. and Davie, J.R. 2003. Chromatin immunoprecipitation: a tool for studying histone acetylation and transcription factor binding. Methods **31**(1): 67-75.

Stipanovich, A., Valjent, E., Matamales, M., Nishi, A., Ahn, J.H., Maroteaux, M., Bertran-Gonzalez, J., Brami-Cherrier, K., Enslen, H., Corbille, A.G., Filhol, O., Nairn, A.C., Greengard, P., Herve, D. and Girault, J.A. 2008. A phosphatase cascade by which rewarding stimuli control nucleosomal response. Nature **453**(7197): 879-84.

Suto, R.K., Clarkson, M.J., Tremethick, D.J. and Luger, K. 2000. Crystal structure of a nucleosome core particle containing the variant histone H2A.Z. Nat Struct Biol **7**(12): 1121-4.

Suzuki, M., Yamada, T., Kihara-Negishi, F., Sakurai, T. and Oikawa, T. 2003. Direct association between PU.1 and MeCP2 that recruits mSin3A-HDAC complex for PU.1-mediated transcriptional repression. Oncogene **22**(54): 8688-98.

Swaminathan, J., Baxter, E.M. and Corces, V.G. 2005. The role of histone H2Av variant replacement and histone H4 acetylation in the establishment of Drosophila heterochromatin. Genes Dev **19**(1): 65-76.

Sweatt, J.D. 2007. Behavioural neuroscience: Down memory lane. Nature **447**(7141): 151-2.

Tachiwana, H., Osakabe, A., Kimura, H. and Kurumizaka, H. 2008. Nucleosome formation with the testis-specific histone H3 variant, H3t, by human nucleosome assembly proteins in vitro. Nucleic Acids Res **36**(7): 2208-18.

Takizawa, T. and Meshorer, E. 2008. Chromatin and nuclear architecture in the nervous system. Trends Neurosci **31**(7): 343-52.

Tao, J., Hu, K., Chang, Q., Wu, H., Sherman, N.E., Martinowich, K., Klose, R.J., Schanen, C., Jaenisch, R., Wang, W. and Sun, Y.E. 2009. Phosphorylation of MeCP2 at Serine 80 regulates its chromatin association and neurological function. Proc Natl Acad Sci U S A

Tao, J., Van Esch, H., Hagedorn-Greiwe, M., Hoffmann, K., Moser, B., Raynaud, M., Sperner, J., Fryns, J.P., Schwinger, E., Gecz, J., Ropers, H.H. and Kalscheuer, V.M. 2004. Mutations in the X-linked cyclin-dependent kinase-like 5 (CDKL5/STK9) gene are associated with severe neurodevelopmental retardation. Am J Hum Genet **75**(6): 1149-54.

Thambirajah, A.A. and Ausió, J. 2009. A moment's pause: putative nucleosome-based influences on MeCP2 regulation. Biochem Cell Biol **87**(5): 791-8.

Thambirajah, A.A., Dryhurst, D., Ishibashi, T., Li, A., Maffey, A.H. and Ausió, J. 2006. H2A.Z stabilizes chromatin in a way that is dependent on core histone acetylation. J Biol Chem **281**(29): 20036-44.

Thambirajah, A.A., Eubanks, J.H. and Ausió, J. 2009a. MeCP2 post-translational regulation through PEST domains: two novel hypotheses: potential relevance and implications for Rett syndrome. Bioessays **31**(5): 561-9.

Thambirajah, A.A., Li, A., Ishibashi, T. and Ausió, J. 2009b. New developments in post-translational modifications and functions of histone H2A variants. Biochem Cell Biol **87**(1): 7-17.

Thoma, F., Koller, T. and Klug, A. 1979. Involvement of histone H1 in the organization of the nucleosome and of the salt-dependent superstructures of chromatin. J Cell Biol **83**(2 Pt 1): 403-27.

Thompson, R.J. 1973. Studies on RNA synthesis in two populations of nuclei from the mammalian cerebral cortex. J Neurochem **21**(1): 19-40.

Tian, F., Hu, X.Z., Wu, X., Jiang, H., Pan, H., Marini, A.M. and Lipsky, R.H. 2009. Dynamic chromatin remodeling events in hippocampal neurons are associated with NMDA receptor-mediated activation of Bdnf gene promoter 1. J Neurochem **109**(5): 1375-88.

Torras-Llort, M., Moreno-Moreno, O. and Azorin, F. 2009. Focus on the centre: the role of chromatin on the regulation of centromere identity and function. EMBO J **28**(16): 2337-48.

Tost, J. 2009. DNA methylation: an introduction to the biology and the disease-associated changes of a promising biomarker. Methods Mol Biol **507**(3-20.

Tsanev, R. and Sendov, B. 1971. Possible molecular mechanism for cell differentiation in multicellular organisms. J Theor Biol **30**(2): 337-93.

Tudor, M., Akbarian, S., Chen, R.Z. and Jaenisch, R. 2002. Transcriptional profiling of a mouse model for Rett syndrome reveals subtle transcriptional changes in the brain. Proc Natl Acad Sci U S A **99**(24): 15536-41.

Urdinguio, R.G., Pino, I., Ropero, S., Fraga, M.F. and Esteller, M. 2007. Histone H3 and H4 modification profiles in a Rett syndrome mouse model. Epigenetics **2**(1): 11-4.

van Daal, A. and Elgin, S.C. 1992. A histone variant, H2AvD, is essential in Drosophila melanogaster. Mol Biol Cell **3**(6): 593-602.

Van Goudoever, J.B., Sulkers, E.J., Halliday, D., Degenhart, H.J., Carnielli, V.P., Wattimena, J.L. and Sauer, P.J. 1995. Whole-body protein turnover in preterm appropriate for gestational age and small for gestational age infants: comparison of [15N]glycine and [1-(13)C]leucine administered simultaneously. Pediatr Res **37**(4 Pt 1): 381-8.

van Holde, K.E., Lohr, D.E. and Robert, C. 1992. What happens to nucleosomes during transcription? J Biol Chem **267**(5): 2837-40.

Vasko, M.R., Guo, C. and Kelley, M.R. 2005. The multifunctional DNA repair/redox enzyme Ape1/Ref-1 promotes survival of neurons after oxidative stress. DNA Repair (Amst) **4**(3): 367-79.

Wade, P.A. 2001. Methyl CpG-binding proteins and transcriptional repression. Bioessays **23**(12): 1131-7.

Wakefield, R.I., Smith, B.O., Nan, X., Free, A., Soteriou, A., Uhrin, D., Bird, A.P. and Barlow, P.N. 1999. The solution structure of the domain from MeCP2 that binds to methylated DNA. J Mol Biol **291**(5): 1055-65.

Walzak, A.A., Veldhoen, N., Feng, X., Riabowol, K. and Helbing, C.C. 2008. Expression profiles of mRNA transcript variants encoding the human inhibitor of growth tumor suppressor gene family in normal and neoplastic tissues. Exp Cell Res **314**(2): 273-85.

Wan, M., Zhao, K., Lee, S.S. and Francke, U. 2001. MECP2 truncating mutations cause histone H4 hyperacetylation in Rett syndrome. Hum Mol Genet **10**(10): 1085-92.

Wang, X., He, C., Moore, S.C. and Ausió, J. 2001. Effects of histone acetylation on the solubility and folding of the chromatin fiber. J Biol Chem **276**(16): 12764-8.

Weaving, L.S., Christodoulou, J., Williamson, S.L., Friend, K.L., McKenzie, O.L., Archer, H., Evans, J., Clarke, A., Pelka, G.J., Tam, P.P., Watson, C., Lahooti, H., Ellaway, C.J., Bennetts, B., Leonard, H. and Gecz, J. 2004. Mutations of CDKL5 cause a severe neurodevelopmental disorder with infantile spasms and mental retardation. Am J Hum Genet **75**(6): 1079-93.

Wei, Y., Yu, L., Bowen, J., Gorovsky, M.A. and Allis, C.D. 1999. Phosphorylation of histone H3 is required for proper chromosome condensation and segregation. Cell **97**(1): 99-109.

Weintraub, H. 1984. Histone-H1-dependent chromatin superstructures and the suppression of gene activity. Cell **38**(1): 17-27.

West, M.H. and Bonner, W.M. 1980. Histone 2A, a heteromorphous family of eight protein species. Biochemistry **19**(14): 3238-45.

Wong, M.L. and Medrano, J.F. 2005. Real-time PCR for mRNA quantitation. Biotechniques **39**(1): 75-85.

Wu, J.I., Lessard, J. and Crabtree, G.R. 2009. Understanding the words of chromatin regulation. Cell **136**(2): 200-6.

Wuebbles, R.D. and Jones, P.L. 2004. DNA repair in a chromatin environment. Cell Mol Life Sci **61**(17): 2148-53.

Wysocka, J., Milne, T.A. and Allis, C.D. 2005. Taking LSD 1 to a new high. Cell **122**(5): 654-8.

Yager, T.D. and van Holde, K.E. 1984. Dynamics and equilibria of nucleosomes at elevated ionic strength. J Biol Chem **259**(7): 4212-22.

Yasui, D.H., Peddada, S., Bieda, M.C., Vallero, R.O., Hogart, A., Nagarajan, R.P., Thatcher, K.N., Farnham, P.J. and Lasalle, J.M. 2007. Integrated epigenomic analyses of neuronal MeCP2 reveal a role for long-range interaction with active genes. Proc Natl Acad Sci U S A **104**(49): 19416-21.

Yoo, A.S. and Crabtree, G.R. 2009. ATP-dependent chromatin remodeling in neural development. Curr Opin Neurobiol **19**(2): 120-6.

Young, J.I., Hong, E.P., Castle, J.C., Crespo-Barreto, J., Bowman, A.B., Rose, M.F., Kang, D., Richman, R., Johnson, J.M., Berget, S. and Zoghbi, H.Y. 2005. Regulation of RNA splicing by the methylation-dependent transcriptional repressor methyl-CpG binding protein 2. Proc Natl Acad Sci U S A **102**(49): 17551-8.

Zalensky, A.O., Siino, J.S., Gineitis, A.A., Zalenskaya, I.A., Tomilin, N.V., Yau, P. and Bradbury, E.M. 2002. Human testis/sperm-specific histone H2B (hTSH2B). Molecular cloning and characterization. J Biol Chem **277**(45): 43474-80.

Zardo, G., D'Erme, M., Reale, A., Strom, R., Perilli, M. and Caiafa, P. 1997. Does poly(ADP-ribosyl)ation regulate the DNA methylation pattern? Biochemistry **36**(26): 7937-43.

Zhang, H., Roberts, D.N. and Cairns, B.R. 2005. Genome-wide dynamics of Htz1, a histone H2A variant that poises repressed/basal promoters for activation through histone loss. Cell **123**(2): 219-31.

Zhang, Y. and Reinberg, D. 2001. Transcription regulation by histone methylation: interplay between different covalent modifications of the core histone tails. Genes Dev **15**(18): 2343-60.

Zheng, C. and Hayes, J.J. 2003. Intra- and inter-nucleosomal protein-DNA interactions of the core histone tail domains in a model system. J Biol Chem **278**(26): 24217-24.

Zhou, Z., Hong, E.J., Cohen, S., Zhao, W.N., Ho, H.Y., Schmidt, L., Chen, W.G., Lin, Y., Savner, E., Griffith, E.C., Hu, L., Steen, J.A., Weitz, C.J. and Greenberg, M.E. 2006. Brain-specific phosphorylation of MeCP2 regulates activity-dependent Bdnf transcription, dendritic growth, and spine maturation. Neuron **52**(2): 255-69.

Zhu, J.K. 2009. Active DNA demethylation mediated by DNA glycosylases. Annu Rev Genet **43**(143-66.

Zilberman, D., Coleman-Derr, D., Ballinger, T. and Henikoff, S. 2008. Histone H2A.Z and DNA methylation are mutually antagonistic chromatin marks. Nature **456**(7218): 125-9.

Zlatanova, J., Caiafa, P. and Van Holde, K. 2000. Linker histone binding and displacement: versatile mechanism for transcriptional regulation. FASEB J **14**(12): 1697-704.